DEVELOPMENT OF A NOVEL HYBRID PROCESS FOR THE CONVERSION OF CELLULOSE INTO HIGH-VALUE CHEMICALS BY APPLYING VOLTAGE IN HOT COMPRESSED WATER

A Thesis Submitted to
the Graduate School of Engineering and Sciences of
İzmir Institute of Technology
in Partial Fulfillment of the Requirements for the Degree of

DOCTOR OF PHILOSPHY

in Chemical Engineering

by
Okan AKIN

July 2017
İZMİR

We approve the thesis of **Okan AKIN**

Examining Committee Members:

Assist. Prof. Dr. Aslı YÜKSEL ÖZŞEN
Department of Chemical Engineering, İzmir Institute of Technology

Prof. Dr. Selahattin YILMAZ
Department of Chemical Engineering, İzmir Institute of Technology

Assist. Prof. Dr. Ali Oğuz BÜYÜKKİLECİ
Department of Food Engineering, İzmir Institute of Technology

Assist. Prof. Dr. Canan URAZ
Department of Chemical Engineering, Ege University

Assoc. Prof. Dr. Zehra ÖZÇELİK
Department of Chemical Engineering, Ege University

28 July 2017

Assist. Prof. Dr. Aslı YÜKSEL ÖZŞEN
Supervisor, Department of Chemical Engineering
İzmir Institute of Technology

Prof. Dr. Seher Fehime ÖZKAN
Head of the Department of Chemical Engineering

Prof. Dr. Aysun SOFUOGLU
Dean of the Graduate School of Engineering and Sciences

ACKNOWLEDGMENT

I would like to express my sincere gratefulness to my supervisor Assist. Prof. Dr. Asli Yüksel Özşen for her encouragement, support and supervision throughout my PhD study. I also would like to express my appreciation to my committee members, Prof. Dr. Selahattin Yılmaz and Assist. Prof. Dr. Ali Oğuz Büyükkileci for their valuable comments and suggestion to help me to surpass the challenges that I encountered during my study. I would like to also express my gratitude to Prof. Dr. Erol Şeker for priceless advices, support and encouragement during my time as a both researcher and student.

I would like to thank to research specialists, Filiz Kurucaovalı, Handan Gaygısız, Esra Tuzcuoglu Yücel for their help, support and valuable advices. I am also grateful to my special friends, Özgün Deliismail, Elif Güngörmüş, Mesut Genişoğlu, Efecan Pakkaner, Bertan Özdoğru for their friendship and support.

Finally, my deepest gratefulness goes to my wife Pelin Oymacı Akın, for her endless support, encouragement and priceless advices in my life. I extent my sincere appreciation to my family, Aydın Akın, Aysel Akın, Halil Oymacı, Nilgün Oymacı, Ozan Akın, Cenk Enhoş, Sima Gazneli Enhoş for their endless support.

ABSTRACT

DEVELOPMENT OF A NOVEL HYBRID PROCESS FOR THE CONVERSION OF CELLULOSE INTO HIGH-VALUE CHEMICALS BY APPLYING VOLTAGE IN HOT-COMPRESSED WATER

In this study, a novel hybrid method of hydrothermal electrolysis implemented for the decomposition of microcrystalline cellulose (MCC) into high value added chemicals such as levulinic acid, 5-hydroxymethylfurfural (5-HMF), and furfural. The hypothesis of the study was that, when direct current (DC) is applied the formation of ionic and radical species can alter the hydrolysis of cellulose. Based on this hypothesis, the purpose of the study was to build an integrated method of hydrothermal electrolysis that can lower energy requirement of cellulose hydrolysis by altering the selectivity.

In order to investigate the individual and coupled effect of operating parameters such as reaction temperature (170-200 ℃), time (30-120 min.), electrolyte concentration (1-50 mM H_2SO_4), constant current (0-2 A), statistical analysis was conducted by a fractional factorial design. Analysis of variance (ANOVA) test was applied to the main hydrolysis products yields of MCC, total organic carbon (TOC) and cellulose conversion. Based on the response surface plots, 1A of current at 200 ºC maximized TOC yield and cellulose conversions to 62% and 81%, respectively.

In order to enhance the selectivity, constant voltage (2.5, 4.0 and 8.0 V) was applied at 200℃. Application of 2.5 V increased TOC (54%) and alter the selectivity of 5-HMF (30%) and levulinic acid (21%). The structural changes in solid residues were analyzed by Fourier Transform Infrared Spectroscopy (FTIR) and found that MCC particles functionalized by carboxylic acid and sulfonated groups by application of 2.5 V. Therefore, change in the selectivity values were conducted with the functionalization of MCC particles due to applied voltage under sub-critical conditions.

ÖZET

SICAK BASINÇLI SUDA VOLTAJ UYGULAYARAK SELÜLOZUN DEĞERLİ KİMYASALLARA DÖNÜŞTÜRÜLMESİ İÇİN YENİ BİR HİBRİT SÜREÇ GELİŞTİRİLMESİ

Bu çalışmada, yeni bir hibrid yöntem olan hidrotermal elektroliz, mikrokristal selülozun (MCC) degerli kimyasallara (levulinik asit, 5-hidroksimetilfurfural (5-HMF), furfural) dönüştürülmesi çalışıldı. Çalışmanın hipotezi, hidrotermal koşullar altında reaksiyon ortamına uygulanan doğru akımın iyonik ve radikal ürünlerin oluşmasına ortam hazırlaması, selülozun hidroliz mekanismasını değiştirebilir. Bu hipoteze dayanarak, çalışmanın amacı, hidrotermal koşullar altında, yüksek katma degerli kimyasallara karşı seçiciliği arttırarak, selüloz hidrolizinin enerji ihtiyacını azaltabilen entegre bir elektroliz yöntemi geliştirmektir.

Reaksiyon paramatrelerinin, sıcaklık (170-200 ℃), reaksiyon zamanı (30-120 dk.), uygulanan doğru akım (0-2 A), elektrolit konsantrasyonun (1-50 mM H_2SO_4), ürünler üzerindeki etkilerini incelemek amacıyla, ½ kesirli çok etkenli deney tasarımı yapıldı. Deneyler sonucu elde edilen, ürün verimleri, toplam organik karbon miktarı, selüloz dönüşümü, varyans analizi (ANOVA) ile istatiksel olarak değerlendirildi. Yanıt yüzeyi yöntemi ile elde edilen verilerde, 200 ℃ sıcaklıkta 1 A sabit doğru akımın uygulanması toplam organik karbon verimini %62've selüloz dönüşümünü %81'e yükseltti.

Değerli kimyasalların oluşumunda, seçiciliği arttırmak amacıyla, sabit voltaj (2.5, 4.0 ve 8.0 V) deneyleri 200 ℃ sıcaklıkta uygulandı. En çarpıcı sonuçlar, 2.5 V sabit voltaj uygulandığında elde edildi. Toplam organik karbon (%54) ve seçicilikte 5-HMF (%30), levülinik asit (%21) değerlerine ulaşıldı. Reaksiyon sonucu elde edilen katının, FTIR analizi sonucunda karboksilik asit ve sülfon fonksiyonel gruplarının, 2.5 V sabit voltaj değerinde daha belirgin hale geldiği gözlemlendi. Seçicilikteki artışların sebebi olarak bu fonksiyonel gruplarının oluşmasına bağlandı.

TABLE OF CONTENTS

LIST OF FIGURES

Figure **Page**

LIST OF TABLES

LIST OF SYMBOLS

g	Harris-Alder g-factor;
k	Boltzmann constant
N_A	Avogadro number
T	Absolute temperature
α	Molecular polarizability of the isolated water molecule
ϵ	Dielectric constant
ϵ_0	Dielectric constant at free space
μ	Dipole moment
ρ	Density
k_B	Boltzmann constant
h	Planck's constant
T	Absolute temperature
κ	Transmission coefficient
K_c^*	Concentration based equilibrium constant
K_γ^*	Activity based equilibrium constants
K_W	Ion dissociation constant
γ	Activity coefficients
V_i	Molar volume
δ	Solubility parameter
$\Delta V^{\neq}$	Activation volume
μ	Dipole moment
a_i	Activity of species i
m^0	Standard molality
κ	Electrolytic conductivity
Λ_0	Molar conductivity of H^+ plus OH^- ions

CHAPTER 1

INTRODUCTION

Increase in the world population resulted in growing energy demand all over the world. Depletion of petroleum stocks and environmental concerns due to emitted greenhouse gases, researches have focused on renewable feedstock of biomass. The growing interest to the biomass as renewable feedstock for the production of value-added products is resulted due to not only environmental concerns but also political stability plays an important role. Due to the uncertainties of petroleum-based economy, many nations have been transferring their petroleum-based economy to biobased. Therefore, a nation lack of petroleum stocks can take advantage of its natural sources (biomass) to produce such value-added products as fermentable sugars and chemicals. Turkey is one of the nations that inadequate petroleum stocks compared to demand on petroleum-based chemicals. Turkey has potential of 15 million tons of agricultural biomass per year as waste. Therefore, petroleum dependency of Turkey can diminish by using its own natural biomass sources.

Conversion of different kinds of biomass sources to value added chemicals has been investigated in literature for last decades (Yan et al. 2010, Wu et al. 2010). Cellulose is the most abundant renewable feedstock in environment. Approximately 50% of wood and agricultural biomass consists of cellulose (Pasangulapati et al. 2012). Thus, focusing on cellulose as model component in the investigation of biomass conversion to valuable chemical can be beneficial in the manner of understanding reaction mechanism. (Cantero, et al. 2013). Some of the literature studies research on the conversion of the carbohydrates such as fructose and glucose (Dibenedetto et al. 2015). These molecules can also be converted to value added chemicals such as levulinic acid, 5-hydroxymethyfurfural (5-HMF), and lactic acid. As it is well known, cellulose has the repeating of D-glucose molecules and therefore, because of decomposition, products of cellulose, hydrolysates, are the product of glucose and its isomer, fructose. Therefore, this project also focuses on hydrolysis of biomass by using microcrystalline cellulose as model component. Using MCC as raw material was chosen to understand the decomposition mechanism clearly and it is primary investigation for the conversion of biomass without pretreatment.

Decomposition of cellulose is challenging for, cellulose is a semicrystalline material and hydrogen bonding between D-glucose chains makes it difficult to dissolve in any medium. Therefore, different reaction mediums such as enzymatic, acid and alkaline mediums have been investigated in literature for the decomposition of cellulose (Ahola et al. 2008, Ashadi, Shimokawa, and Ogawa 1996). However, there are some disadvantages of these reaction mediums. Bioconversion of cellulose by enzymes lasts quite long in comparison to other methods. Fan et. al. reported that 30% conversion of cellulose in a batch reactor takes 16h (Lee, Gharpuray, and Fan 1982). On the other hand, biohydroylsis is the huge cost due to the expensive enzyme requirement. Therefore, sustainability and industrial scale decomposition of cellulose is not promising unless operating cost decline. Degradation of cellulose in an acid medium has been investigated in literature as well (Amarasekara and Wiredu 2011). Acid has the ability to hydrolyze the cellulose by breaking the both β(1-4)glycosidic bond and intra- and inter-molecular hydrogen bonding (Sasaki et al. 2005). Cellulose degradation by acid has been discouraged due to the corrosive nature of acids that resulted in the use of expensive corrosion resistant stainless steel reactor. Moreover, in the manner of environmental concerns, acid disposal is thoughtful consideration.

Due to the presence of intra- and inter molecular hydrogen bond linkages at the crystalline region in cellulose, makes cellulose hard to soluble and reactive (Sasaki et al. 2005). Therefore, organic solvents and different acid types are effective but not environmentally friendly process. Consequently, improvement of a process that is both effective and environmentally benign is challenging. However, hydrothermal degradation of biomass is a promising process in the manner of both environmental and effectiveness of reaction medium. There have been different kinds of studies reported that hydrothermal conditions is effective reaction medium regarding the conversion of biomass to valuable chemical intermediates (Sasaki et al. 2005). In this manner, sub-critical and supercritical water as reaction medium has unique properties for various organic reactions (Pinkowska, Wolak, and Zlocinska 2011, Prado et al. 2014, Rogalinski et al. 2008). Water has some unique properties at around the critical point (T_c=374.2 ºC, P_c=22.1 MPa and ρ_c=0.323 g. cm^{-3}). Depending on the condition of temperature and pressure, hot compressed water supports (HCW) either free radical or polar and ionic reactions. In other words, HCW is an adjustable solvent for specified reactions (Kruse and Dinjus 2007) . Studies related to conversion of cellulose and cellulosic biomass to value-added chemical intermediates in subcritical and supercritical water medium has been reported (Tolonen et al. 2015,

Resende and Savage 2010). Hot compressed water has gotten attention from both industry and academia due its adjustable properties, hence, also in our study hot compressed water was chosen as reaction medium because of environmental benign properties and effective features in cellulose hydrolysis compared to acid and enzymatic media. Sasaki and coworkers investigated the reaction mechanism of cellulose hydrolysis in sub and supercritical water. They reported that in subcritical region ionic product concentration increases which defines the reaction pathway in a way of liquid products. On the other hand, in supercritical region radical based reactions become favorable which resulted in gaseous products (Sasaki et al. 1998). In this project, it is aimed to produce liquid products, hence, water in subcritical region is chosen as reaction medium.

As it is important for all reactions, selectivity and yield of conversion of reactant plays an important role in the optimization of reaction conditions. Hence, adjustable solvent properties are inadequate in the formation of value added chemicals with high yield and selectivity. Therefore, researches have been investigating to increase selectivity of reactions by using catalysis. Different kinds of catalysis have been investigated and reported in literature regarding the conversion of biomass to valuable chemicals (Cao et al. 2015, Chen et al. 2011). Chen and coworkers reported that edition of oxidizing agent in reaction medium increases the yield of reaction towards to 5-HMF. Other than oxidizing agents, electrochemical methods have been reported for the oxidation of organic compounds (Sasaki et al. 2010, Yuksel, Sasaki, and Goto 2011). Yuksel and coworkers reported that hydrothermal electrolysis of glycerol under subcritical water conditions resulted in higher yield of lactic acid formation. Therefore, hydrothermal electrolysis can be used to increase the yield of the product of cellulose decomposition in subcritical water conditions. In our knowledge, there is no study that conducts the hydrothermal electrolysis in decomposition of cellulose under subcritical water conditions.

The purpose of the study is to build an integrated method of electrolysis under hydrothermal conditions that can lower the energy requirement of cellulose hydrolysis by increasing the selectivity to high value added chemicals. Thus, in this study, novel hybrid process of hydrothermal electrolysis of microcrystalline cellulose to value added chemicals such as 5-HMF, levulinic acid and furfural was investigated. The effect of constant current and constant voltage application into the reaction medium under hydrothermal conditions and interaction of electrolysis with reaction temperature, time and electrolyte concentration was investigated within the statistical significance.

CHAPTER 2

HOT-COMPRESSED WATER AS REACTION MEDIUM

In this chapter, the main properties of water at hydrothermal conditions and its phase behavior along with the thermo-physical properties are addressed. Most importantly, the electrical properties of water including ionic product, electrical conductivity and dielectric constant are discussed, as these properties play important role in electrochemical decomposition of biomass. Moreover, utilization of biomass to value added chemicals in sub- and supercritical water conditions is also discussed.

2.1. Properties of Hot-Compressed Water

The properties of hot-compressed water have been well established in literature that opened up new opportunities to use it in chemical reactions (Franck 1970, Marshall and Franck 1981b). There has been numerous study reported in literature using pure water as reaction medium in its sub-critical (Sasaki, Adschiri, and Arai 2004) and supercritical states (Zhu, Ma, and Zhu 2010, Watanabe et al. 2004). Water becomes attractive as reaction medium due to its versatile properties (low dielectric constant, high diffusivity, low density) of in critical state. These properties of water can be adjusted by changing its temperature and pressure (Kruse and Dinjus 2007). For instance, dielectric constant decreases ($\epsilon \cong 10$) and ionic product concentration increases to 10^{-11} in the temperature range 200 ºC and 300 ºC (Marshall and Franck 1981a). The water properties can be adjusted by changing the temperature and pressure and hence, selectivity and yield of a chemical reaction can be adjusted accordingly. The best way to understand unusual properties in critical region begins with investigation of phase diagram of water (Figure 2.1).

The critical point of water is reached as the temperature and pressure increases up to a point where the two phases, the liquid and vapor coalesce into a single phase. Along the saturation line, the density of water diminishes while the vapor density increases as its pressure increases until the densities become equivalent at the critical

point. This point is characterized as the critical temperature point T_c (374 ^oC) and critical pressure point P_c (22.1 MPa) (Figure 2.1) (Kruse and Dinjus 2007).

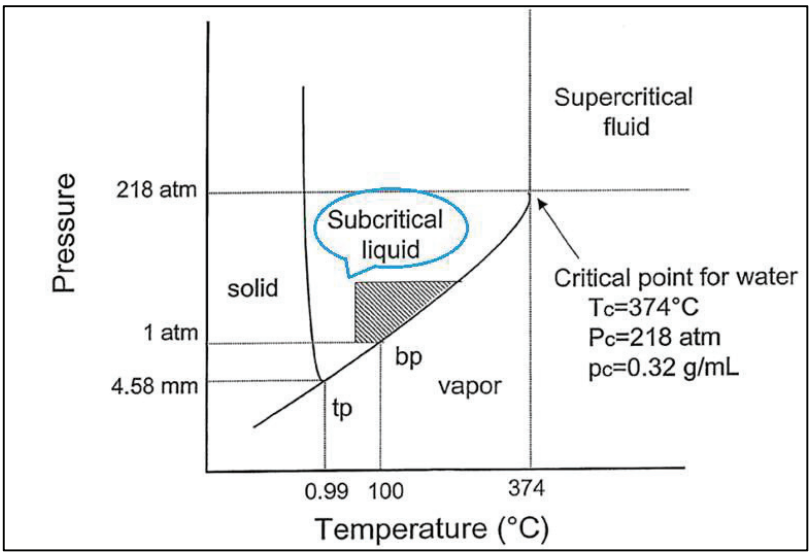

Figure 2.1. Phase diagram of water
(Source: Kruse and Dinjus 2007)

2.1.1. Dielectric Constant of Water and Its Effect on Reaction Kinetics

Dielectric constant is a dimensionless number describes the ability of a solvent that can be polarized under applied electrical field. Dielectric constant allies with the polarity. Water has high polarity of in its ambient conditions due to hydrogen bonding network (Harvey and Friend 2004). Thus, high dielectric constant of a solvent is associated with greater ability to solve polar compounds. Water has higher dielectric constant of 78.2 in ambient (T=25 °C) temperature, in comparison to liquids such as paraffin ($\epsilon \cong 2.25$) (Harvey and Friend 2004). The increase in the temperature decreases the static dielectric constant of water rapidly (Figure 2.2). The following expression (Eqn. 2.1, Eqn. 2.2) is derived for the dielectric constant. Parameters are listed in Table 2.1, for the calculation of dielectric constant.

$$\frac{\epsilon - 1}{\epsilon + 2} = A\frac{\epsilon}{(2\epsilon + 1)(\epsilon + 2)} + B \qquad (2.1)$$

where A and B are represented as;

$$A = \frac{N_A \mu^2 \rho g}{\epsilon_0 k\, T}, B = \frac{N_A \alpha}{3\epsilon_0}\rho \tag{2.2}$$

In where g is the Harris-Alder g-factor; Boltzmann constant (k); Avogadro number (N_A); Absolute temperature (T); molecular polarizability of the isolated water molecule (α); The dielectric constant (ϵ) and free space (ϵ_0), dipole moment (μ), and density (ρ).

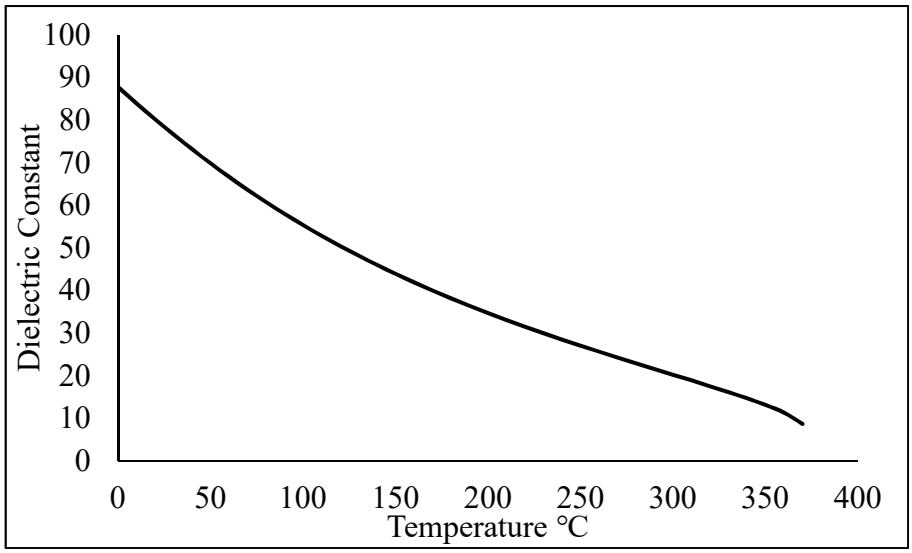

Figure 2.2. Change of dielectric constant of water with temperature (Source: Uematsu and Frank 1980)

Table 2.1. Parameters used in the calculation of dielectric constant (Source:Brunner 2014)

Parameter	Value
Permittivity of free space, ϵ_0	$[4 \times 10^{-7}\ \pi(299{,}792{,}458)^2]^{-1}$ $C^2\ J^{-1}\ m^{-1}$
Mean molecular polarizability, α	1.636×10^{-40} $C^2\ J^{-1}\ m^{-1}$
Molecular dipole moment, μ	6.138×10^{-30} C m
Boltzmann constant, k	1.380658×10^{-23} mol^{-1}
Avogadro number, N_A	6.0221367×10^{23} mol^{-1}
Molar mass of water, Mw	0.018015268 kg

The importance of dielectric constant arises from its effect on chemical kinetics due to the changes in solvent properties of water. The common definition of a chemical

reaction is the mechanistic model. For instance, for an elementary reaction (Eqn.2.3) general rate expression is given in Eqn. 2.4. The kinetics of a reaction in mechanistic models can be associated with the transition state theory (Savage et al. 1995).

$$A + B \rightarrow D + E \tag{2.3}$$

$$r = k\, C_A C_B \tag{2.4}$$

The transition state theory conducts the kinetics of an elementary reaction through a transition-state intermediate species ($M^{\neq}$) in Eqn.2.5. (Pearson 1981)

$$aA + bB \leftrightarrow M^{\neq} \rightarrow products \tag{2.5}$$

$$k = \kappa \frac{k_B T}{h} K_c^* \tag{2.6}$$

In where, k is the rate constant of transition-state, k_B is the Boltzmann constant, h is the Planck's constant, T is the absolute temperature and κ is the transmission coefficient and K_c^* is the equilibrium constant in terms of concentration. Concentration based equilibrium (K_c^*) constant can be described in terms of thermodynamic (K_a^*) and activity (K_γ^*) based equilibrium constants (Eqn. 2.7). The rate constant can be rewritten in terms of thermodynamic and activity based coefficients in Eqn. 2.8.

$$K_c^* = \frac{K_a^*}{K_\gamma^*} \tag{2.7}$$

$$k = \kappa \frac{k_B T}{h} \frac{K_a^*}{K_\gamma^*} \tag{2.8}$$

Equilibrium constant can be related to the change in the Gibbs' free energy, ΔG^* and Eqn. 2.8 arranged as follows ;

$$k = \kappa \frac{k_B T}{h} \exp\left(\frac{-\Delta G^*}{RT}\right) \tag{2.9}$$

Eqn.2.9 is used for the correlation of reaction kinetics in where linear free-energy relationships conducted (Brunner 2014). The rate constant can be described in terms of activity coefficients (Eqn.2.10). Activity coefficients (γ) can be derived from the solvent properties regarding to molar volume (V_i) and solubility parameter (δ) as indicated in equation (2.11.

$$k = k_0 \frac{\gamma_A \gamma_B}{\gamma_{M*}} \tag{2.10}$$

$$RT ln\gamma_i = V_i(\delta_i - \bar{\delta})^2 \tag{2.11}$$

Combining the activity coefficient expression with the rate constant yields the prediction of the effect of solvent with different solubility parameters (Eqn. 2.12**(2.**).

$$ln\frac{k}{k_0} = \frac{V_A(\delta_A - \bar{\delta})^2 + V_B(\delta_B - \bar{\delta})^2 - V_{M*}(\delta_{M*} - \bar{\delta})^2}{RT} \tag{2.12}$$

Transition state theory yields the change in the activation volume as fallows;

$$\left(\frac{\partial ln k}{\partial p}\right) = \left(\frac{\partial ln K_X^{\neq}}{\partial p}\right)_T + \left(\frac{\partial ln\alpha}{\partial p}\right)_T = -\frac{\Delta V^{\neq}}{RT} + \left(\frac{\partial ln\alpha}{\partial p}\right)_T \tag{2.13}$$

where k is the reaction rate constant, K equilibrium constant, α transmission coefficient and $\Delta V^{\neq}$ is the activation volume. The solvent activation volume can be described with the following relation.

$$\Delta V_{M*} = \Delta V_A + \Delta V_{B.} \tag{2.14}$$

The relation of activation volume of transition state ((2.13) and combination to (2.14 yields that reaction rate constant varies linearly with the solvent solubility parameter $\bar{\delta}$. This relation is also verified and reported in experiments that uses different liquids

(Pearson 1981). Thus, dielectric constant can be used for the solution phase reaction kinetics that implemented for polar molecules. Kirkwood derived a relation ((2.1) between energy of a dipole and dipole moment μ in terms of dielectric constant (Connors 1990).

$$\Delta G \sim \frac{\epsilon - 1}{2\epsilon + 1} \tag{2.15}$$

2.1.2. Ionic Dissociation Constant and Electrolytic Conductivity of Water

The dissociation of water to its positive and negative ions is important for electrochemical reactions under hydrothermal conditions due to the current efficiency. The dissociation of water can be written as;

$$2H_2O \leftrightarrow H_3O^+ + OH^- \tag{2.16}$$

The dissociation of water is an endothermic reaction and equilibrium constant for this reaction is described in terms of activities ((2.17).

$$K_W = \frac{a_{H_3O^+} a_{OH^-}}{a_{H_2O}^2} \tag{2.17}$$

In where a_i is the activity of species *i.* Ion concentration is measured in terms of molality and it is 10^{-14} for the water in ambient conditions. As the temperature and pressure changes, the ionic constant of water changes accordingly (Figure 2.3). Increase in the temperature yields higher ionic product concentration favoring the proton-based catalytic reactions. However, ionic product concentration of water decreases above the 250 ℃ due to the low density of water yielding the destruction of hydrogen bond network. Thus, dissociation of water at higher temperature is restricted due to the low density (Brunner 2014). The change of ionic dissociation constant of water (pKw) as a function of temperature and density is provided by the International Association for the Properties of Water and Steam (IAPWS) (Eqn. 2.18, Eqn. 2.19).

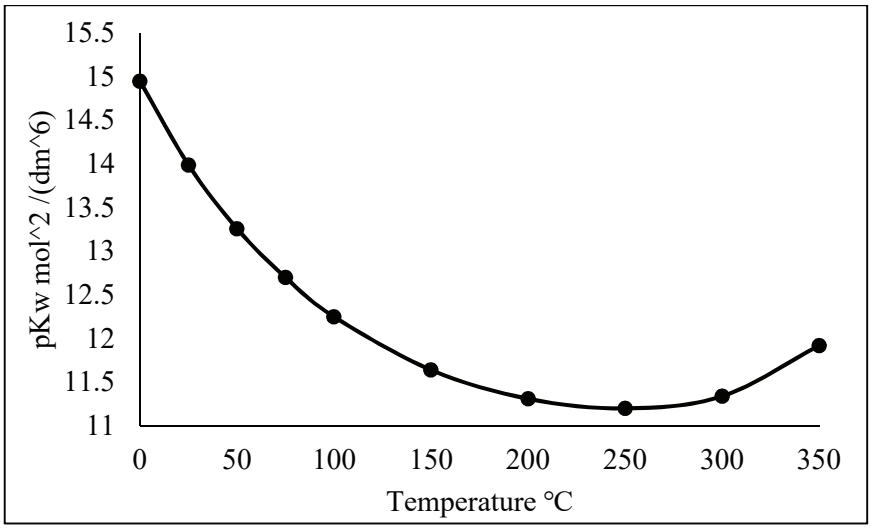

Figure 2.3. Change of ionic dissociation constant of water with temperature (Source: Bandura and Lvov 2006)

Ionization constant as a function of density and temperature is expressed with the following equations (Eqn. 2.18, Eqn. 2.19).The ionization constant equation includes the equilibrium constant of the ionization reaction in the ideal gas state pK_W^G.

$$pK_W = -2n\left[log_{10}(1+Q) - \frac{Q}{Q+1}\rho(\beta_0 + \beta_1 T^{-1} + \beta_2\rho)\right] + pK_W^G + 2log_{10}\frac{m^0 M_W}{G} \quad (2.18)$$

$$Q = \frac{\rho}{\rho_0}\left[\left(\alpha_0 + \alpha_1 T^{-1} + \alpha_2 T^{-2}\rho^{2/3}\right)\right] \quad (2.19)$$

$$pK_W^G = \gamma_0 + \gamma_1 T^{-1} + \gamma_2 T^{-2} + \gamma_3 T^{-3} \quad (2.20)$$

In where Mw is the molecular weight of water, pK_W^G is the ionization constant of water at ideal-gas state, m^0 is the standard molality (1 mol kg^{-1}), G=1000 g kg^{-1}, ρ is the mass density (g cm^{-3}), T is the absolute temperature (K) and $\gamma_0, \gamma_1, \gamma_2, \gamma_3$ $\alpha_0, \alpha_1, \alpha_2$ $\beta_0, \beta_1, \beta_2$ are parameters given in Table 2.2.

Table 2.2. Empirical parameters for (Source: Bandura and Lvov 2006)

Coeffcient	Value	Units
n	6	
α_0	-0.864671	
α_1	8659.19	K
α_2	-22786.2	$(g\ cm^{-3})^{-2/3}\ K^2$
β_0	0.642044	$(g\ cm^{-3})^{-1}$
β_1	-56.8534	$(g\ cm^{-3})^{-1}\ K$
β_2	-0.375754	$(g\ cm^{-3})^{-2}$
γ_0	6.141500×10^{-1}	
γ_1	4.825133×10^{4}	
γ_2	-6.770793×10^{4}	
γ_3	1.010210×10^{7}	

Electrolytic conductivity of water is important due to the usage as reaction medium for hydrothermal electrolysis of microcrystalline cellulose in this study. As ionic product concentration is related to the electrolytic conductivity of water, the relation is built accordingly. IAPWS has released a dimensionless electrolytic conductivity (κ_r) of water as follows;

$$\kappa_r = 10^{-3}\ \Lambda_{0,r}\ K_{W,r}^{1/2} \rho_r \tag{2.21}$$

In where $\kappa_r = \kappa/\kappa^{ref}$, $\Lambda_{0,r}=\Lambda_0/\Lambda^{ref}$, $K_{W,r} = K_W/{K_W}^{ref}$, $\rho_r = \rho/\rho^{ref}$, κ is the electrolytic conductivity (specific conductance) of water, K_w is the ion product of water, ρ is the density of water, and Λ_0 is the molar conductivity of H^+ plus OH^- ions in water. Reference values: $\kappa^{ref} = 10^2 S\ m^{-1}$, $\Lambda^{ref} = 10^{-4} m^2 S mol^{-1}$, ${K_W}^{ref} = 1\ (mol\ kg^{-1})^2$, $\rho_{ref} = 10^3 kg\ m^{-3}$.

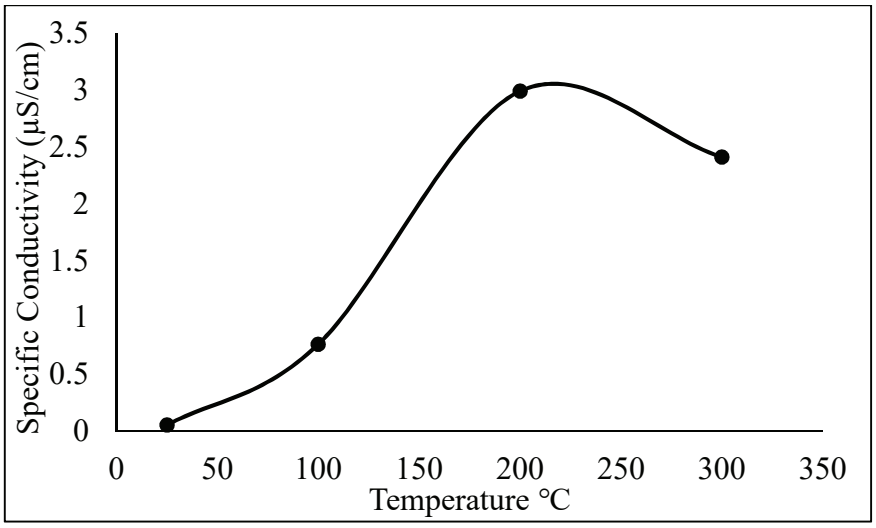

Figure 2.4. Specific electrolytic conductivity of water
(Source:Bandura and Lvov 2006)

Electrolytic conductivity of water increases up to 250 °C (Figure 2.4), above this temperature, decreases due to low density of water resulted in the disruption in hydrogen bonding network. Hydrolysis of biomass takes place via protonation of β(1-4)glycosidic bond of cellulose and under hypothermal conditions, high ionic product concentration is favored. In the case of hydrothermal electrolysis of microcrystalline cellulose, electrolytic conductivity plays an important role in terms of current efficiency. Therefore, experimental conditions were decided considering the water properties mainly ionic product concentration and electrolytic conductivity.

CHAPTER 3

HYDROLYSIS OF MICROCRYSTALLINE CELLULOSE IN HOT-COMPRESSED WATER

Utilization of biomass will remain an important topic because it is a renewable resource. The conversion of simple biomass compounds such as sugars and starch has been investigated widely (Alvarez and Vazquez 2004, Bodirlau, Spiridon, and Teaca 2010, Nagamori and Funazukuri 2004). Biomass has been investigated widely in both academia and industry due to its potential. In order to find more efficient and sustainable way of utilization of biomass, different kinds of researches has been published. In this purpose, different methods in utilization of biomass have been reported so far; enzymes (Badgujar and Bhanage 2016, Annamalai, Rajeswari, and Balasubramanian 2014) mineral acid (Li et al. 2017), ionic liquids (Zheng et al. 2016), solid acid catalysts (Kilic and Yilmaz 2015), sub- and supercritical water (Sasaki et al. 2000). Electrochemical methods have also been reported, Zhang and coworkers studied electrochemical degradation of lignin (Zhang et al. 2014), Xu and coworkers studied electrolysis of corn strove to sugars (Xu et al. 2014).

Recent studies have been focused on the conversion of cellulosic materials due to the dual use of derived products in food and nonfood purposes. The mixture of cellulose, hemicelluloses and lignin has been investigated widely by both academia and industry. GF Biochemicals cooperation, which is located in Italy, is the high volume producer of levulinic acid from lignocellulosic biomass. There are not much in number as bulk producers using biomass as feedstock due to the challenges of biomass utilization, such as high activation energy for hydrolysis, high cost in separation of decomposition products (Brunner 2014). Real biomass includes additional compounds such as proteins and others. However, biomass includes substantial amount of water in its structure. Therefore, decomposition of biomass in sub and supercritical water can play an important role in the further exploitation of this resource.

Utilization of biomass with high-temperature and supercritical water can be carry through liquefaction, total gasification, and oxidation (Figure 3.1).

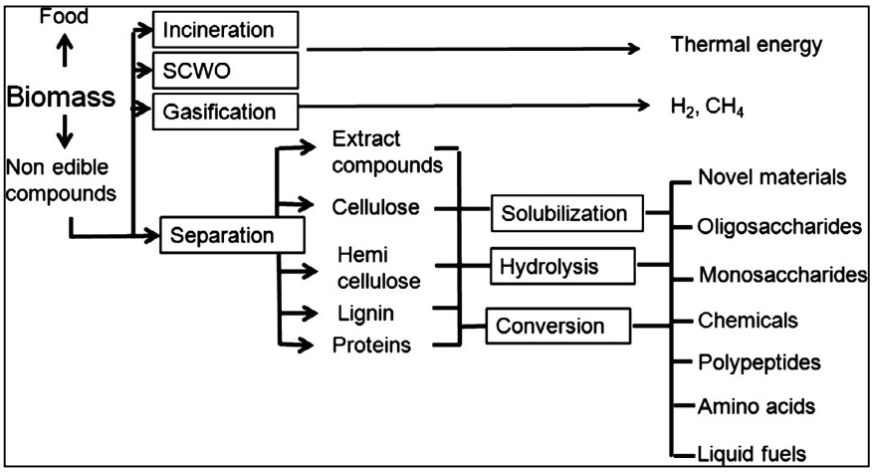

Figure 3.1. Utilization of biomass by different processes
(Source: Brunner 2014)

3.1. Cellulose as Model Compound and Decomposition in Sub- and Super Critical Water

In this study, microcrystalline cellulose is used as model compound due to the its crystalline structure which makes it insoluble and resistant to attack by catalyst. Cellulose has low solubility and high rigid structure due to the intra- and intermolecular hydrogen bonds (Figure 3.2, arrows). The challenge regarding the solvability of cellulose arises due to the intermolecular hydrogen bonds, which make intermolecular bonds inaccessible to solvent compound. This structure makes cellulose resistant to enzymes and swelling in water. Due to the compressibility and density properties of water, cellulose becomes partially soluble in supercritical water region (Peterson et al. 2008). However, reported studies showed that hot compressed water can rapidly solubilize cellulose and hydrolyze to its building block as glucose (Sasaki, Adschiri, and Arai 2004, Knezevic, van Swaaij, and Kersten 2009).

Different kinds of biological sources can be used as cellulose. Hence, different physical and chemical structure of cellulose can affect its behavior. Therefore, experiments should conduct for the same batch of cellulose source. However, results of several studies in cellulose conversion near critical water exhibits similar behavior (Cantero, Bermejo, and Cocero 2013, Ding and Wang 2008, Resende and Savage 2010). Recently, detailed mechanism of cellulose decomposition in subcritical and supercritical water was reported as hydrolysis, retro-aldol condensation, keto-enol tautorism and dehydration (Sasaki et al. 1998, Goto and Yokoe 1996).

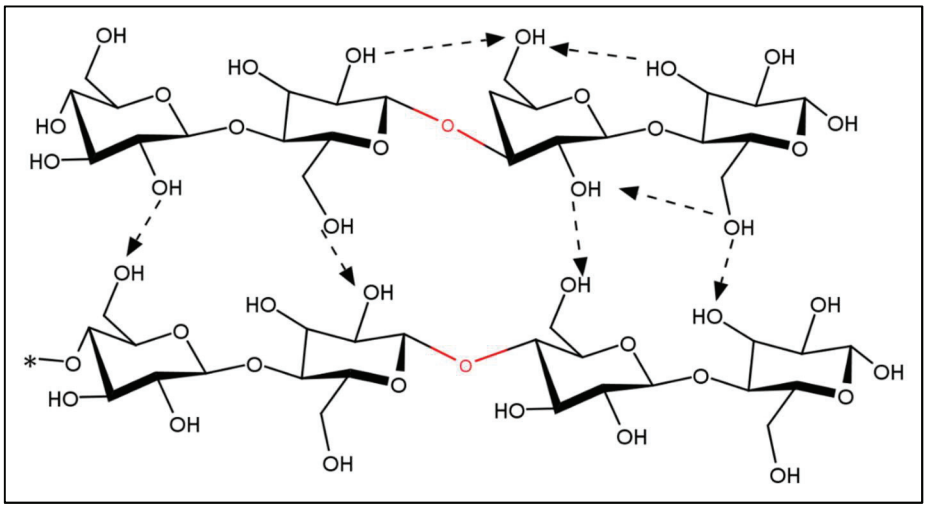

Figure 3.2. Structure of microcrystalline cellulose with ending and repeating group

The reaction pathway can be divided into three main parts: 1st part is cellulose is hydrolyzed to oligosaccharides; 2nd part is the saccharides are hydrolyzed to glucose (Figure 3.3) and; 3rd part, glucose isomerization and dehydration to 5-HMF and levulinic acid. The products of cellulose hydrolysis, in the first step, are oligosaccharides and small saccharides such as cellobiose (Cantero, Bermejo, and Cocero 2013).

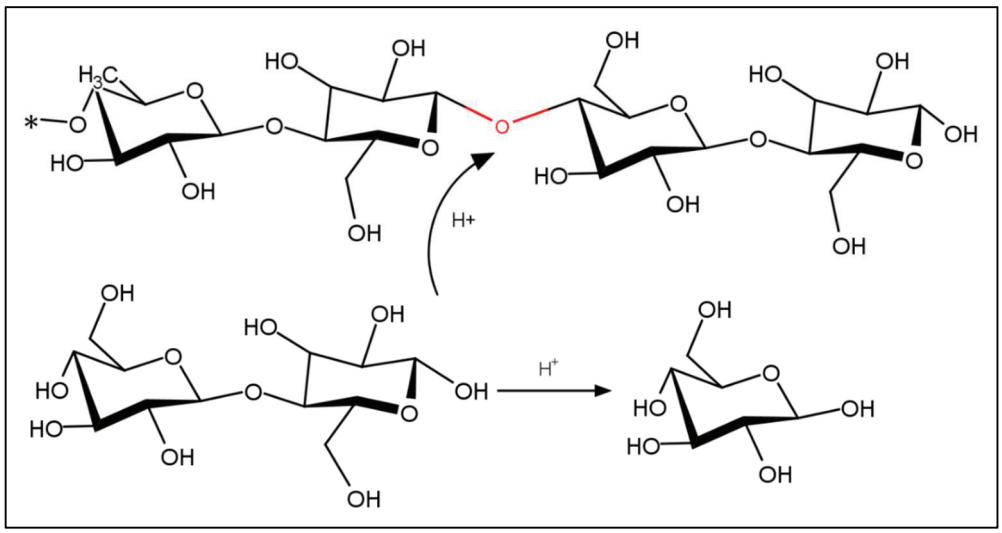

Figure 3.3. Cellulose hydrolysis to cellobiose and glucose

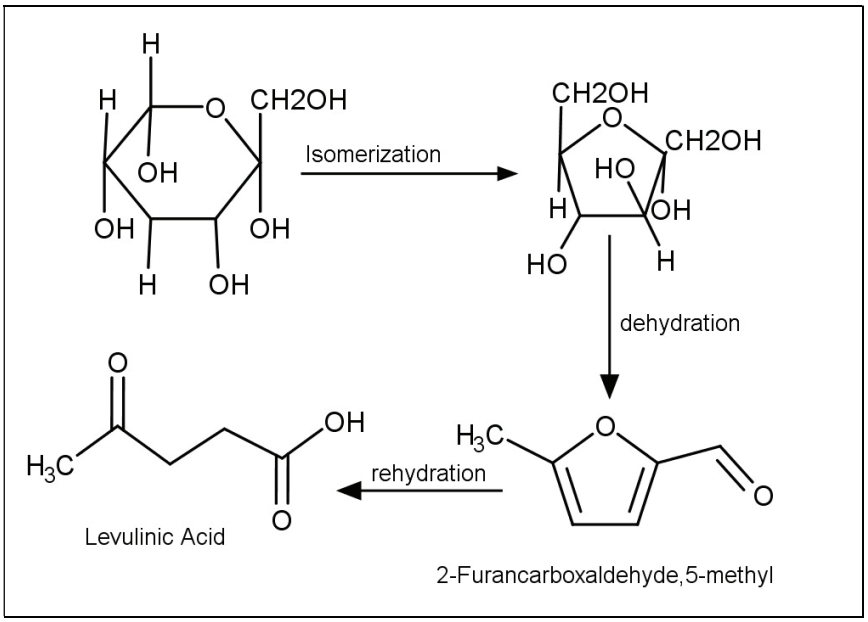

Figure 3.4. Glucose isomerization to fructose, dehydration and rehydration to 5-HMF and levulinic acid, respectively

3.2. Reaction Kinetics and Product Distribution of Cellulose Decomposition in Sub- and Supercritical Water

As the building block of cellulose is glucose and degradation products formed due to the further reactions of glucose, the conversion of glucose to valuable chemical intermediates is a matter of interest more than decades (Cao et al. 2015, Chen and Wilson 2007). As mentioned before, supercritical region resulted in more gaseous products when compared to sub critical region. During hydrolysis of glucose in high-temperature water, gaseous products can be neglected up to a temperature of T=300 ºC, at a pressure of P=40 MPa, and a residence time of up to t=5 min. The main hydrolysis products are 1,6-anhydroglucose, fructose, erythrose, glycolaldehyde, pyruvaldehyde, and dihydroxyacetone. All products are soluble in water. Hydrolytic reactions of glucose at temperatures T=300–400 ºC, pressures P=25–40 MPa, and residence times t=0.02–2 s reveal a number of parallel and secondary reactions(Brunner 2009). Eventually, the hydrolysis products react to acids, aldehydes, and alcohols. The hydrolysis of glucose in high-temperature and supercritical water was reported by Saito and coworkers and they claimed that D-Glucose was converted into aldehydes, organic acids and furans, with mainly organic acids obtained at 240 ºC (Saito et al. 2009). Findings of Saito and

coworkers are in good agreement with study of Oomari and coworkers and reaction paths (Figure 3.5) (Oomori et al. 2004).

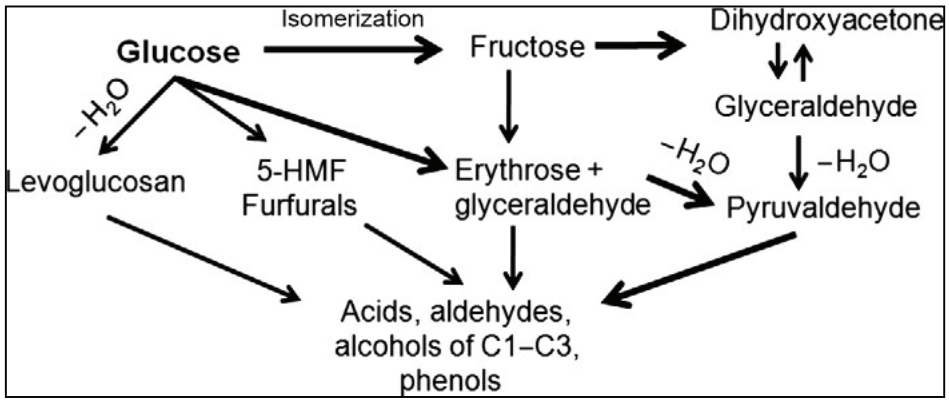

Figure 3.5. Reaction paths for the decomposition of glucose under hydrothermal conditions (Source: Brunner 2009)

Lui reported that fructose, 5-HMF, and levoglucosan are formed as a result of glucose hydrolysis in subcritical region. Figure 3.6 indicates formation of main products with respect to residence time of reactant in tubular reactor. Fructose is formed firstly due to its low temperature stability. As the residence time increases yield of 5-HMF increases, hence, fructose and levoglucosan is converted to the 5-HMF (Liu 2000).

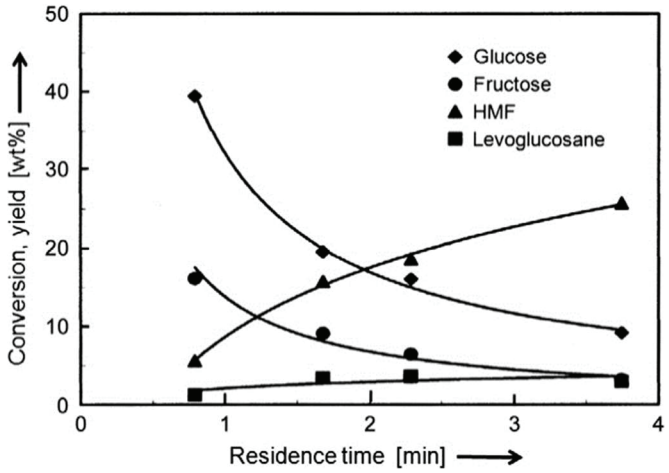

Figure 3.6. Conversion of glucose in subcritical water region, T=250 ºC, P=24 MPa (Source: Liu 2000)

Klinger and coworkers reported that the conversion of glucose in high temperature water already begins at temperature below T=160 ºC. At a temperature of T=200 ºC about

20% and T=240 ºC about 50% of glucose is converted as shown in Figure 3.7 (Klingler and Vogel 2010). As the temperature increases over T=300 ºC, glucose conversion rate increases. Conversion becomes so fast that approximately 90% of glucose is converted in one second at T=350 ºC (Kabyemela et al. 1999).

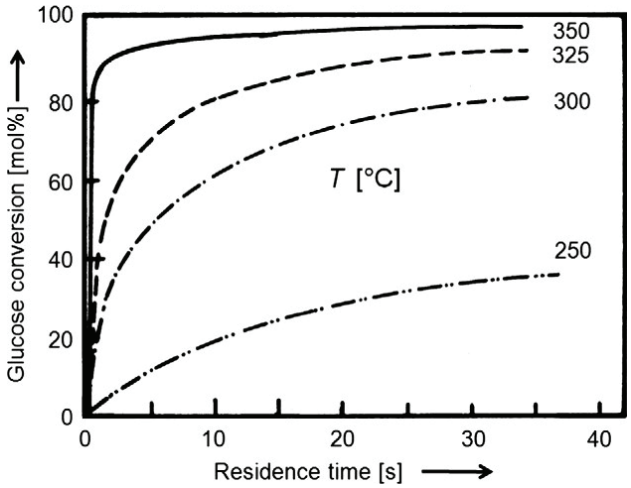

Figure 3.7. Temperature dependence of glucose conversion in subcritical water at temperature of T=250-350 ºC, P=24 MPa (Source:Klingler and Vogel 2010)

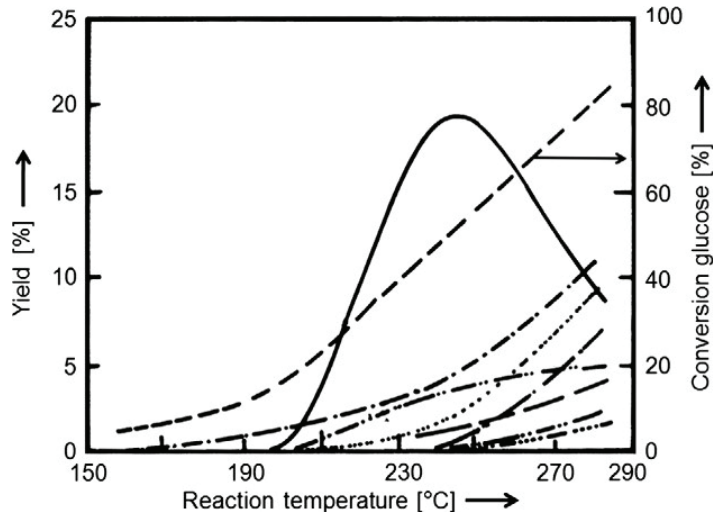

Figure 3.8. Conversion of glucose with subcritical water in dependence on temperature. Residence time t=60 s, P=10-25 MPa. Conversion: ---------, glucose; Yield: fructose;-.-.-.-. - 5-HMF; -..-,1,6 anhydroglucose; …. formic acid (Source: Naguchi et al. 2006)

Decomposition products were mainly obtained via keto-enol tautomerism to fructose, via dehydration to 1,6-anhydro-b-D-glucose and 5-HMF, and organic acids

(lactic acid, formic acid, acetic acid, and glycolic acid) which further decomposed to aldehydes via retro-aldol condensation (Figure 3.8) (Kabyemela et al. 1999). Higher weight of molecular products (e.g., fructose) are decomposed to smaller molecules with increasing residence time and temperature. Product distribution for temperatures from T=250 to 420 ºC is shown in Figure 3.8. At T=300 ºC, the main products are glycolaldehyde and 5-HMF (Figure 3.9-left). With increasing residence time, more 5-HMF is formed, whereas fructose, mannose, 1,6-anhydroglucose, and pyruvaldehyde yields decrease (Klingler and Vogel 2010).

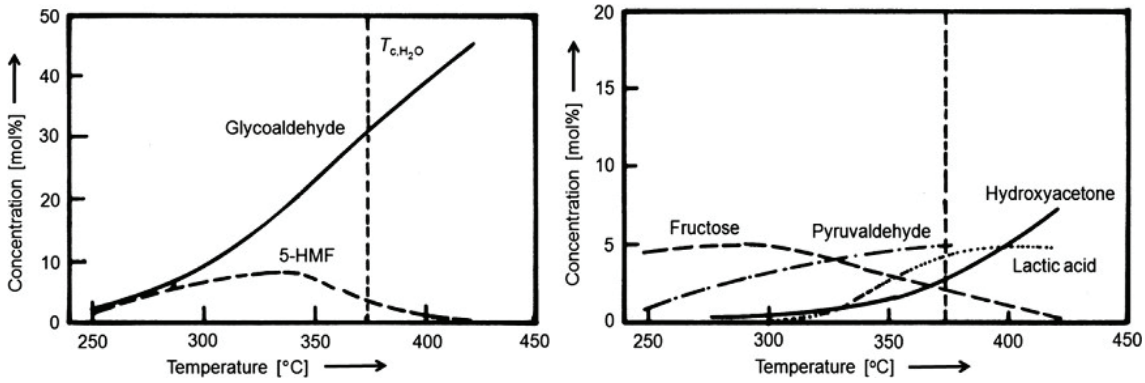

Figure 3.9. Conversion of glucose and its products in high temperature and supercritical water region (Source: Klingler and Vogel 2010).

Many studies reported that cellulose decomposition reaction rate can be controlled via manipulating the temperature and pressure in near- and supercritical water region without using catalyst (Sasaki, Adschiri, and Arai 2004). Kinetics of cellulose decomposition in water is generally modeled as fist order reaction with a following equation;

$$k_T = k_0 exp\left(-\frac{E_{a,C}}{RT}\right) \tag{3.1}$$

Generally, consistent values for the activation energy between temperatures of T=200-350 ºC are reported. Schwald and coworkers reported an activation energy of cotton cellulose degradation as E_a=129.1 kJ mol^{-1} (Schwald and Bobleter 1989). On the other hand, Adschiri and coworkers reported higher activation energy E_a=165 kJ mol^{-1} for unspecified origin of cellulose (Adschiri et al. 1993). Moreover, Rogalinski and coworkers reported that activation energy for microcrystalline cellulose is

E_a=154.4 kJ mol^{-1} (Rogalinski et al. 2008). Adschiri and coworkers also reported that activation energy of cellulose decomposition at higher temperature T=350-370 ^oC changes drastically, it is value reported as 548 kJ mol^{-1}.

Sasaki and coworkers reported that hydrolysis of cellulose particle mainly took place at their external or inner surface in subcritical region (Sasaki, Adschiri, and Arai 2004). They proposed a mathematical modeling that is help to quantify reaction rate constant with respect to temperature. A shrinking-core model is a useful mathematical expression for the reaction that takes place in surface of a particle with changing volume. Hence, following equation is used regarding the cellulose degradation;

$$\frac{dV(X)}{dt} = -k_s.S(X) \tag{3.2}$$

Where k_s (cm.s^{-1}) is the surface reaction rate constant, and S (cm^2) and V (cm^3) are the surface area and the volume of the particle respectively. A cellulose particle composed of a large number of microfibrils, and that the microfibril comprises a number of crystallites, which are combined in series, it is supposed that a cylindrical- shaped grain is more suitable than the sphere-shaped grain for microcrystalline cellulose. Therefore, the model with cylindrical grain was employed. In this model, a solid particle is assumed composed of cylindrical grains of radius [rg (μm)] (Sasaki, Adschiri, and Arai 2004). Hence, there is no change in density of the particle; conversion can be expressed in terms of volume of particle;

$$X = 1 - \left(\frac{V(X)}{V(0)}\right) \tag{3.3}$$

$$\frac{dX}{dt} = 2 * \frac{k_s}{r_{g0}}(1-X)^{\frac{1}{2}} \tag{3.4}$$

By integrating this equation an expression in terms of space-time is derived;

$$k = \frac{k_s}{r_{g0}} = \frac{1-(1-X)^{1/2}}{\tau} \tag{3.5}$$

where k (s^{-1}) is the overall conversion rate constant of microcrystalline cellulose. Reaction rate constant can be found by plotting conversion versus residence time. Sasaki and coworkers were reported the reaction rate kinetics of cellulose decomposition in Figure 3.10. The slope of the lines gives the reaction rate constant that corresponds for reaction temperature.

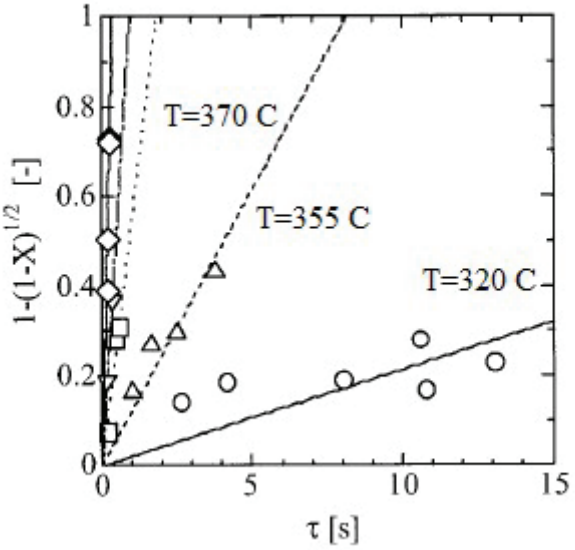

Figure 3.10. Relationship between the $1-(1-X)^{1/2}$ and the residence time (τ) in subcritical and supercritical region (Source: Sasaki, Adschiri, and Arai 2004)

Arrhenius plots of the *k* values in other words defining the activation energy of cellulose decomposition to observe the effect of temperature on cellulose conversion plays an important role in defining the reaction mechanism. Sasaki and coworkers reported that the microcrystalline cellulose conversion in subcritical and supercritical water consisted of two Arrhenius-type reactions with a crosspoint of about 370°C (Figure 3.11). Below 370°C, the reaction was heterogeneous surface hydrolysis of cellulose without its swelling microcrystalline cellulose, and the apparent activation energy, Ea=145.9 ±4.6 kJ mol^{-1} and the preexponential factor $A=10^{11.9\pm0.4}$ is reported. On the other hands, above 370°C the conversion rate of microcrystalline cellulose became much faster than that below 370°C, and the kinetic parameters were found to be Ea =547.9 ±27.8 kJ mol^{-1} and $A=10^{44.6\pm2.2}$, respectively (Sasaki, Adschiri, and Arai 2004).

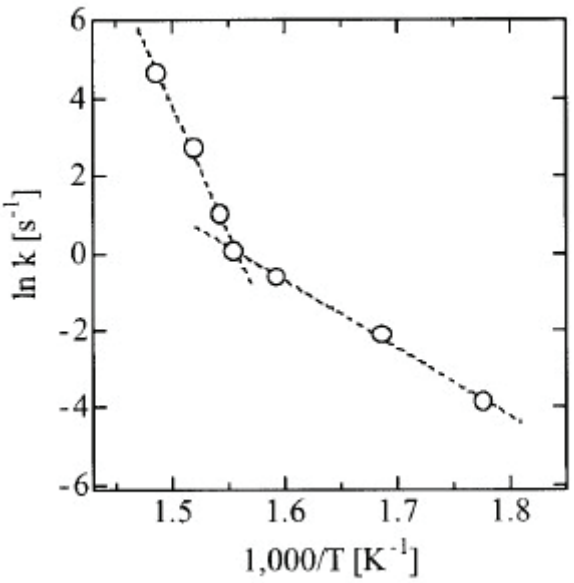

Figure 3.11. Arrhenius plot of the rate constant of conversion of microcrystalline cellulose (k) in subcritical and supercritical water region at 25 MPa based on the shrinking core model (Source: Sasaki, Adschiri, and Arai 2004)

The sharp change in the conversion of microcrystalline cellulose is based on the contribution of swelling or dissolution and pyrolytic depolymerization of microcrystalline cellulose. Sasaki and coworkers stated that decomposition mechanism may shifted from an ionic reaction mechanism to a radical one by decreasing density water density by increasing the temperature. However, there has been no any study reported that clearly suggest reaction mechanism so far.

Decomposition products of cellulose are mainly; glucose, the monomeric building block, fructose, which is formed from glucose by isomerization, pyruvalaldehyde, levoglucosan and HMF, and acids. Figure 3.12 indicates the yield of glucose and HMF as a result of decomposition of cellulose at different temperature and constant pressure of 25 MPa. For temperatures between T=270 and 310 ºC, the maximum of glucose concentration is shifted to lower residence times. At T=310 ºC, also for HMF, a maximum occurs, indicating that this product is itself further converted.

Table 3.1 indicates the formation and decomposition kinetics of products of cellulose decomposition. Reaction kinetics is assumed to first order rate law for formation and decomposition (Brunner 2009).

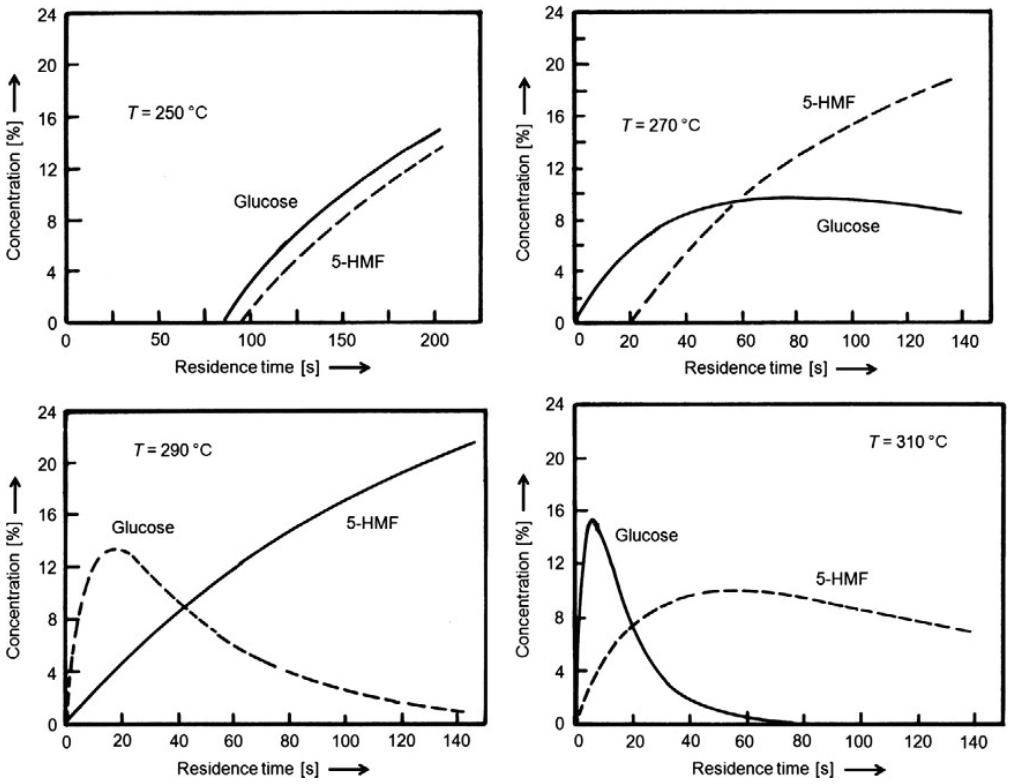

Figure 3.12. Yield of glucose and 5-HMF of cellulose decomposition in hot compressed water at different temperature and P=25 MPa (Source: Brunner 2009)

Table 3.1. Rate constant of formation (k_f) and decomposition (k_d) for main degradation products (Source: Brunner 2009)

T (°C)	Glucose		HMF		Pyruvaldehyde	
	$k_f(s^{-1})$	$k_d(s^{-1})$	$k_f(s^{-1})$	$k_d(s^{-1})$	$k_f(s^{-1})$	$k_d(s^{-1})$
250	0.002	0.006	0.0018	0.005	0.001	0.007
270	0.004	0.03	0.003	0.008	0.0017	0.01
290	0.024	0.12	0.00025	0.005	0.0036	0.013
310	0.075	0.31	0.006	0.043	0.015	0.045

CHAPTER 4

APPLICATION OF ELECTROCHEMISTRY

In this chapter, fundamentals and application of electrochemistry is discussed. In order to initialize a chemical reaction, the required minimum energy of the reaction, in other words activation energy must be supplied into the reaction medium. Catalyst have been used for the purpose to reduce the activation energy but there has been limitation in some areas in usage of catalysts. In these cases, electrochemical reactions become more attractive due to the attractive advantages such as low operating cost, high selectivity to product of interest, etc. There has been numerous study has been reported regarding to synthesis of organic chemicals via electrochemical reactions (Wu et al. 2017, Sasaki et al. 2010, Pospisil et al. 1995). Especially, studies regarding to degradation of organic compounds in waste water streams via electrolysis has promising reported results (Rajkumar and Palanivelu 2004, Radha, Sridevi, and Kalaivani 2009). Electrochemical decomposition of organic compounds in hot-compressed water has been also reported. For instance, Sasaki and coworkers investigated the degradation of 1-butanol and glucose to carboxylic acids by electrolysis in hydrothermal conditions (Sasaki et al. 2010, Sasaki et al. 2011). Moreover, Zhang and coworkers studied electrochemical degradation of lignin (Zhang et al. 2014), Xu and coworkers studied electrolysis of corn strove to sugars (Xu et al. 2014). In electrochemical reactions, the electrode potential is adjusted to manipulate the electrochemical reaction rates. Thus, electrode potentials (redox potential) has major effect on electrochemical reactions.

4.1. Activation Energy and Overpotential

The behavior of an electron in electrode can be predicted by considering the Fermi-Level (E_F) (Waldvogel 2015). The Fermi level is associated with the energy of the highest occupied orbitals (HOMO) and lowest occupied orbitals (LUMO) (Figure 4.1). In order to transfer an electron, the energy barrier (activation energy), must be overcome by the reacting species. In order to produce a current, the potential difference must be above the equilibrium value.

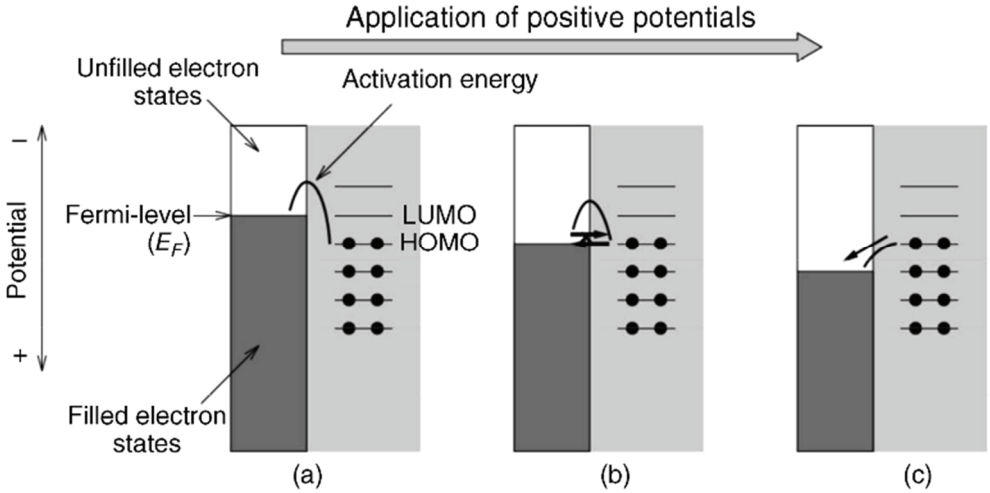

Figure 4.1. The Fermi-Level of orbital energies as HOMO and LUMO in solution and electron transfer from electrode to substrate (a), counter electron transfer (b) and substrate to electrode (c) (Soruce: Waldvogel 2015)

Even though the electrode potential plays important role in electrochemical reactions, mass transfer is also crucial that can affect the reaction rate. In electrochemical reactions, mass transfer limitation can take place either by electron transfer or diffusion of an activated species to the electrode surface depending on the electrode potential. An example of a scanning voltammogram is given in Figure 4.2. In voltammogram, electrode potential scanned with a constant rate and the change in the current is measure simultaneously. The first region of voltammogram up to an electrode voltage value there is not flow of current across electrodes. This is due to the lower potential than the standard potential. However, at higher potential, electron transfer rate increases dramatically in which electrochemical reaction is limited both mass transport and electron transfer. At higher potential, electron transfer reaches it maximum value resulted in constant current due to the mass transport limitation. In quite solution, current decreases with increasing electrode potential. This is due to the concentration polarization at interface (Figure 4.3) resulted in the depletion of substrate in the vicinity of electrode which is resulted in a decline in current value.

The empirical equation (Eqn. 4.1) is derived by Buttler and Volmer that conducts the change of current density (i) on an electrode with the overpotential (η) assuming that both a cathodic and an anodic reaction occurs at the same electrode.

$$i = i_a - i_c = i_0 \left[\exp\left(\frac{\alpha n F}{RT}\right) - exp\{-(1-\alpha) n F \dot{\eta}/RT\} \right] \quad (4.1)$$

In where i_a and i_c are the anodic and cathodic current respectively. i_0 and α is the exchange current density and the charge transfer density, respectively. Number of electrons is represented as (n). F and ή is the Faraday constant and overpotential, respectively.

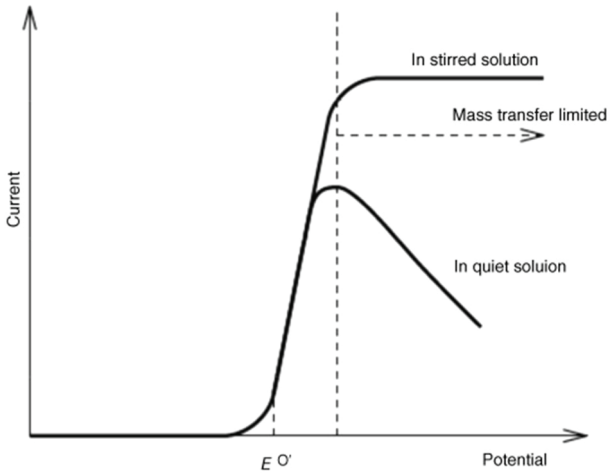

Figure 4.2. Scanning voltammogram of a solution in stirred and quite medium (Source: Waldvogel 2015)

When the limiting step of electrochemical reaction is the mass transfer of substrate to anodic surface a diffusion layer is formed and the thickness of this layer changes over time. In this case, limiting current density (i_d) is described related to diffusion layer thickness (δ) and diffusion coefficient of substrate (D), electrolyte concentration (c).

$$i_d = nFDc/\delta \quad (4.2)$$

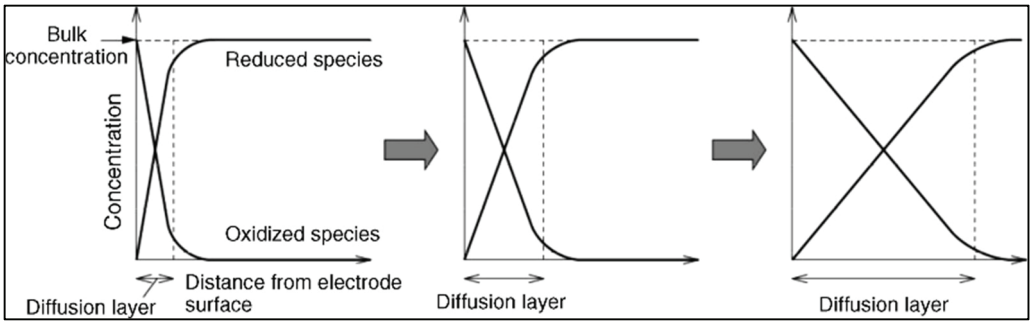

Figure 4.3. Concentration polarization at the interphase of anode in quite solution (Source: Waldvogel 2015)

CHAPTER 5

HYPOTHESIS OF THE STUDY

Sub- and supercritical water as reaction medium have attracted attention due to its versatile properties such as ionic product concentration (10^{-11}, 200-300 °C range) and dielectric constant (ε≈10 near critical) (Marshall and Franck 1981a). Self-dissociation products of water as hydroxide (OH^-) and hydronium ion (H_3O^+) play crucial role in the protonation of β(1-4),glycosidic bond of cellulose that resulted in formation of decomposition products. In order to depolymerize microcrystalline cellulose, hydronium ion must access to intra- and inter-molecular hydrogen bonds. Thus, diffusion of protons with versatile properties (low density, high diffusivity) of near critical water becomes more effective. High ionic product concentration also yields to low energy for the migration of electroactive species in electrochemical methods. Therefore, electrochemical reactions at near critical conditions become more economically feasible (Asghari and Yoshida 2008).

The hypothesis of this is that application of direct current into reaction medium under hydrothermal condition would create activated species in terms of ionic and radical molecules due the redox reactions of water and sulfuric acid (Fig.5.1). Formation of these molecules can alter the decomposition of cellulose as in the postulated reaction mechanism Figure 5.2. Formation of radicals regarding to redox reactions of sulfuric and water is reported in literature. Davis and coworkers studied the formation of persulfate via electrolysis of sulfuric acid solution based on radical mechanism (Davis, Baygents, and Farrell 2014). They reported that different radical species ($SO_4^{-\bullet}, HSO_4^{\bullet}, OH^{\bullet}$) and ionic products ($SO_4^{2-}, H_3O^+, OH^-$) can be formed during electrolysis of sulfuric acid solution at different electrode potentials.

Application of direct current under hydrothermal condition is resulted in the reactions at positive anode (Eqn. 5.1 and Eqn. 5.2) and at negative cathode (Eqn. 5.3 and Eqn. 5.4). Eqn. 5.2 yield the formation of H^+ ion which can generate an acid layer around anode that can yield the protonation of β(1-4),Glycosidic bond of cellulose.

$$4OH^-_{(aq)} - 4e^- \rightarrow 2H_2O_{(l)} + O_{2(g)} \quad (5.1)$$

$$2H_2O_{(l)} - 4e^- \rightarrow 4H^+{}_{(aq)} + O_{2(g)} \quad (5.2)$$

$$4H^+_{(aq)} + 4e^- \rightarrow 2H_{2(g)} \quad (5.3)$$

$$4H_3O^+_{(aq)} + 4e^- \rightarrow 2H_{2(g)} + 4H_2O_{(l)} \quad (5.4)$$

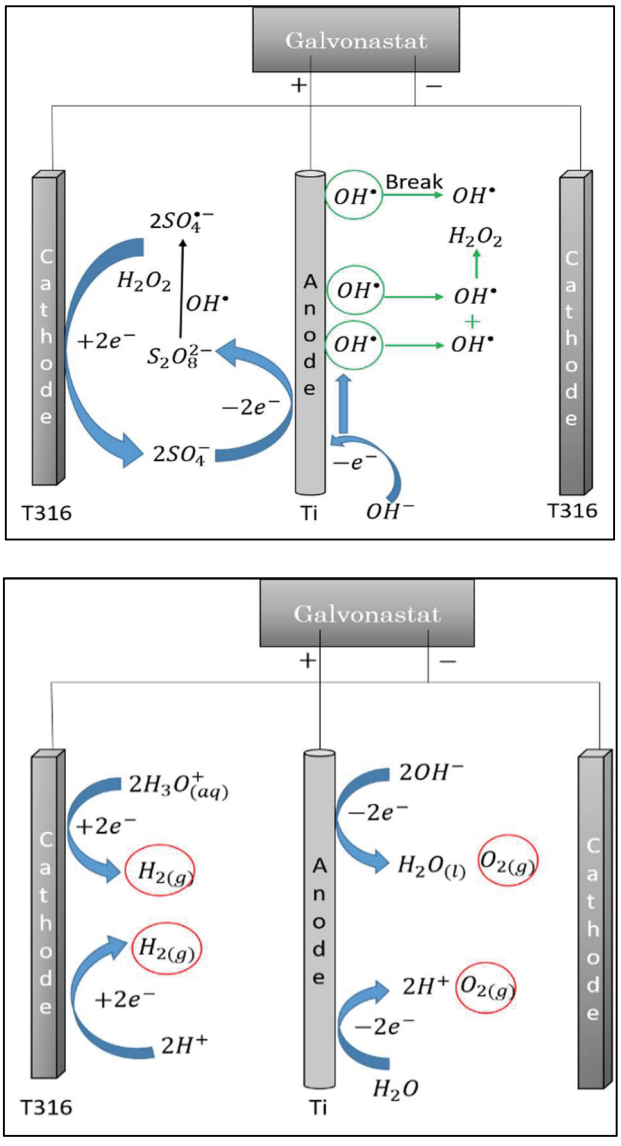

Figure 5.1. Electrochemical reaction of water and sulfuric acid that yields a) radical, b) ionic products

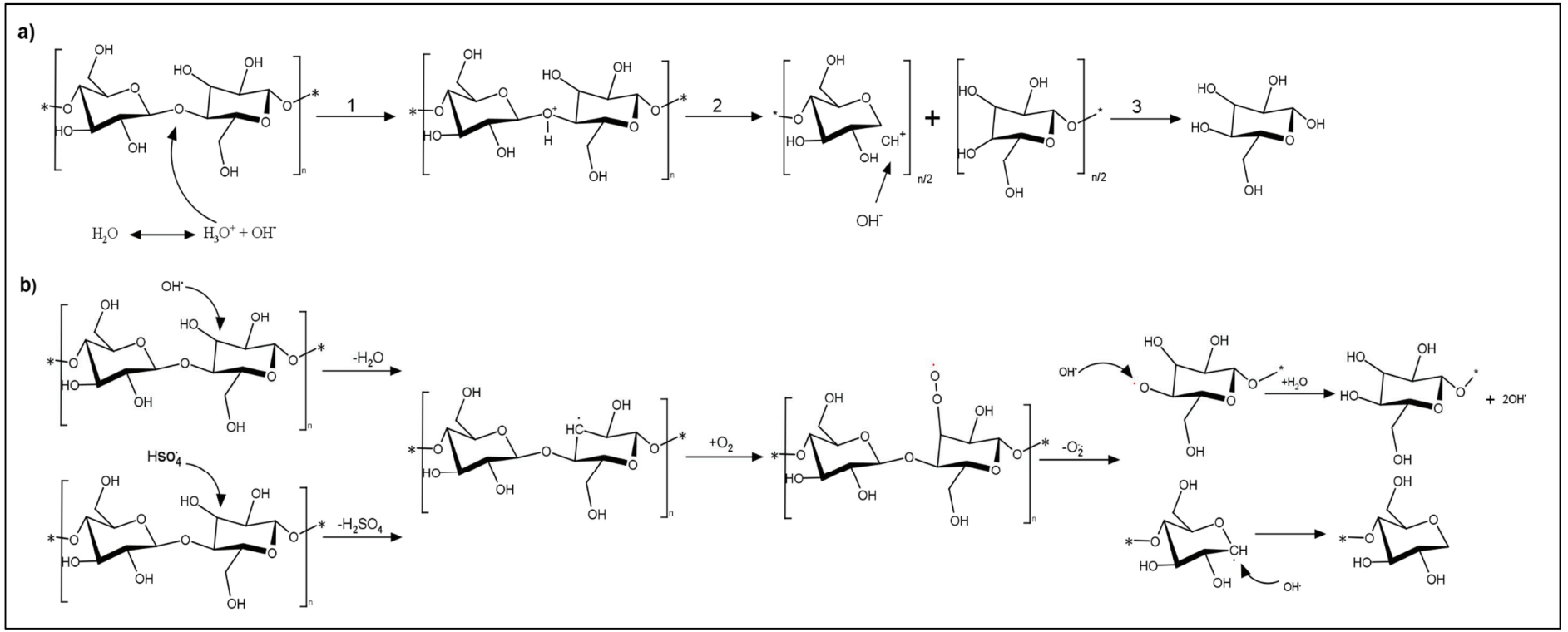

Figure 5.2. Postulated reaction mechanism of decomposition of cellulose based on a) ionic b) radical products of hydrothermal electrolysis

CHAPTER 6

EXPERIMENTAL STUDY

6.1. Materials

Microcrystalline cellulose (MCC, Sigma Aldrich 31.069-7, <20 μm) was used as the model compound of biomass. Sulfuric Acid (Merck, 96-98% purity, CAS-NO 84721) was used as electrolyte and external proton source. Standard chemicals that are used for the calibration of analytical methods such as High Performance Liquid Chromatography (HPLC) and Gas Chromatography-Mass Spectroscopy (GC-MS) are listed in Table 6.1. Ultra-pure water was used as reaction medium with the accepted electrical conductivity range of 0.4-1 μs.

Table 6.1. Standard chemicals used for the calibration of analytical methods.

#	Chemical Name	Cas Number	Brand
1	Pyruvic Acid	107360-25G	Aldrich
2	Glucose	1.00063.2500	Merck
3	Fructose	F0127-1006	Sigma Aldrich
4	DL-Glyceroladhyde	141339.1212	Pancreac
5	Glycolic acid	124737-256	Sigma Aldrich
6	Glycoaldehyde	G6805-1G	Aldrich
7	Lactic Acid	141034.1211	Panreac
8	Glycerol	141339.1212	Pancreac
9	Formic Acid	1.00264.2500	Merck
10	Acetic Acid	1.00063.2500	Merck
11	Levulinic Acid	L2009-50G	Aldrich
12	Hydroxymethylfurfural	W501808-25G-K	SAFC
13	Furfural	8.04012.0500	Merck

6.2. Experimental Procedure

Hydrothermal electrolysis experiments were carried out in a 450 mL of batch reactor (Parr 5500 series) made of T316, which is illustrated in Figure 6.1. Hydrothermal electrolysis experiments were carried out at a constant current (0-2 A) passing through the electrodes. Specially designed cylindrical type electrode (12 mm diameter, 94 mm length), made of titanium, was used as anode and cylindrical reactor wall (165 mm in length, 76 mm outer diameter) was acted as cathode

All experiments were conducted in 200 ml of ultra-pure water containing 8 gr of microcrystalline cellulose. Sulfuric acid was added to the reaction medium as external proton source at different concentrations (0-50 mM). Reaction medium was purged by nitrogen gas at 20 bar of pressure to remove the dissolved oxygen within the water, for 10 minutes.

In electrochemical experiments, specially designed cylindrical type anode (12 mm diameter, 94 mm length) made of Titanium (Figure 6.1-b) and reactor wall, as cathode, separated by teflon part. The conductivity between anode and direct current (DC) power supply was controlled via electrical conductivity meter.

Reaction medium was heated to desired temperature with an external electrical heater (1) and reaction time was set as zero when the desired reaction temperature is reached. In order to observe the effect of heating period, first sample was taken at the time of desired temperature is reached and labeled as 0 minute. 2 ml of samples were collected (10) from the cooling unit (4) at predetermined reaction time intervals. The liquid products were filtered from 0.2 μu PTFE filters to the vials for further analysis. DC supply (GW Instekt) (2) was used in two different operations as constant current and constant voltage modes. The change in the voltage (V) or current (A) values was monitored during the reaction and recorded accordingly. The reaction was stopped by powering off the DC supply and cooling the reaction medium via cooling jacked. The gas products were collected to polypropylene (PP) bags when the medium temperature cooled down to (8) 50 ℃. Liquid product and solid residue were separated by using filter paper. Then, separated solid residue rinsed with ultra-pure water and dried in vacuum oven at 60 ℃ for three days.

Anode material was cleaned after each experiment. The cleaning procedure begins with removal of tarry material by using sponge and aluminum oxide powder. Then, anode

mechanically polished by using sandpaper (grade 900) and rinsed with ultra-pure water. Iso-propyl alcohol was used for further removal of particles from anode surface by using sonication bath. The same procedure applied to the reactor wall for complete removal of tarry material.

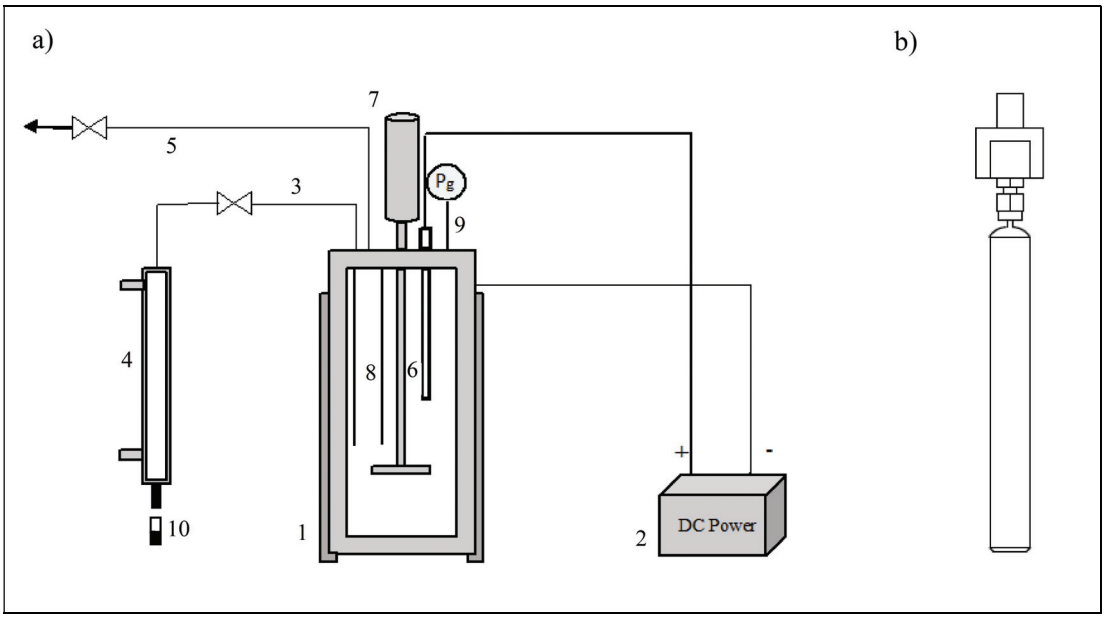

Figure 6.1. Schematic representation of a) experimental set-up and b) cylindrical anode material

6.3. Liquid Product Analysis

Liquid products collected during the reactions were analyzed by means of analytical methods as High Performance Liquid Chromatography (HPLC) and Gas Chromatography-Mass Spectroscopy (GC-MS). Total organic carbon (TOC) of liquid samples were measured in order to define the conversion of microcrystalline cellulose.

6.3.1. High Performance Liquid Chromatography (HPLC)

Liquid degradation products of microcrystalline cellulose was analyzed by means of HPLC (Agilent 1200 and 1100). Sugar column (Shodex SH1100) was used for the separation of degradation products. As eluent, Sulfuric acid (3.75 mM) with flow rate of 0.5 ml/min and 50 °C of column temperature found as the optimized operating conditions

for clear separation of main degradation products. The optimization of operating parameter of HPLC was carried on at different flow rate (0.4-0.6 ml/min) and column temperature (40-60 ℃). The operating conditions, which clear separation of standard chemicals was obtained, was selected as the optimized conditions to operate HPLC. Refractive index detector (RID) were used for the detection of separated chemicals. Optical unit temperature was set as 40 ℃ for all measurements. Figure 6.2 indicates the chromatogram of standard chemicals used for the determination of degradation products. Code numbers of standard chemicals are listed in Table 6.1.

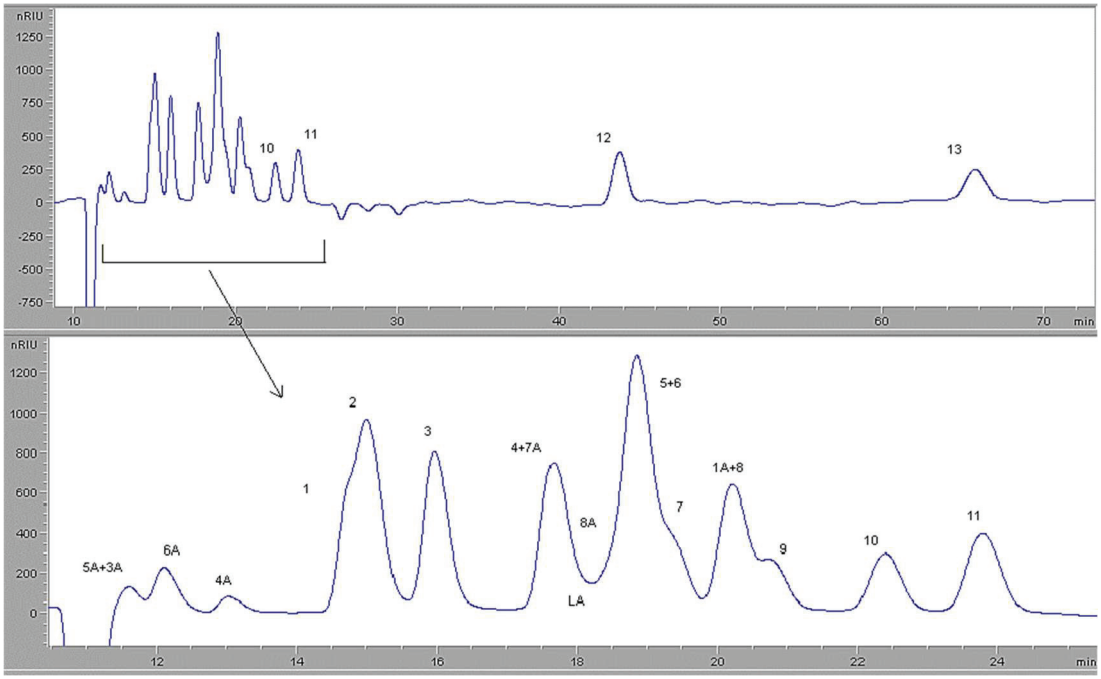

Figure 6.2. Chromatogram of mixture of standard chemicals (100ppm)

Calibration curves of standard chemicals were conducted in concentration interval of 10-5000 ppm with nine-point measurement. There are two ranges of calibration for Glucose (Figure 6.3) since, calibration curves deviates from linearity at lower concentrations. Therefore, some of the standard chemicals were calibrated in two regions for better quantification. Calibration curves and governing equations are given in Appendix A.

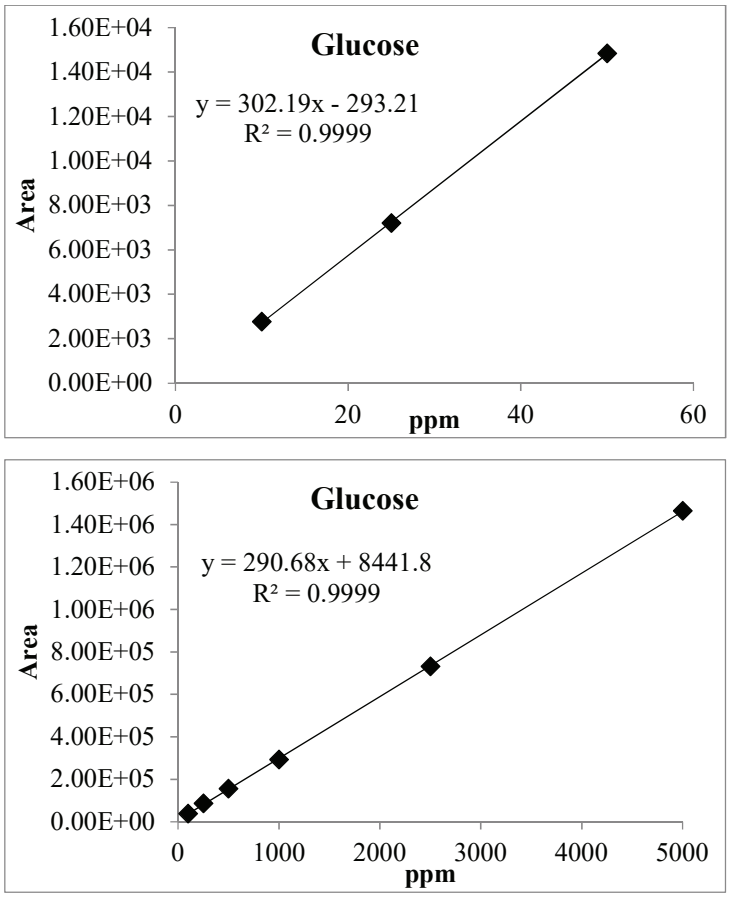

Figure 6.3. Calibration curves for Glucose at a) 10-60 ppm and b) 60-5000 ppm

6.3.2. Gas Chromatography-Mass Spectroscopy (GC-MS)

GC-MS (Agilent 6890 N/5973 N Network) was used for the analysis of liquid products that cannot be identified by HPLC analysis. Stabilwax®-DA (Crossbond® Carbowax® polyethylene glycol, 30-meter-long, 0.32 mm inner diameter, 1 µm particle size) column was used. GC-MS analysis were conducted in two different modes as SCAN and Selected Ion Methodology (SIM). SIM method was used for the detection and quantification of standard chemicals within the liquid products. SCAN mode was used to identify the intermediate products of cellulose degradation. GC analysis was conducted with the following method; initial oven temperature set as 40 °C and then, first heating (8 °C/min) to 140 °C kept for 5 minutes, second heating (10 °C/min) to 220 °C and kept for 10 minutes. Total run time of method is 37.50 minutes. GC-MS chromatograms were analyzed by using MSD ChemStation E.0202.1431 software. Analyzed chromatograms are identified by using National Institute of Standard (NIST), MS search and compounds are tabulated in Table 6.2.

Table 6.2. List of cellulose degradation compounds detected by GC-MS analysis

Compound Name	Retention Time	Characteristic Ions
2-Butanone	4.323	43,72,29,27,57,15,28,42,44,39
Furan,2-methyl	10.813	82,53,81,39,27,54,51,50,28,52
2-Butanone, 3-hydroxy-	12.217	45,43,88,27,29,42,55,46,44,73
2-Propanone,1-hydroxy-	12.561	43,31,74,15,29,42,45,44,27,28
2-Cyclopenten-1-one	13.646	82,39,54,53,28,27,55,26,81,51
2(3H)-Furanone,5-methyl	14.8656	55,98,43,27,70,39,26,42,15,99
Acetic acid	15.061	43,4560,15,42,29,14,28,41,18
Furfural	15.449	96,95,39,38,29,37,97,40,67,42
Ethanone,1-(2-furanyl)-	16.353	95,110,39,43,38,15,96,67,68,40
Propanoic Acid	16.68	74,28,45,29,73,27,57,55,26,56
Formic acid	16.838	29,46,45,28,17,44,16,12,13,30
2-Furancarboxaldehyde,5-methyl	18.16	110,109,53,27,39,51,81,43,50,
2-Butanone,4-hydroxy	19.917	43,70,31,55,61,27,15,42,45,73
2-Furanmethanol	20.401	98,41,8197,39,53,42,69,70,27
2(5H)-Furanone,5-methyl	21.442	55,98,43,83,27,54,26,69,39,29
Hexanoic acid	21.599	60,73,41,43,87,27,61,45,55,29
1,4-Pentanediol	22.573	45,42,71,41,43,31,27,44,56,58
2-Cyclopenten-1-one,2-hydroxy-3-methyl	24.092	112,69,55,41,43,83,56,84,27,39
Heptanoic Acid	24.197	60,73,43,41,87,55,29,27,71,70
2-Pentenoic Acid	24.232	55,29,27,39,100,45,41,54,56,43
2-Butenoic acid, 2-methyl	24.719	100,55,29,85,27,39,54,82,53,41
5-Hexyl-2-furaldehyde	24.834	109,81,110,53,180,123,95,97,96
2-5Furandicarboxaldehyde	26.354	124,123,95,67,125,53,50,42,51
Levoglucosenone	26.519	98,96,39,53,68,97,42,41,70,29
Formic Acid,2-propenyl ester	28.129	57,39,41,29,58,31,40,27,30,28
Propanoic acid, anhydride	29.052	57,29,27,28,26,58,56,43,74,45
5-Acetoxymethyl-2-furaldehyde	29.127	126,43,79,109,53,97,127,81,52
Isopropyl Palmitate	29.183	43,102,60,57,256,41,61,55,71
Pentanoic acid, 4-oxo-	31.096	43,56,45,55,73,29,27,15,28,42
1,4:3,6-Dianhydro-à-d-glucopyranose	31.413	69,29,57,41,70,98,31,43,85,86
Furancarboxaldehyde,5-(hydroxymethyl)-	33.122	97,126,41,39,69,29,53,125,109

6.3.3. Total Organic Carbon (TOC)

Total Organic Carbon (TOC) of liquid phase were measured by Shimadzu TOC-VCPH Analyzer with Total Nitrogen Measuring Unit (TNM-1). The calibration range of organic content is 5-100 ppm of carbon. Analysis were conducted by diluting the samples in order to obtain measurements within the calibration range. Each measurement requires approximately 50 ml of samples after dilution. TOC analysis were conducted for the all samples taken during the reaction time. Samples were diluted with range of 50-250 times for TOC analysis. Results obtained from TOC analysis conducted with the carbon balance, product yield and selectivity of degradation compounds.

6.4. Analysis of Solid Residue

Structural and chemical analysis of solid residue of degradation of cellulose were conducted by X-Ray diffraction and Fourier Transform Infrared Spectroscopy (FTIR), respectively. Morphological property of solid residue was also analyzed by scanning electron microscopy (SEM).

6.4.1. Fourier Transform Infrared Spectroscopy (FTIR)

The change in the chemical bonds of cellulose or solid residue was analyzed via FTIR. FTIR analyses were conducted with scan rate of 2 cm^{-1} from 600 cm^{-1} to 4000 cm^{-1} wavenumber by Perkin Elmer Frontier-Spectra two. Attenuated total reflectance method was used for the analysis of each sample.

6.4.2. X-Ray Diffraction

The structure of microcrystalline cellulose and solid residue after hydrothermal electrolysis reaction were characterized using Philips X'Pert Pro MRD (Cu Kα radiation λ=1.54nm, 40 kV, 40 mA) between scanning range of 5^o and 90^o.

6.4.3. Scanning Electron Microscopy

Morphological properties of solid residues and microcrystalline cellulose were analyzed by Scanning Electron Microscopy (SEM), (Quanta 250 SEM) with ETD detector. Due to the charging problem of solid particles, SEM images were analyzed via drift mode.

CHAPTER 7

CONSTANT DIRECT CURRENT ELECTROLYSIS OF MICROCRYSTALLINE CELLULOSE IN HOT COMPRESSED WATER

In this chapter, constant direct current electrolysis of microcrystalline cellulose (MCC) in hot-compressed water conditions was investigated. In order to investigate the both individual and coupled effect of operating parameters, ½ fractional factorial design with 2-level of four factors; reaction time, temperature, H_2SO_4 concentration and applied direct current with 3 center points and 2 replicates were built and Analysis of Variance (ANOVA) test was applied to the responses. Responses such as yield of cellulose degradation products (Levulinic acid, 5-HMF, Furfural), cellulose conversion and total organic carbon in liquid (TOC) was analyzed and surface counter plots were obtained by using response surface methodology (RSM).

7.1. Experimental Procedure and Methods

Hydrothermal electrolysis experiments were carried out in a 450 mL of batch reactor (Parr 5500 series) made of T316. All experiments were conducted in 200 ml of deionized water containing 8 gr of MCC. As an electrolyte and proton source, sulfuric acid was added at different concentrations (1-50 mM).

Reaction medium was heated to desired temperature with an external electrical heater and the reaction time was set as zero when the desired reaction temperature is reached. In order to observe the effect of heating period, first sample was taken at the time of desired temperature is reached. 2 ml of samples were collected at reaction times of 0, 15, 30, 60, 90, and 120 minutes.

Hydrothermal electrolysis experiments were carried out at a constant current (0-2 A) passing through the electrodes. Cylindrical type electrode made of titanium, was used as anode and cylindrical reactor wall as cathode.

7.1.1. Factorial Design of Constant Current Experiments

Experimental design is a statistical way for better understanding of multivariable systems that have interactions between parameters affecting the response of a system. As the model equation ((7.1) is fitted to the data, both coupled and individual effects on responses are analyzed accordingly.

In this study, effect of parameters as reaction Current (A), Temperature (B), Time (C) and H_2SO_4 concentration (D) on responses such as conversion of cellulose, conversion of TOC, yields of 5-HMF, levulinic acid and furfural were statistically analyzed by using surface response methodology (RSM) to optimize desired responses. Experimental design was built by ½ fractional factorials design with two level (Table 7.1) of four factors (A, B, C, and D) with three center points and two replicates for corner points. A total number of 19 experimental runs were built and given in Table 7.2.

The second order regression model based on second order Taylor approximation (Eqn. 7.1) was used to optimize the responses (Yield of products, TOC and cellulose conversions). ANOVA test was applied to each response with an alpha value of 0.05. The significance of operating parameters on responses and interaction of parameters were analyzed statistically by the (Eqn. 7.2)

$$Y_i = \beta_0 + \beta_1 x_{i1} + \beta_2 x_{i2} + \cdots + \beta_k x_{ik} + \beta_{11} x_{i1}^2 + \beta_{22} x_{i2}^2 + \cdots + \beta_{kk} x_{ik}^2 + \beta_{12} x_{i1} x_{i2} + \beta_{13} x_{i1} x_{i3} + \cdots + \beta_{k-1,k} x_{i,k-1} x_{ik} + \epsilon_i \quad (7.1)$$

$$Yield = \beta_0 + \beta_1 A + \beta_2 B + \beta_3 C + \beta_4 D + \beta_{11} A^2 + \beta_{22} B^2 + \beta_{33} C^2 + \beta_{44} D^2 + \beta_{12} AB + \beta_{23} BC + \beta_{34} CD + \beta_{13} AC + \beta_{24} BD + \epsilon \quad (7.2)$$

Table 7.1. Boundary conditions for factorial design of experiments

Values	Temperature °C	Reaction time (min)	H_2SO_4 (mM)	Direct current (DC)
High	230	30	1	0
Low	170	120	50	2

7.2. Liquid Products of Microcrystalline Cellulose Decomposition by Applied Constant Current in Hot-Compressed Water

High performance liquid chromatography (HPLC) and Gas chromatography mass spectroscopy were used to determine and quantified liquid products of cellulose decomposition under hydrothermal electrolysis conditions. Selected ion methodology (SIM) was used for the quantification of major products of glucose, fructose, levulinic acid, 5-HMF and furfural. Yield of product was calculated based on the carbon amount of species produced and initial amount of carbon in cellulose (**(7.3**Eqn. 7.3). Carbon amount of cellulose was found as 42-45% by TOC analysis. For all experiments, carbon balance was calculated as above 90%. Conversion of cellulose and TOC yield were calculated by using Eqn. 7.4 and Eqn. 7.5, respectively.

$$\text{Yield of Product } i \ \% = \frac{(\text{Number of carbon of species } i) * (\text{Mole of species } i \text{ produced})}{\text{Moles of carbon in cellulose}} * 100 \quad (7.3)$$

$$\text{Converted Cellulose \%} = \frac{\text{Initial amount of cellulose (gram)-Residual amount at the end (gram)}}{\text{Initial amount of cellulose (gram)}} * 100 \quad (7.4)$$

$$\text{TOC Yield \%} = \frac{\text{Total Organic Carbon (TOC)}}{\text{Moles of carbon in cellulose}} * 100 \quad (7.5)$$

A standard HPLC chromatogram of degradation products of microcrystalline cellulose under hydrothermal conditions are given in Figure 7.1. Sample calculation for HPLC analysis results are given in APPENDIX C. The change in the intensity with sampling time of 0, 60 and 120 minutes are investigated for all experiments that built by fractional factorial design. In order to observe the reaction time effect on cellulose conversion which was calculated by measuring the mass of residue at the end of reaction, the attributed reaction time was considered for yield data used as response in ANOVA analysis. Calculated values of cellulose conversion, yield of TOC and degradation products are given in Table 7.2.

Table 7.2 Fractional factorial design and responses as cellulose conversion, total organic content and yield of liquid products

Design	Temperature (°C)	Time (min)	H_2SO_4 (mM)	Current (A)	Cellulose conversion	TOC %	Glucose %	Fructose %	5-HMF %	Furfural %	Levulinic Acid %
----	170	30	1	0	11.38	29.00	0.36	0.48	0.04	0.07	0.04
+--+	230	30	1	2	81.25	60.71	12.20	7.94	7.00	1.51	3.00
-+-+	170	120	1	2	11.25	8.10	1.71	1.94	0.18	0.16	0.68
++--	230	120	1	0	70.63	40.48	8.47	*	5.29	2.55	11.50
--++	170	30	50	2	29.00	22.00	4.17	3.21	0.74	0.35	1.57
+-+-	230	30	50	0	77.13	61.50	4.64	1.74	3.57	2.20	36.00
-++-	170	120	50	0	48.75	29.07	6.36	0.95	3.57	0.92	7.20
++++	230	120	50	2	74.38	39.38	0.60	0.24	0.27	0.48	28.98
---+	170	30	1	0	11.38	28.81	0.20	0.28	0.03	0.07	0.04
+--+	230	30	1	2	78.75	61.20	11.93	6.03	7.44	1.48	3.20
0+-+	170	120	1	2	7.50	8.21	1.58	1.90	0.17	0.13	0.50
++--	230	120	1	0	68.75	41.00	9.00	*	5.50	2.45	12.00
--++	170	30	50	2	30.75	22.35	4.20	3.69	0.96	0.48	1.40
+-+-	230	30	50	0	82.63	62.02	4.63	2.85	2.82	2.43	37.00
-++-	170	120	50	0	46.88	28.48	6.60	1.90	3.63	0.83	7.10
++++	230	120	50	2	77.00	39.52	0.44	0.26	0.35	0.47	29.90
0000	200	75	25.5	1	81.13	62.62	15.41	7.79	3.71	1.05	12.44
0000	200	75	25.5	1	81.38	62.20	15.70	7.20	3.50	1.04	*
0000	200	75	25.5	1	80.00	62.00	15.20	7.50	4.00	0.92	11.91

* Data does not exist

(+) High, (0) Middle, (-) Low values of design variables

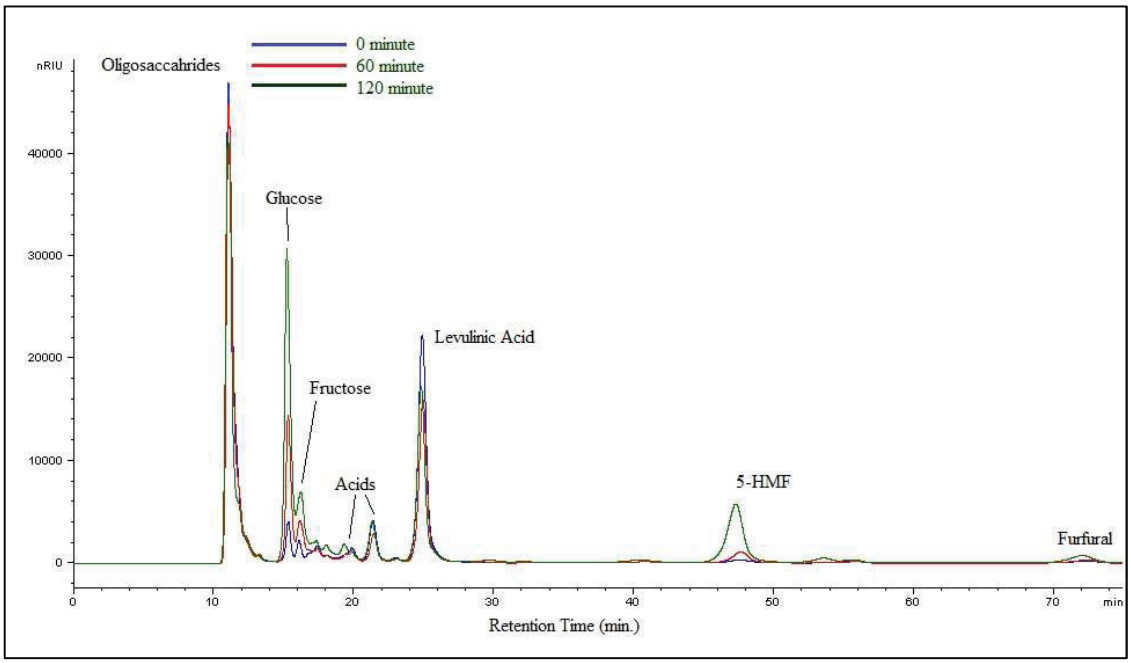

Figure 7.1. HPLC of cellulose decomposition products at sampling time of 0, 60 and 120 minutes of reaction under hydrothermal electrolysis conditions.

7.2.1. Analysis of Variance (ANOVA) of Cellulose Conversion and Total Organic Carbon (TOC)

In order to investigate the both individual and coupled effect of operating parameters on cellulose conversion, ANOVA test was applied to given data with the confidence interval of 95% (α=0.05). The summary of ANOVA analysis for cellulose conversion is given in Table 7.3. Individual parameters as applied current, sulfuric acid concentration, reaction time and temperature and interaction of these parameters with current were investigated via F-value and P-value of statistical results. As the model equation (Eqn.7.1) is fitted to the experimental data and the proposed model equation (Eqn. 7.6) is obtained. The R^2 with a value of 0.99 indicates that model is well fit to the observed response. The model accuracy is also confirmed by histograms including normal probability and residual plots (Figure 7.2). T-tests of operating parameters (direct current, temperature, H_2SO_4, time) defined the coefficient of main effects and their second orders with interaction terms in the model given as Eqn. 7.6. Cellulose conversion value can be predicted by using proposed model equation in the range of boundary conditions.

$$Converted\ Cellulose = -9.721 + 4.152\,A + 0.06025\,B + 0.01167\,C + 0.03806\,D - 2.4298\,A^2 + 0.00869\,A*B - 0.011347\,A*C - 0.01242\,A*D \quad (7.6)$$

Some of the interaction terms were removed due to the lack of fit ($p>0.05$) indicating that there is no significant interaction between these parameters. However, their effect on responses was considered as disturbance in the system causing error in the measure responses. The total error of measurements are given in Table 7.3. As an individual parameter, reaction time has the p-value of 0.708, which is higher than the confidence interval indicating that time has no significant effect on the conversion of cellulose. However, interaction parameter (current*time) showed that coupled effect of current and time was significant and thus, model did not avoid time as insignificant parameter. The importance of reaction time is due to the formation of degradation products effect the reaction conditions such as pH value of medium. Therefore, coupled effect of reaction time and current become significant due to the increased H^+ concentration.

Table 7.3. ANOVA analysis results for cellulose conversion with 95% of confidence interval

Source	DF	Sum of Squares	Mean of Squares	F Value	P-Value
Model	8.00	96.71	12.09	542.06	0.000
Linear	4.00	75.06	18.76	841.37	0.000
Current	1.00	0.31	0.31	13.69	0.004
Temperature	1.00	68.43	68.43	3068.57	0.000
Time	1.00	0.00	0.00	0.15	0.708
H_2SO_4	1.00	6.31	6.31	283.06	0.000
Square	1.00	14.92	14.92	668.79	0.000
Current*Current	1.00	14.92	14.92	668.79	0.000
2-Way Interaction	3.00	6.74	2.25	100.75	0.000
Current*Temperature	1.00	1.09	1.09	48.73	0.000
Current*Time	1.00	4.17	4.17	187.06	0.000
Current*H_2SO_4	1.00	1.48	1.48	66.47	0.000
Error	10.00	0.22	0.02		
Total	18.00	96.93			

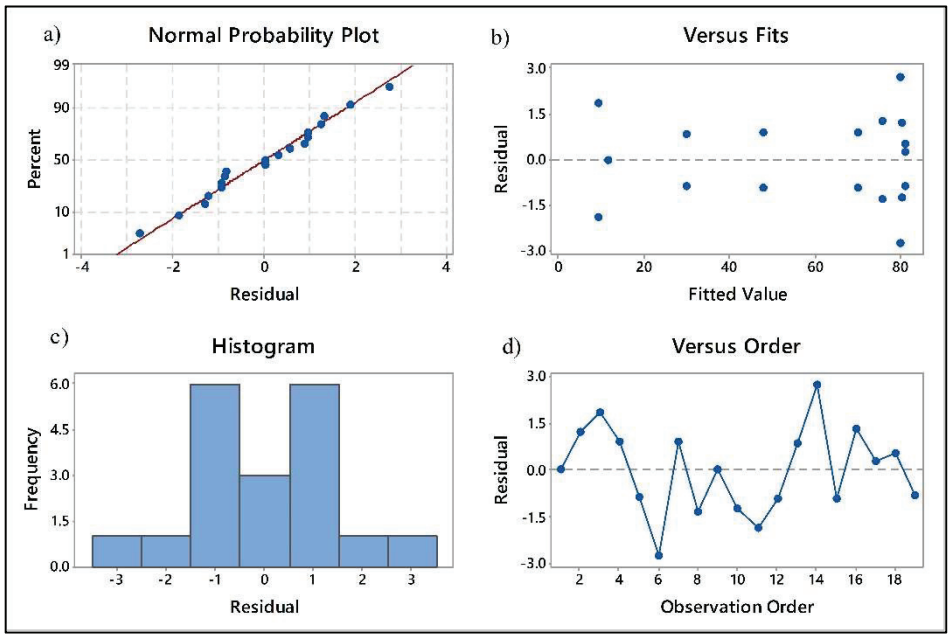

Figure 7.2. Histogram plots of converted cellulose, a) normal probability plot of residuals b) residuals versus predicted values, c) frequency histogram of residuals, d) observation orders of residuals

Normal probability and histogram plots indicates the distribution of residuals based on the measurement of cellulose conversion values. Based on the residual distribution (Figure 7.2-a), ANOVA test is applicable to the experimental data. In order to the check the applicability of ANOVA test to responses, histogram plots for all responses were separately investigated. ANOVA test of TOC yield ($p>0.05$) is given in Table 7.4. The parameters such as reaction temperature, direct current, reaction time and sulfuric acid concentration has significant effect on the formation of organic carbon in liquid phase. The most significant term was temperature followed by reaction time and current applied. Quadratic model equation is fitted to the experimental data with the R^2 value of 0.99 and is evaluated as model equation (Eqn. 7.7).

$$\text{TOC Conversion} = -31.280 + 33.774\,A + 0.37351\,B - 0.11753\,C + 0.21319\,D - 25.908\,A*A + 0.10524\,A*B - 0.03992\,A*C - 0.14478\,A*D \quad (7.7)$$

Table 7.4. ANOVA analysis results for TOC yield with 95% of confidence interval

Source	DF	Sum of Squares	Mean of Squares	F Value	P-Value
Model	8	6473.57	809.20	9355.12	0.000
Linear	4	4365.38	1091.34	12617.03	0.000
Current (A)	1	216.67	216.67	2504	0.000
Temperature (B)	1	3300.57	3300.57	38157	0.000
Time (C)	1	803.18	803.18	9285.60	0.000
H_2SO_4 (D)	1	44.95	44.95	519.71	0.000
Square	1	1695.76	1695.76	19604.71	0.000
Current*Current	1	1695.76	1695.76	19604.71	0.000
2-Way Interaction	3	412.43	137.48	1589.38	0.000
Current*Temperature	1	159.50	159.50	1843.93	0.000
Current*Time	1	51.63	51.63	596.95	0.000
Current*H_2SO_4	1	201.30	201.30	2327.25	0.000
Error	10	0.86	0.09		
Total	18	6474.43			

The residual plots of model for TOC yield (Figure B.1-a, Appendix B) shows that residuals are normally distributed, indicating that model is applicable.

Response surface plots (RSPs) (Figure 7.3) of cellulose conversion was plotted by the hold value of 25mM H_2SO_4 at different reaction temperatures of 170 ºC, 200 ºC and 230 ºC. As it is seen from RSPs, temperature has the highest impact on cellulose degradation for, as the temperature increases, ionic product concentration reaches its maximum value up to 220 ºC in sub-critical water region (Dinjus and Kruse 2004). In order to depolymerize MCC, hydronium ions (H_3O^+) must access to inter- or intra-molecular hydrogen bonding. Thus, diffusion of protons (H^+) plays a crucial role together with versatile properties (low density, high diffusivity) of water in sub-critical region. Therefore, the trend in cellulose conversion and TOC yield are mostly related to the ionic product concentration of reacting medium. The change in the ionic product concentration due to applied direct current cannot be measured in-situ. Thus, effect of applied current is discussed considering mainly trend of TOC yield and cellulose conversion values.

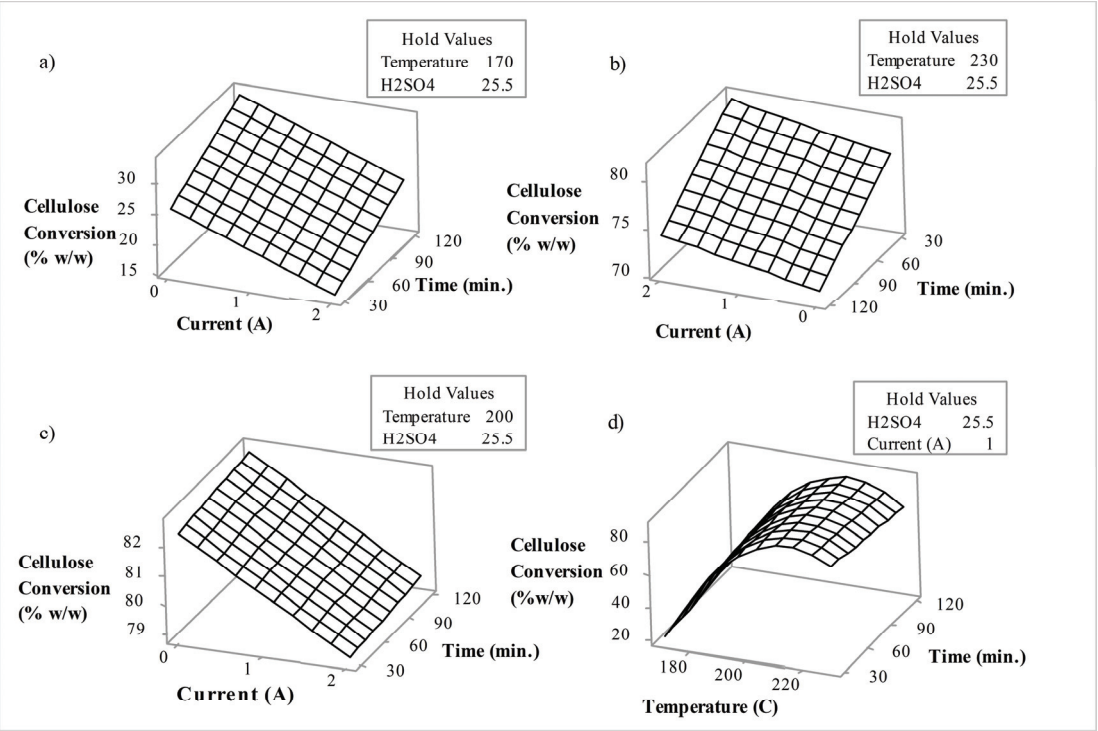

Figure 7.3. Surface response plot of cellulose conversion holding values of 25 mM at a) 170℃ b) 230 ℃ c) 200 ℃ and d) 1 A of direct current

Figure 7.3-a indicates the effect of current on cellulose conversion at 170 ℃ and 25.5 mM of sulfuric acid concentration. Application of current has diverse effect on cellulose conversion (Figure 7.3-a) which can be attributed to decrease in the ion product concentration due to the reduction and oxidation reactions of hydrogen ion (H^+) and hydroxyl ion (OH^-) forming hydrogen and oxygen gases, respectively. Thus, protonation of β(1-4),glycosidic bond is hindered due to lower concentration of hydrogen ion under applied direct current. However, increase in the reaction temperature to 200 ℃ (Figure 7.3-c) decreased the diverse effect of applied direct current in cellulose conversion. Moreover, applied direct current has positive effect on cellulose conversion when the reaction temperature is 230 ℃ (Figure 7.3-b).Thus coupled effect of reaction temperature and direct current is considered as an interacting parameter. Increase in the reaction temperature resulted in higher diffusivity concentration of ions that penetrate into microcrystalline structure, hence higher cellulose conversion was obtained (Figure 7.3-d). However, further increment in reaction temperature (230 ℃) resulted in the lower cellulose conversion at higher reaction time (Figure 7.3-b). For instance, cellulose conversion decreases from 80% to 70% when the reaction time increased to 30 minutes to 120 minutes. Decrease in the cellulose conversion is due to the formation of

tarry products from decomposition product of cellulose which is supported by the TOC yield (Figure 7.4-d). Decrease in the TOC yield (Figure 7.4-d) supports the formation of tarry products. For instance, 5-HMF polymerize and forms tarry materials under hydrothermal conditions (Chuntanapum and Matsumura 2009). Therefore, cellulose conversion decreases due to the weight based calculations. Application of direct current at 230 ℃ of reaction temperature has positive effect on cellulose conversion independent of reaction time. Therefore, based on the surface response plot of TOC yield (Figure 7.4-c), application of direct current hinders the formation of char and yields higher TOC yield. However, TOC yield reaches its maximum value at 1 A of current (60%). Applied 2 A of direct current resulted in lower TOC yield (Figure 7.4-a) even though the cellulose conversion is similar to that of 1 A of applied current. Therefore, application of 2 A of current resulted in the formation of gaseous products due to the further degradation of aldehydes, ketones and carboxylic acids.

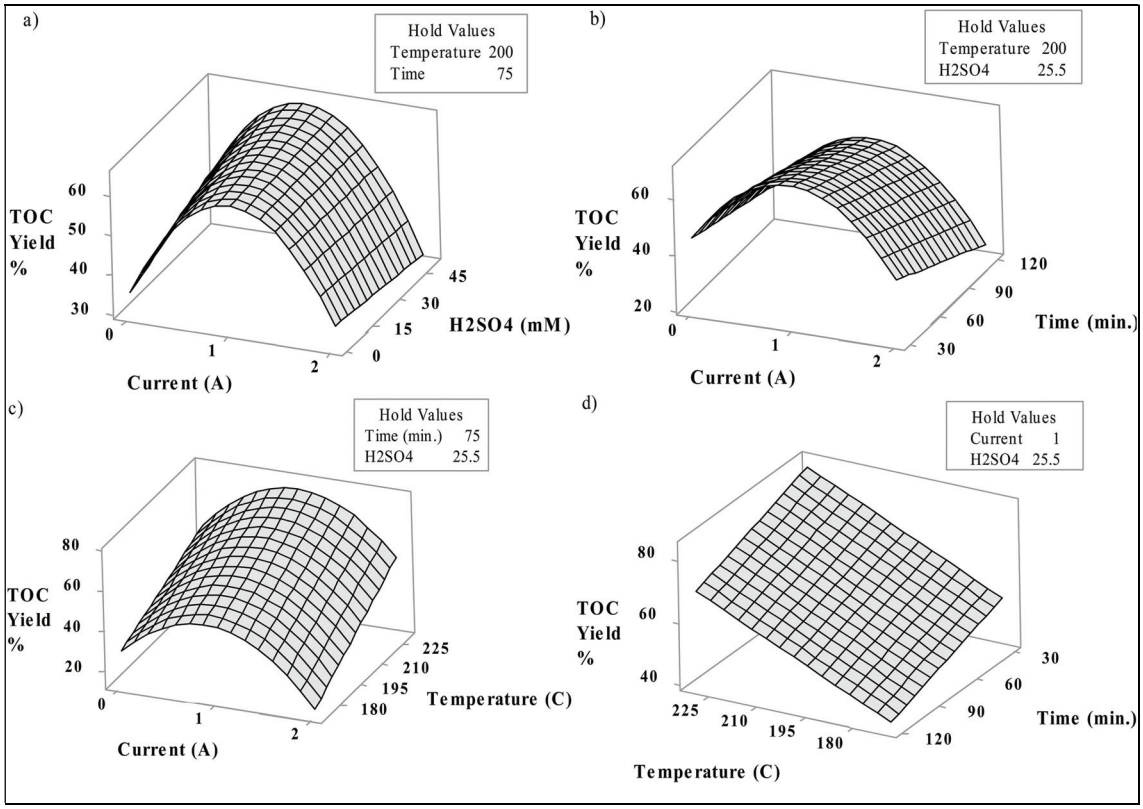

Figure 7.4. Response surface plot of TOC yield a) current vs H_2SO_4, b) current vs time, c) current vs temperature, d) temperature vs time

Application of direct current might have increased the H^+ concentration around positive anode that resulted in an acid layer formation (Yu, Baizer, and Nobe 1988). Formation of an acid layer around anode can increase the decomposition of cellulose to soluble products (Oligosaccharides, Glucose, Fructose, Furfural, 5-HMF and Levulinic acid). For instance, TOC yield increased from about 30 % to 60% when 1 A of direct current applied at the same conditions (Figure 7.4-a). However, further increment in current resulted in sharp decrease of TOC conversion. Similar trend was also observed for all reaction temperatures (Figure 7.4-c). The current effect on TOC conversion at low acid concentration (1mM H_2SO_4) support the idea of electrochemically generated acid layer around anode material due to dissociation of water molecules that resulting in the protonation of β(1-4) Glycosidic bonds. Moreover, applied current diminished the needed acid concentration from 50 mM to 1 mM to obtain the same TOC yield (Table 7.2)

Water as a reaction medium exhibits narrow potential window for electrochemical reactions. In other words, application of high potential to the reaction medium resulted in the formation of hydrogen and oxygen gases and hence, higher concentration of activated species as ionic (H^+, OH^-) and radical species ($SO_4^{-\bullet}, HSO_4^{\bullet}, OH^{\bullet}$) in the presence of sulfuric acid (Davis, Baygents, and Farrell 2014). Formation of highly active species resulted in the further degradation of liquid products to gaseous products (CO_2, H_2). Thus, applied 2 A of current resulted in lower TOC yield by keeping cellulose conversion similar to that of current free experiments. GC-TCD analysis of gaseous products supports the results obtained from cellulose conversation and TOC yield.

7.2.2. Analysis of Variance (ANOVA) of Glucose, Fructose, 5-HMF and Furfural

Protonation of β(1-4),glycosidic bonds of cellulose yields to formation of oligosaccharides such as cellotriose, cellopentose. Further decomposition resulted in the formation of glucose molecules, building block of cellulose. ANOVA test to glucose yield ($p>0.005$) showed that all parameters has significant effect as individually. However, interaction term of current with reaction temperature has the p value of 0.713 which is higher than confidence interval. Therefore, coupled effect of current and temperature is removed from the model and its effect is considered as disturbance in responses

(Table 7.5). Hence, model equation is given (Eqn. 7.8 **(7.8)**) by neglecting the interaction of temperature and applied current.

$$\text{Glucose Yield \%} = -10.822 + 27.427\,A + 0.05508\,B + 0.05722\,C + 0.02143\,D - 10.619\,A*A + 0.00060\,A*B - 0.06774\,A*C - 0.05666\,A*D \quad (7.8)$$

Table 7.5. ANOVA analysis results for Glucose yield with 95% of confidence interval

Source	DF	Sum of Squares	Mean of Squares	F Value	P-Value
Model	7.00	525.23	75.65	1792.29	0.000
Linear	4.00	60.89	15.23	415.57	0.000
Current (A)	1.00	0.74	0.74	20.07	0.001
Temperature (B)	1.00	44.66	44.66	1219.05	0.000
Time (C)	1.00	3.58	3.58	97.77	0.000
H_2SO_4 (D)	1.00	11.92	11.92	325.39	0.000
Square	1.00	284.85	284.85	7776.08	0.000
Current*Current	1.00	284.85	284.85	7776.08	0.000
2-Way Interaction	2.00	179.49	89.74	2656.76	0.000
Temperature*H_2SO_4	1.00	148.66	148.66	4400.83	0.000
Current*H_2SO_4	1.00	30.83	30.83	912.70	0.000
Error	11.00	0.37	0.04		
Total	18.00	525.60			

As a result of ANOVA test, the most significant effect on glucose yield is found as temperature and its interaction by sulfuric acid (Table 7.5). Interaction of temperature and sulfuric acid has major effect on glucose yield since, protonation of intra- and inter molecular cellulose bonds resulted in the formation of glucose. In order to visualize, response surface plots of glucose yield (Figure 7.5) is conducted within interactions of operating parameters. The effect of direct current (Figure 7.5-a-b-d) on glucose yields resembles as in the TOC yield. Application of 1 A of direct current at reaction temperature 170 °C increased glucose yield (3.2%) in comparison to current free (glucose yield 13%) reaction conditions. Electrochemically generated activated species as radicals and ionic compounds could have increased the rate of cellulose decomposition. However, 2 A of

current loaded experiments for longer reaction times (75 and 120 min.) resulted in lower glucose yield. This could be due to further reactions of glucose such as isomerization to fructose, retro-aldol condensation to eryhtrose, glycoaldehyde, and glyceraldehyde (Yin and Tan 2012).

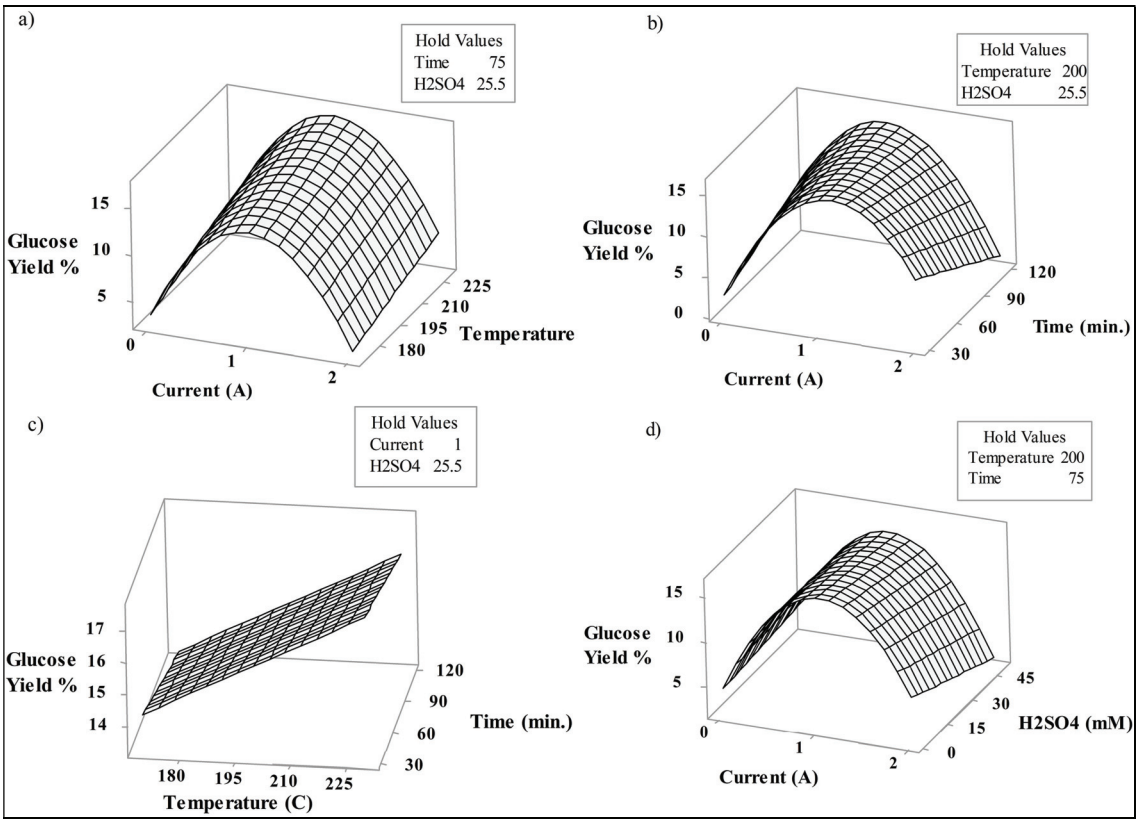

Figure 7.5. Response surface plot of Glucose yield a) current vs temperature, b) current vs time, c) temperature vs time d) current vs H_2SO_4

Isomerization of glucose yields to fructose. In isomerization reaction mechanism, both hydroxyl (OH^-) and hydrogen ion (H^+) concentration plays an important role (Cantero, Bermejo, and Cocero 2015). Thus, ionic product concentration has similar effect on fructose as in the case of both TOC and glucose yield observations. Table 7.6 indicates the ANOVA test summary and it is seen that current ($p=0.982$) and reaction time ($p=0.579$) are insignificant as an individual. However, coupled effect of current and reaction time has p value near to zero indicating that coupled effect is significant. However, interaction of current and sulfuric acid concentration has no significant effect ($p>0.05$) and thus removed from the model equation (Eqn. 7.9).

Table 7.6. ANOVA results for converted Fructose with 95% of confidence level

Source	DF	Sum of Squares	Mean of Squares	F Value	P-Value
Model	7	128.56	18.37	51.63	0.000
Linear	4	36.26	9.07	25.48	0.000
Current (A)	1	0.00	0.00	0.00	0.982
Temperature (B)	1	14.85	14.85	41.75	0.000
Time (C)	1	0.12	0.12	0.33	0.579
H_2SO_4 (D)	1	13.55	13.55	38.08	0.000
Square	1	41.10	41.10	115.55	0.000
Current*Current	1	41.10	41.10	115.55	0.000
2-Way Interaction	2	30.33	15.16	42.62	0.000
Current*Temperature	1	6.43	6.43	18.06	0.002
Current*Time	1	30.26	30.26	85.08	0.000
Error	9	3.20	0.36		
Total	16	131.76			

$$Fructose\ Yield\ \% = -13.58 + 17.89\,A + 0.0753\,B + 0.04053\,C - 0.05311\,D - 4.340\,A*A - 0.02987\,A*B - 0.04322\,A*C \quad (7.9)$$

Response surface plots of fructose yield and interaction of operating parameters are shown in Figure 7.6. Interactions of direct current with temperature (Figure 7.6-a) and reaction time (Figure 7.6-b) has major effect on fructose yield. Fructose yield reaches its highest yield of 7.5% at applied 1 A of direct current and 230 ℃ of reaction temperature. As the sulfuric acid concentration increases (Figure 7.6-d) the fructose yield decreases due the further reactions of fructose that yields in products such as furans and carboxylic acids (Promdej and Matsumura 2011).

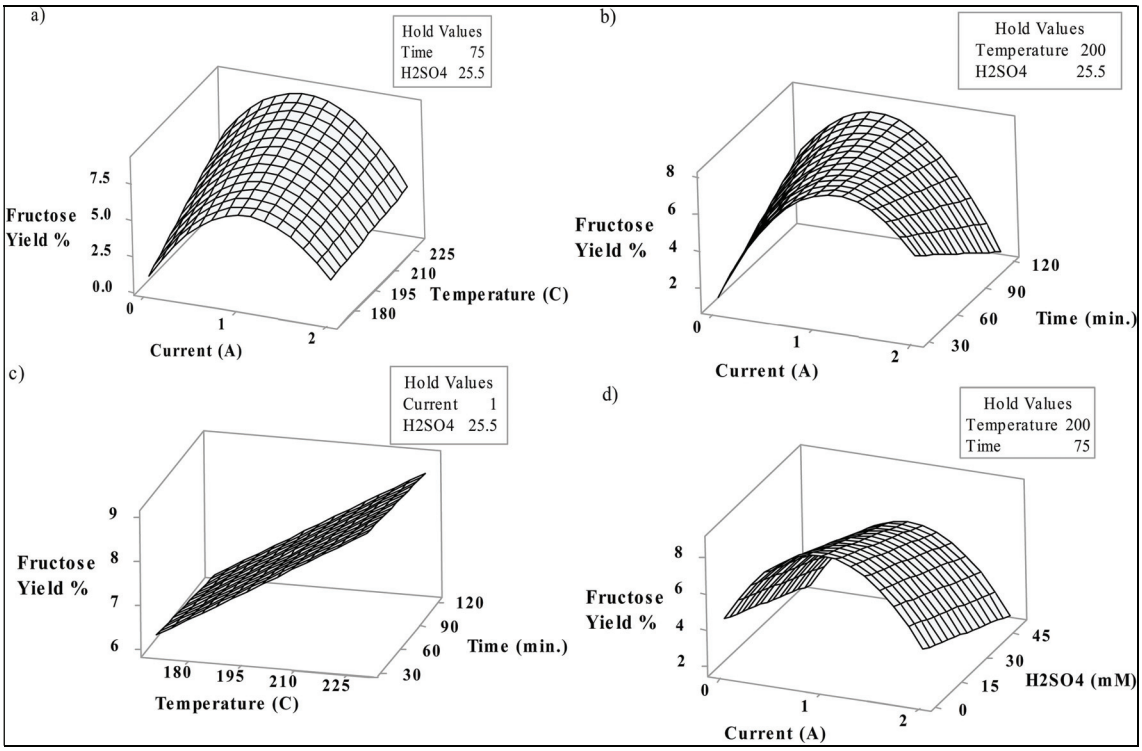

Figure 7.6. Response surface plots of Fructose yield a) current vs temperature, b) current vs time, c) temperature vs time d) current vs H_2SO_4

Dehydration of fructose yields to 5-HMF (Antal, Mok, and Richards 1990), further rehydration of 5-HMF resulted in the formation of levulinic acid and formic acid. Furfural is also formed by abstraction of formaldehyde from 5-HMF. Thus, statistical analysis is conducted and following model equations Eqn. 7.10, Eqn. 7.11 and Eqn. 7.12 are obtained to calculate the yields of 5-HMF, furfural and levulinic acid respectively.

$$5-\text{HMF Yield\%} = -7.959 + 4.298\,A + 0.04129\,B + 0.03203\,C + 0.01393\,D - 1.139\,A*A + 0.00646\,A*B - 0.03708\,A*C - 0.03878\,A*D \quad (7.10)$$

$$\text{Furfural Yield\%} = -5.584 + 2.234\,A + 0.032250\,B + 0.005500\,C + 0.00633\,D + 0.0329\,A*A - 0.010250\,A*B - 0.006333\,A*C - 0.006990\,A*D \quad (7.11)$$

$$\text{Levulinic Acid Yield\%} = -55.513 - 0.312\,A + 0.34217\,B - 0.09800\,C + 0.32510\,D - 0.918\,A*A - 0.04415\,A*B + 0.11968\,A*C - 0.02360\,A*D \quad (7.12)$$

Table 7.7. indicates the significant parameters that effect the formation of 5-HMF, furfural, and levulinic acid. F-value represents a quantitative that shows the degree of influence on responses as product yields. Thus, temperature has the highest F-value and it is the most significant effecting individual parameter for the production of 5-HMF, levulinic acid and furfural. The effect of sulfuric acid concentration is in the second place after the reaction temperature for the yields of 5-HMF and levulinic acid, except furfural. Sulfuric acid as Brϕnsted acid is found and reported widely for the hydrolysis of cellulose and dehydration of fructose to 5-HMF (Li et al. 2014, Jeong et al. 2010). Reaction time has least significant effect (F=14.91) in formation of 5-HMF and levulinic acid. However, coupled effect of direct current and time (F=802.31) demonstrates significant effect on 5-HMF production. Moreover, in comparison to individual effects of current and time, there is a dramatic increase in F-values for both 5-HMF and levulinic acid. In contrast, current demonstrates the significant individual effect on furfural yield after reaction temperature. In order for better observation of interactions, response surface plots of 5-HMF (Figure 7.8-a-b-c), levulinic acid (Figure 7.8-d-e-f) and furfural (Figure 7.8-g-h-j) demonstrates the effecting parameters as direct current, reaction temperature and reaction time. Table 7.2 also indicates the quantities of yields for better observation. Application of 2 A of direct current at 230 ℃ for 30 minutes at 1 mM H_2SO_4 yields to highest yield of 5-HMF (7%). In current free experiments, RSPs (Figure 7.8-b) showed that increase in acid concentration resulted in higher 5-HMF yield. When current was applied after addition of higher acid concentration (25 mM and 50 mM H_2SO_4), diverse effect in which HMF yield was diminished from % 6.84 to 3.73% was observed. Moreover, interaction of current and reaction time exhibited similar trend in 5-HMF yield, in which, 2 A of applied current at reaction time of 30 min. and 120 min. resulted in HMF yields of 5.27% and 1.48%, respectively. Similar interaction of current with acid concertation and reaction time support the idea of electrochemically generated acid layer. On the other hand, levulinic acid yield increased with reaction time when 2 A of direct current was applied (Figure 7.8-e), however, TOC yield (Figure 7.4) and cellulose conversion decreased (Figure 7.3) in the same conditions. Thus, application of current resulted in further polymerization of 5-HMF to tarry material while increasing the levulinic acid yield. Maximum yield of levulinic acid (37%) was observed without applying current for 30 minutes of reaction at 230 ºC in 50 mM H_2SO_4 of reaction medium(Table 7.27). Application of direct current in this conditions resulted in decrease in the levulinic acid yield to 16%. The decrease in the levulinic acid concentration could

be due to further reactions to lactic acid, acetaldehyde, gamma-valoralactone (GVL), 2-butanone (dos Santos et al. 2015, Promdej and Matsumura 2011). However, when reaction time increased (e.g. 120 min.) at 2 A of current, levulinic acid yield increased from 16% to 28%. Figure 7.7 indicates the predicted parameters to maximize both TOC and levulinic acid yield values. By using mode equations for both TOC ((7.7) and levulinic acid yield ((7.12), it was predicted that reaction that was carried out with the addition of 50mM H_2SO_4 by applied direct current of 0.02 A at reaction temperature of 230 ºC would maximize TOC conversion and levulinic acid yield as 62% and as 36%, respectively.

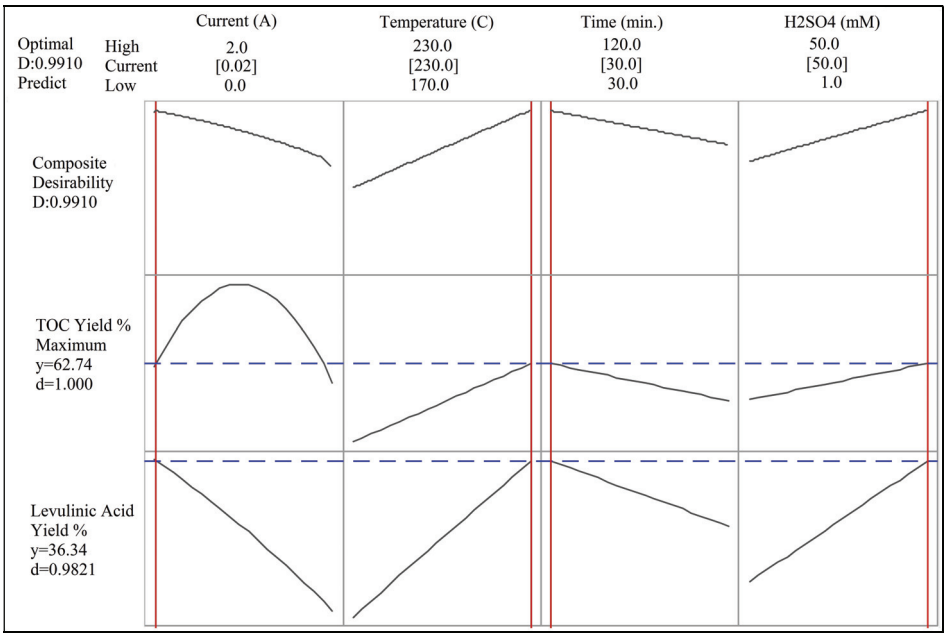

Figure 7.7. Predicted operating parameters for maximum TOC and Levulinic acid yields

Table 7.7. ANOVA test results of 5-HMF, levulinic acid, and furfural yield

	(5-HMF)					Levulinic Acid				
Source	DF	Sum of Squares	Mean of Squares	F Value	P-Value	DF	Sum of Squares	Mean of Squares	F Value	P-Value
Model	8	105.83	13.23	238.16	0.000	8	2774.65	346.83	2508.62	0.000
Linear	4	45.96	10.74	193.34	0.000	4	2275.66	568.92	4114.95	0.000
Current (A)	1	3.37	3.37	60.62	0.000	1	108.42	108.42	784.20	0.000
Temperature (B)	1	32.83	32.83	591.09	0.000	1	1278.96	1278.96	9250.67	0.000
Time (C)	1	0.83	0.83	14.91	0.003	1	15.23	15.23	110.15	0.000
H_2SO_4 (D)	1	5.93	5.93	106.74	0.000	1	873.05	873.05	6314.79	0.000
Square	1	3.28	3.28	59.02	0.000	1	1.50	1.50	10.84	0.000
Current*Current	1	3.28	3.28	59.02	0.000	1	1.50	1.50	10.84	0.009
2-Way Interaction	3	59.60	19.87	357.63	0.000	3	497.49	165.83	1199.45	0.000
Current*Temperature	1	0.60	0.60	10.81	0.008	1	28.06	28.06	202.98	0.008
Current*Time	1	44.55	44.56	802.31	0.000	1	464.08	464.08	3356.68	0.000
Current*H_2SO_4	1	14.44	14.44	259.96	0.000	1	5.35	5.35	38.68	0.000
Error	10	0.56	0.06			9	1.24	0.14		0.000
Total	18	10.39				17	2775.89			

	Furfural				
Source	DF	Sum of Squares	Mean of Squares	F Value	P-Value
Model	8	12.89	1.61	290.99	0.000
Linear	4	9.60	2.40	433.68	0.000
Current (A)	1	2.61	2.61	471.08	0.000
Temperature (B)	1	6.97	6.97	1258.81	0.000
Time (C)	1	0.02	0.02	4.06	0.000
H_2SO_4 (D)	1	0.00	0.00	0.76	0.000
Square	1	0.00	0.00	0.49	0.000
Current*Current	1	0.00	0.00	0.49	0.498
2-Way Interaction	3	3.28	1.09	197.58	0.498
Current*Temperature	1	1.51	1.51	273.25	0.000
Current*Time	1	1.30	1.30	234.73	0.000
Current*H_2SO_4	1	0.47	0.47	64.75	0.000
Error	10	0.06	0.02	0.01	0.000
Total	18	12.94	0.055		

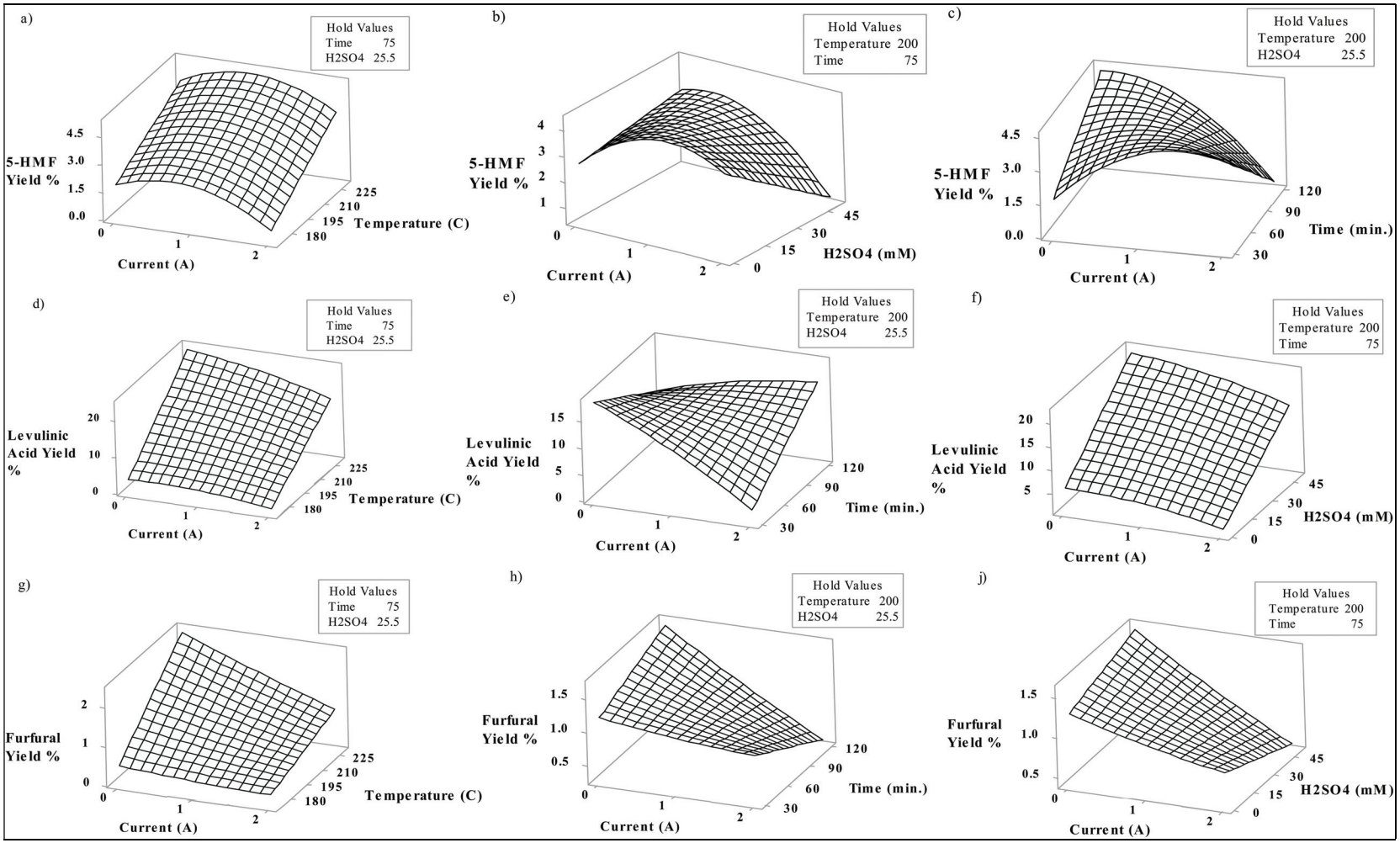

Figure 7.8. Surface response plots of 5-HMF (a-c), levulinic acid (d-f), furfural yields (g-j) with effecting parameters of applied current, reaction temperature and time, acid concentration (H_2SO_4)

7.3. Gas Products of Microcrystalline Cellulose Decomposition under Applied Direct Current in Hot Compressed Water

Gas samples were collected to the polypropylene (PP) bags with sampling time of 30, 60, 120 minutes and after cooling at the end of reaction. Collected samples were analyzed by gas chromatography thermal detector (GC-TCD). Cellulose degradation products such as aldehydes and ketones further degrade to gaseous products as carbon dioxide, hydrogen, carbon monoxide under hydrothermal conditions (Chuntanapum et al. 2008, Castello, Kruse, and Fiori 2013). Possible reactions involved in the formation of gas products as CH_4, C_2H_4, C_3H_6 reported as the gas products of cellulose decomposition (Gao et al. 2012) are illustrated as follows;

$$CO + H_2O \leftrightarrow CO_2 + H_2 \quad (7.13)$$

$$CO + 3H_2 \leftrightarrow CH_4 + H_2O \quad (7.14)$$

$$2CO + H_2 \leftrightarrow 1/2C_2H_4 + CO_2 \quad (7.15)$$

$$2CO + H_2 \leftrightarrow 1/3C_3H_6 + CO_2 \quad (7.16)$$

$$H_2O \leftrightarrow H_2 + 1/2O_2 \quad (7.17)$$

Figure 7.9. indicates the formation of gaseous decomposition products of cellulose under hot-compressed water and applied direct current conditions at sampling times. Analysis of samples taken at the end of reaction after the cooling of reaction medium to ambient conditions were not shown in figures. The results were given within the text. As the reaction temperature increased from 200 ℃ to 260 ℃, hydrogen concentration in the gas products increased from 0.52 to 2.83 µg/ml (Figure 7.9-a) at the sampling time of 120 min. Application of 2 A of direct current resulted in the formation hydrogen in concentration of 53.8 µg/ml (Figure 7.9-a). This is mostly due to the hydrolysis of water under applied current. However, application of 1 A of current did not yield hydrogen gas formation (Figure 7.9-a) in which maximum TOC yield was achieved. Reduction of hydrogen ion yields to formation of hydrogen gas at anode, hence, protonation of β(1-4),glycosidic bond of cellulose is not favored at 2 A of current. Thus, lower TOC yield was obtained at 2 A of applied current in comparison to that of 1 A of current.

Therefore, application of current (1 A) enhanced decomposition mechanism of cellulose through the formation of TOC instead of gaseous and tarry products.

For the experiments that 2A of direct current applied, the collected gas samples at sampling time of 120 minutes and at the end of reaction (after cooling of reaction medium) showed that there was a dramatic decrease in hydrogen concentration from 95.48 to 36.71 µg/ml and carbon dioxide concentration from 427.14 to 284.83 µg/ml concentrations, respectively. In addition, carbon monoxide amount increased from 47.89 to 92.24 µg/ml which indicates that water gas shift reaction is favored the carbon monoxide formation as the reaction temperature cooled from 230 ºC to ambient temperature. Methane formation (Figure 7.9-c, circle) was also observed as gas products and an increase in acid concentration from 1 to 50 mM yields to 0.27 and 0.51 µg/ml, respectively.

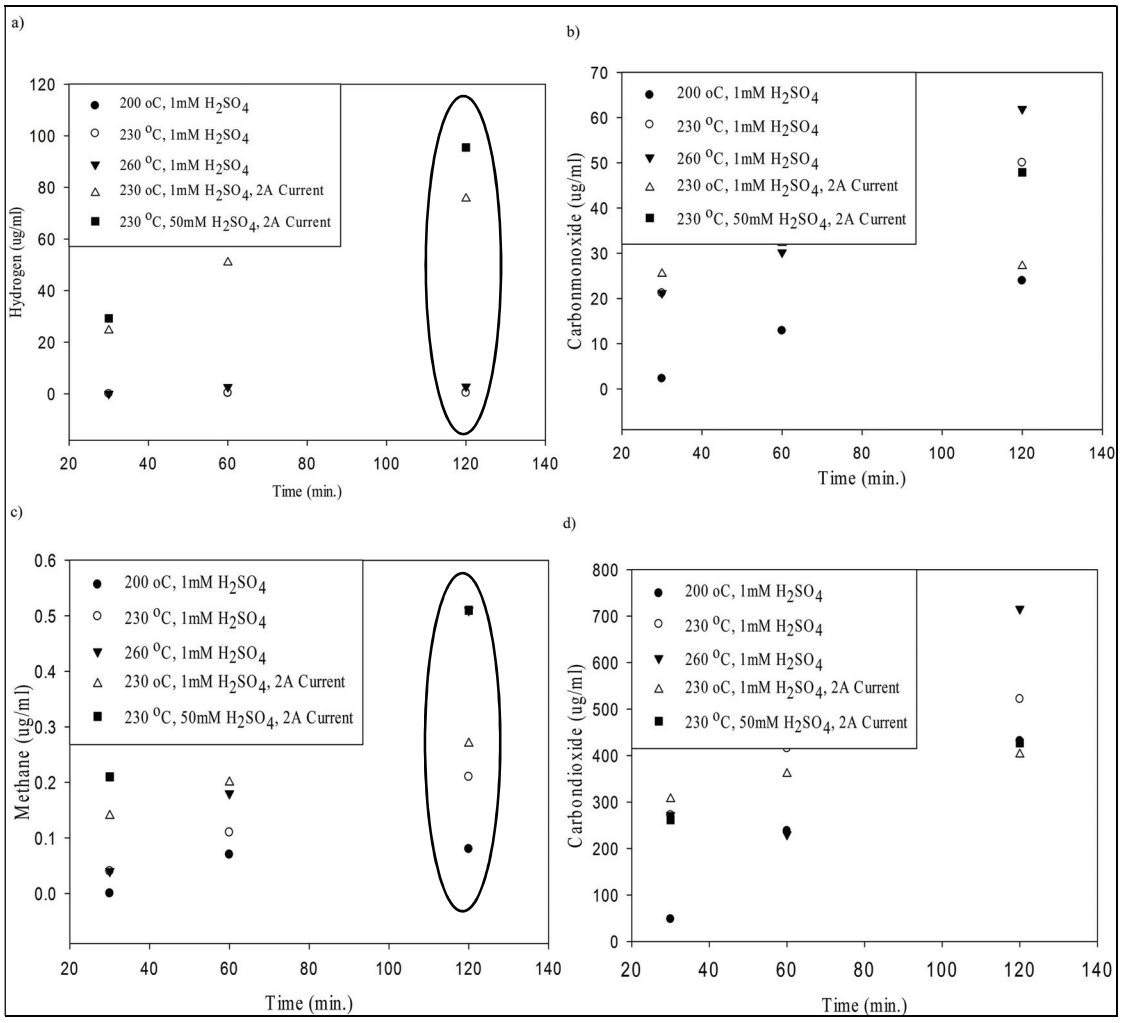

Figure 7.9. Gaseous products of cellulose of decomposition, a) hydrogen, b) carbonmonoxide, c) methane, d) carbondioxide under hydrothermal and applied constant current conditions.

7.4. Analysis of Solid Residue of Microcrystalline Cellulose Decomposition under Applied Current in Hot Compressed Water

Solid residue that is obtained at the end of decomposition reaction of cellulose in hot compressed water with and without direct current was analyzed by scanning electron microscopy and FT-IR for structural and chemical properties, respectively. Crystalline structure of MCC is shown in Figure 7.10-a with clear observation of crystal layers with the particle size of approximately 30 μm. The residue obtained from hydrothermal decomposition of MCC at 230 ℃ and 1 mM H_2SO_4 without applied current is shown in Figure 7.10-b. The structural change of MCC is clearly observed (Figure 7.10-b) under hydrothermal conditions. Moreover, shrinking in the particles are clearly observed. At higher reaction temperature of 260 ºC, formation of solid spheres (circle) that are embedded in char (arrow) is observed (Figure 7.10-c). Cellulose decomposition product of 5-HMF can polymerize and forms tarry materials in hot-compressed water conditions (Chuntanapum, Shii, and Matsumura 2011). Application of current (2 A, 230 ºC) to the reaction medium resulted in the formation of carbon spherical particles as tarry material (Figure 7.10-d) with particle size of 1-3μm. Formation of carbon microspheres supports the idea of decrease in cellulose conversion when the 2 A of current is applied to the reaction medium in which reaction time has negative effect on cellulose conversion. Clear image of microspheres showed that there was no formation of char material around. As it was found from GC-TCD results, applied current (2 A) to the reaction medium increased the gaseous product concentration such as carbon dioxide, hydrogen and carbonmonoxide. Thus, applied current (2A) may restrict the formation of char.

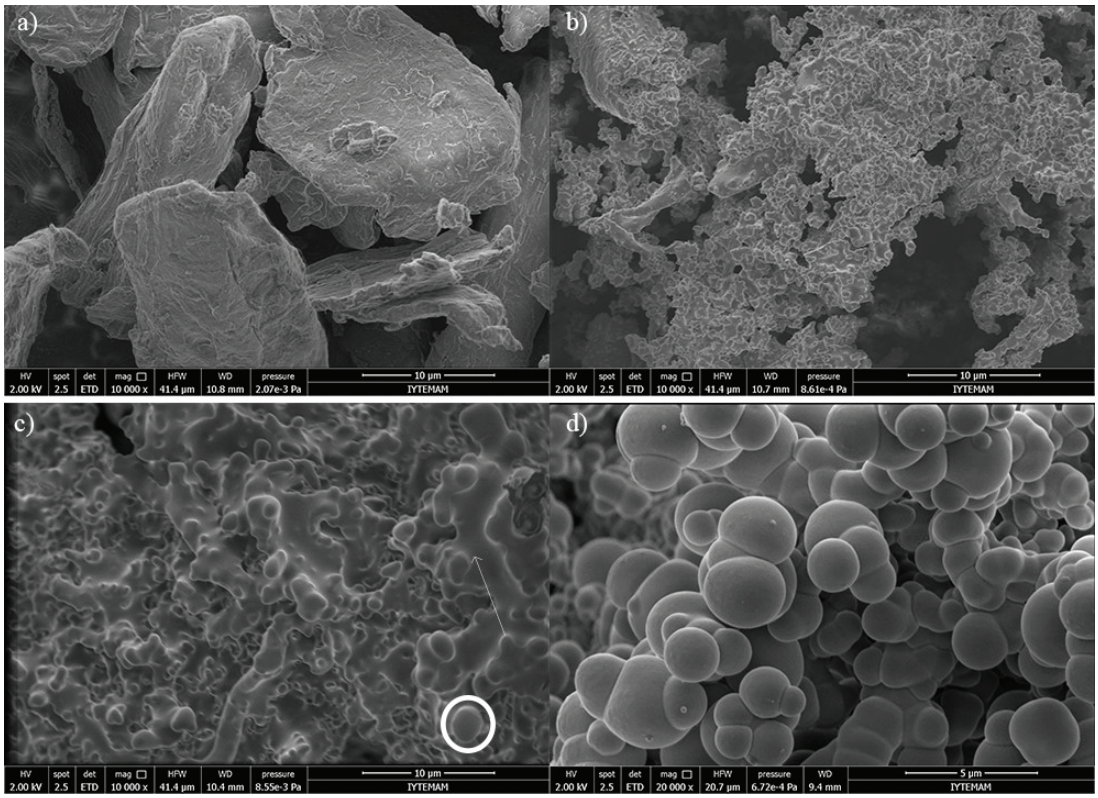

Figure 7.10. SEM images of a) microcrystalline cellulose and solid residues of b) 230 ºC, 0 A c) 260 ºC, 0 A and d) 230 ºC at 2 A of current applied

Spectrum obtained by FTIR analysis of solid residues is shown in Figure 7.11. The peaks at 2877 cm^{-1} are attributed to stretching vibration of C-H. The O-H stretching vibration at 3341 cm^{-1} corresponds to intramolecular hydrogen bond of microcrystalline cellulose. This peak disappeared at 2 A of applied current and 50 mM H_2SO_4 conditions indicating that intra-molecular hydrogen bonds are protonated and cleavage. In addition, application of 2 A of current diminished the peak at 892 cm^{-1}, which is attributed to β-D-glucopyranosyl, in reaction temperature of 230 ºC with reaction time of 30 min. Thus, hydrothermal treatment of cellulose resulted in hydrolysis reaction that destructs the inter-molecular hydrogen bonds (Chung, Lee, and Choe 2004). Moreover, the broad peak start from 1530 cm^{-1} to 1750 cm^{-1} shows the existence of aldehydes and ketones that absorbed to solid residuals (Gao et al. 2012). This broad spectrum was observed at the residues in which glycosidic bond disappeared. The main characteristic peaks of spectrum 1031 and 1057 cm^{-1} are assigned as C-OH and C-O stretching vibrations. The peaks at 1104 and 1160 cm^{-1} can be attributed as C-O and C-C stretching vibration of cellulose ether, respectively. These peaks were disappeared in residues obtained at 230 ºC, 50 mM

H_2SO_4, 2 A of current at 120 min. The peak at 1643 cm^{-1} is due to adsorbed water molecules in MCC structure.

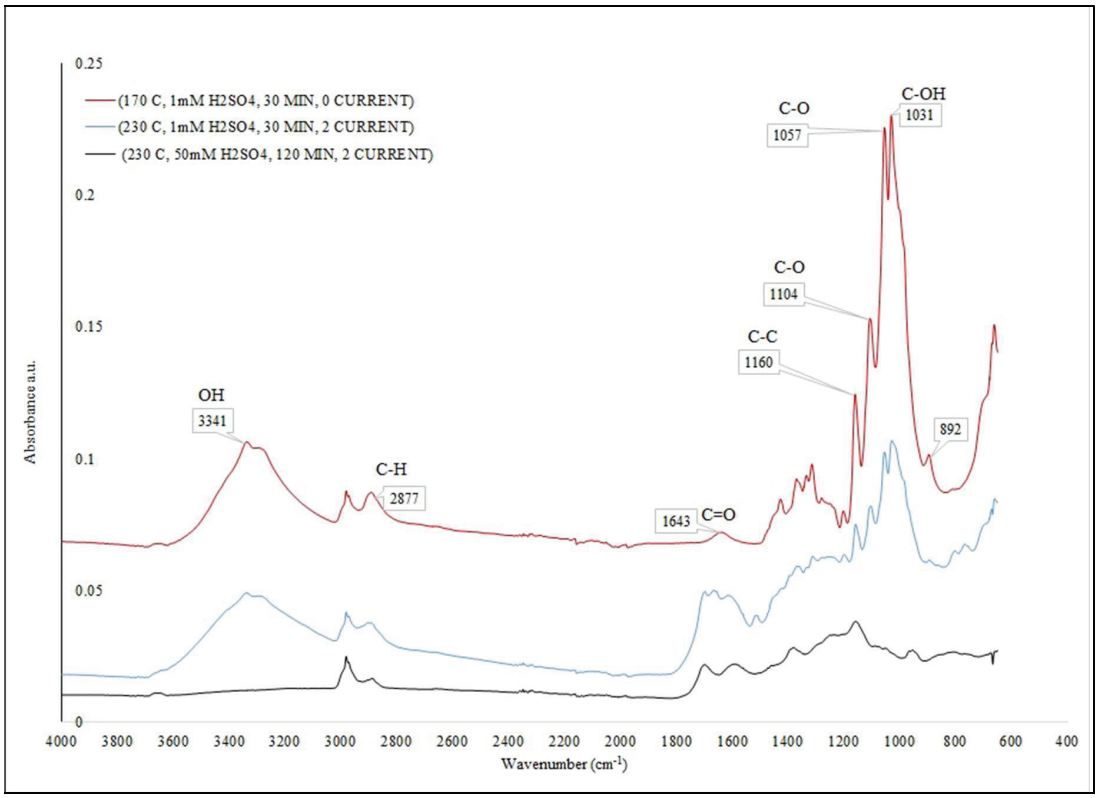

Figure 7.11. FT-IR spectrum of solid residua of MCC decomposition under applied current and hydrothermal condition

CHAPTER 8

CONSTANT VOLTAGE ELECTROLYSIS OF MICROCRYSTALLINE CELLULOSE IN HOT COMPRESSED WATER

In this chapter, electrochemical degradation of microcrystalline cellulose (MCC) under applied constant voltage between anode and cathode in hot-compressed water is discussed. Effect of applied constant voltage on product yield and selectivity values of Glucose, Fructose, 5-HMF, Levulinic acid, Formic acid, Furfural, total organic carbon (TOC) yield is conducted. Constant voltage was applied with range of 2.5 to 8.0 V between cylindrical anode (made of Titanium) and cathode as reactor wall (T316) for 240 minutes of reaction time at constant reaction temperature of 200 ℃. External proton source and as an electrolyte, H_2SO_4 (5-25 mM) was used.

In order to understand the effect of constant voltage on product distribution and selectivity values discussion is built along with the SEM-EDX and FTIR analysis of solid residue obtained at the end of reaction.

8.1. Experimental Procedure and Methods

Microcrystalline cellulose with the concentration of 4 g / 100 ml of UP water, was used in all experiments. Table 8.1 indicates the experimental conditions that is implemented for constant voltage decomposition of MCC. Electrochemical degradation of MCC under hydrothermal conditions were carried out in a 450 ml (Parr 5500 series) of batch reactor equipped with a specially designed titanium anode. Experimental set-up was illustrated and explained in detail at chapter 6 (Experimental study). Hydrothermal electrolysis experiments were carried out at a constant temperature of 200 °C for 240 minutes of reaction time by application of constant voltage values (2.5, 4.0 and 8.0 V). Liquid samples were collected through the reaction with the interval of 30 minutes and filtered for further analysis as HPLC, TOC and GC-MS.

Table 8.1. Applied voltage and electrolyte concentration of constant voltage experiments

Experiment #	Voltage (V)	H_2SO_4 (mM)
1	0	0
2	2.5	0
3	4.0	0
4	8.0	0
5	0	5
6	2.5	5
7	4.0	5
8	8.0	5
9	0	25
10	2.5	25
11	4.0	25
12	8.0	25

Products of MCC decomposition such as aldehydes, ketones and carboxylic acids were identified by HPLC-refractive index (RI) detector. Gaseous product was collected to polypropylene (PP) bags at the end of reaction. Gas Chromatography equipped with a Thermal Conductivity Detector (GC-TCD) (Agilent 6890 N) were used to analyze gas products. TOC analyzer (Shimadzu TOC- VCPH) was used to monitor TOC conversions in the liquid products and solid residues. Fourier Transmission Infrared Spectroscopy (FT-IR) analyses of solid residues were conducted by Perkin Elmer Frontier-Spectra two with scan rate of 4 cm^{-1} from 600 cm to 4000 cm^{-1} wavenumber.

The change in the current values during reaction under constant voltage values of 2.5 V, 4.0 V and 8.0 V were given in Figure 8.1. In the absence of the electrolyte (Figure 8.1-a) the initial current value of 0.03 A for all voltage values. This could be due to lack of electrolyte resulted in the limiting current value. Hydrolysis of cellulose resulted in the formation of organic acids that can act as electrolyte in reaction medium. Thus, current value increased for 4.0 V and 8.0 V (Figure 8.1-a). In contrast, current decreased when 2.5 V was applied. This could be due to formation of tarry material around electrode that increased the resistance. Moreover, application of 2.5 V under electrolyte free conditions selectively produce furfural instead of organic acids. Therefore, the decrease in current could also be resulted from reaction medium product distribution. Addition of sulfuric acid (5 mM and 25 mM) as an electrolyte resulted in higher current values. The most dramatic results in terms of product selectivity were obtained at 2.5 V in which current values in range 0.01-0.04 A. Optimization result in ANOVA analysis (Figure 7.7) support this observation and validate the statistical optimization results.

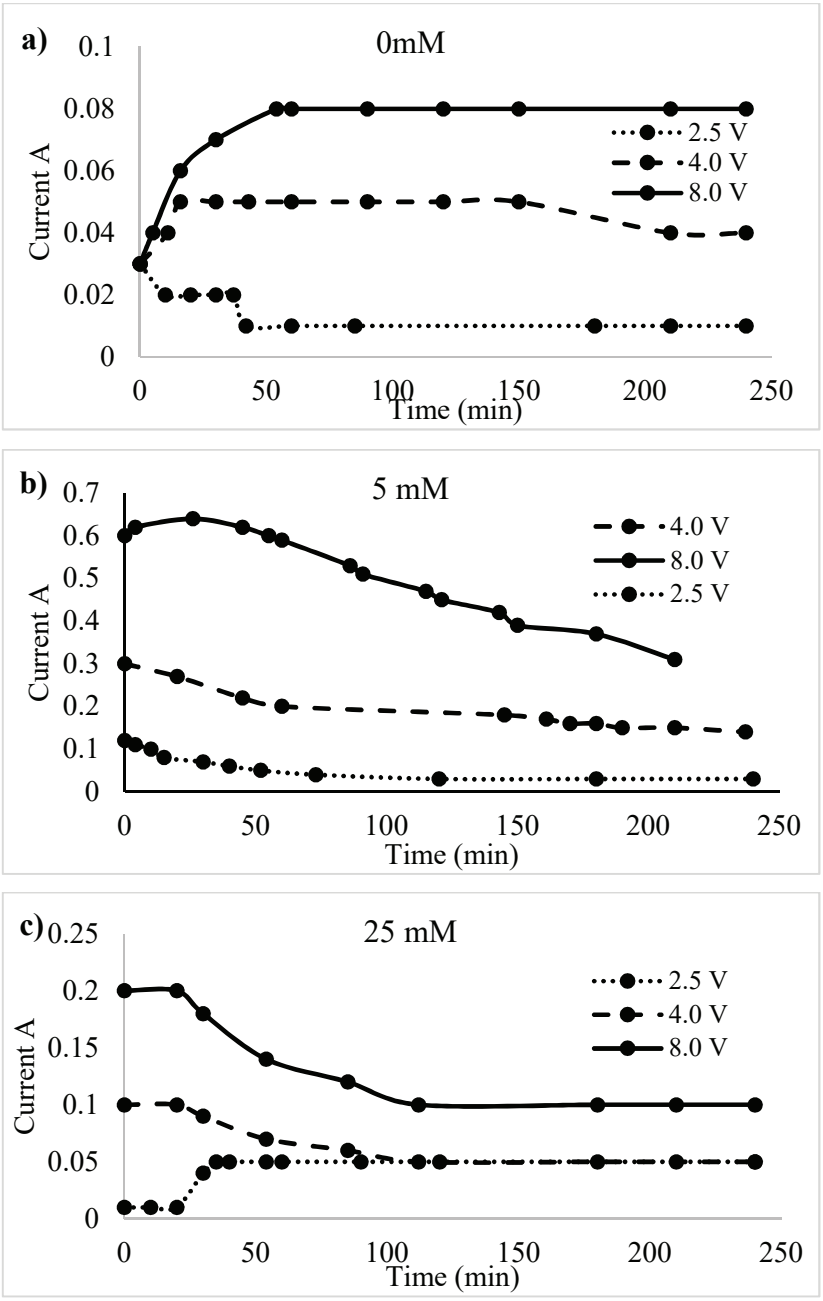

Figure 8.1. Change in the current (A) during reaction at constant voltage (2.5 V, 4.0 V and 8.0 V) in H_2SO_4 concentration of a) 0 mM, b) 5 mM and c) 25 mM

8.2. Total Organic Carbon Yield of Electrochemical Decomposition of Microcrystalline Cellulose under Constant Voltage in Hot-Compressed Water

Ionic product concentration plays crucial role in destruction of intra- and inter hydrogen bonds of cellulose that yields the formation of further degradation products. Cellulose decomposition mechanism in sub-critical conditions is explained via ionic

based reactions (Sasaki et al. 2000). Results of constant current experiments showed that application of constant current (1 A) to reaction medium resulted in the maximum value of TOC yield in comparison to 2 A and current free reactions. An increase in ionic concentration due to self-dissociation of water under applied current resulted in higher TOC yields, in comparison to higher current values (2 A) that yields the formation of gaseous products due to radical based mechanism in decomposition of cellulose (Akin and Yuksel 2016). Total organic carbon yield of liquid was analyzed in order to investigate the effect of constant voltage on protonation of intra- and inter molecular hydrogen bonds of microcrystalline cellulose. Yield of TOC was calculated based ((7.3) on carbon amount of initial cellulose in the reaction medium. Figure 8.2 indicates the formation of decomposition of products in terms of total organic carbon (TOC) yield under applied constant voltage (0, 2.5, 4.0 and 8.0 V) at different electrolyte concentrations (0, 5 and 25 mM). MCC decomposition was carried out in subcritical water conditions without electrolyte as control experiment. Application of constant voltage values of 2.5 and 4.0 V without electrolyte (0 mM of H_2SO_4) resulted in lower TOC (11%) (Figure 8.2-a) compared to voltage free (0 V) reaction (TOC , 13%). Water self-disassociation products as hydronium (H_3O^+) and hydroxyl (OH^-) ions could be reduced or oxidized in cathode and anode, respectively, in the absence of electrolyte. Thus, decrease in the TOC yield could be due to limitation in protonation of β(1-4),glycosidic bond due to the low concentration of ion products. In contrast, potential difference of 8.0 V resulted in TOC yield of 13% at reaction time of 180 minutes, in which, current free experiment yields 10%. An increase in the overpotential resulted in the rate of dissociation of water to its products. Application of voltage under hydrothermal conditions also yields the formation of radical species such as hydroxyl radical ($OH^{\bullet -}$) (Rossmeisl, Logadottir, and Nørskov 2005). Increase in radical species concentration could also result in the formation of decomposition products via radical based mechanism. In the presence of electrolyte (5 mM of H_2SO_4) increased the TOC yield to 50% (Figure 8.2-b) in subcritical water conditions. Application of 2.5 V and 8.0 V voltages to reaction medium containing 5 mM of sulfuric acid increased the TOC yield to 54% and 60%, respectively. The coupled effect of applied current and sulfuric acid was also reported in the study of constant current decomposition of MCC under hydrothermal conditions (Akin and Yuksel 2016). Interaction of applied voltage and sulfuric acid is due to the oxidation of sulfuric acid that yields the formation of sulfate radical ($SO_4^{\bullet -}$) near anode (Davis, Baygents, and Farrell 2014). In contrast, application of 4.0 V did not

enhance the TOC yield. Therefore, interaction of applied voltage with the parameters effecting TOC yield is indistinguishable. It is due to the fact that TOC formation is also effected by the formation of carboxylic acids that are formed during the decomposition of cellulose. Addition of sulfuric acid increases the concentration of degradation products, hence, effect of applied voltage at higher sulfuric acid concentration showed different patterns in TOC yield (Figure 8.2-c). Applied 2.5 V resulted in the higher TOC yield in reaction medium with 25 mM of sulfuric acid.

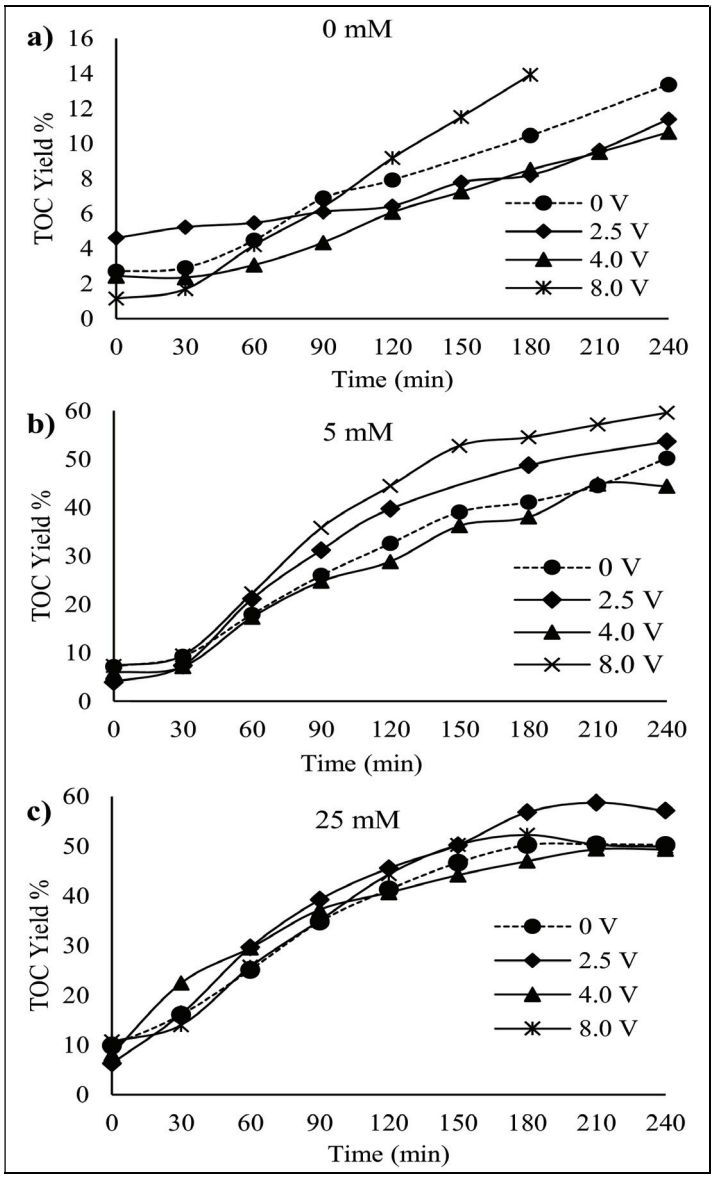

Figure 8.2. Total organic carbon yield of MCC decomposition in H_2SO_4 concentration of a) 0 mM b) 5mM and c) 25 mM

8.3. Product Yield of Electrochemical Decomposition of Microcrystalline Cellulose under Constant Voltage in Hot-Compressed Water

MCC decomposition products such as glucose, fructose, 5-HMF, levulinic acid and furfural under applied constant voltage (2.5, 4.0, and 8.0 V) in hot compressed water (200 ℃) conditions was investigated with and without electrolyte (0, 5, and 25 mM of H_2SO_4). The yield values of products were calculated as described in materials and method section. Control experiment was carried under without acid and application voltage in 200 ℃ of reaction time. The selectivity and yield values of products of hydrothermal decomposition of cellulose under applied voltage is given in Figure 8.3. Under hydrothermal condition, glucose selectivity (Figure 8.3-a) and yield (Figure 8.3-b) values reached to 19.6% and 5.75%, respectively. Application of constant voltage of 4.0 V decreased the glucose selectivity and yield values to 15% and 1.7% respectively. In addition, 2.5 V of potential difference also declined the glucose selectivity and yield values to 9.7% and 1.2%, respectively. This could be due to same effect of voltage as it was in TOC yield. In the absence of electrolyte, ion products of water can be involved redox reactions that can hinder the protonation of cellulose. However, application of 8.0 V resulted in higher selectivity to glucose (Figure 8.3-a) in comparison to 2.5 V, 4.0 V and voltage free experiments. The same trend was also observed in glucose isomerization to fructose (Figure 8.3-c and Figure 8.3-d). However, under hydrothermal conditions, yield of fructose was much higher than that was in voltage applied experiments. This could be explained by series reactions in which fructose was further converted to 5-HMF by dehydration. Application of 8.0 V alter the decomposition reaction pathway in favor of furfural (Figure 8.3-e) and 5-HMF (Figure 8.3-g) production. There are two proposed reaction pathways for the conversion of fructose to furfural under hydrothermal conditions (Aida et al. 2007). One is the removal of formaldehyde from 5-HMF and the other one is the cleavage of C-C bond in fructose that yields pentose formation and further dehydration of pentose yields to furfural formation (Luijkx, van Rantwijk, and van Bekkum 1993). The increment in the yield values of furfural (Figure 8.3-f) and 5-HMF (Figure 8.3-h) was observed simultaneously. Therefore, it could be said that furfural might be formed by the cleavage of C-C bond in fructose because of the low yield of fructose (8.0 V) in comparison to hydrothermal reaction (0 V) (Figure 8.3-d). Otherwise,

5-HMF concentration was expected to decrease with the increase of furfural yield in the reaction pathway of formaldehyde extraction from 5-HMF.

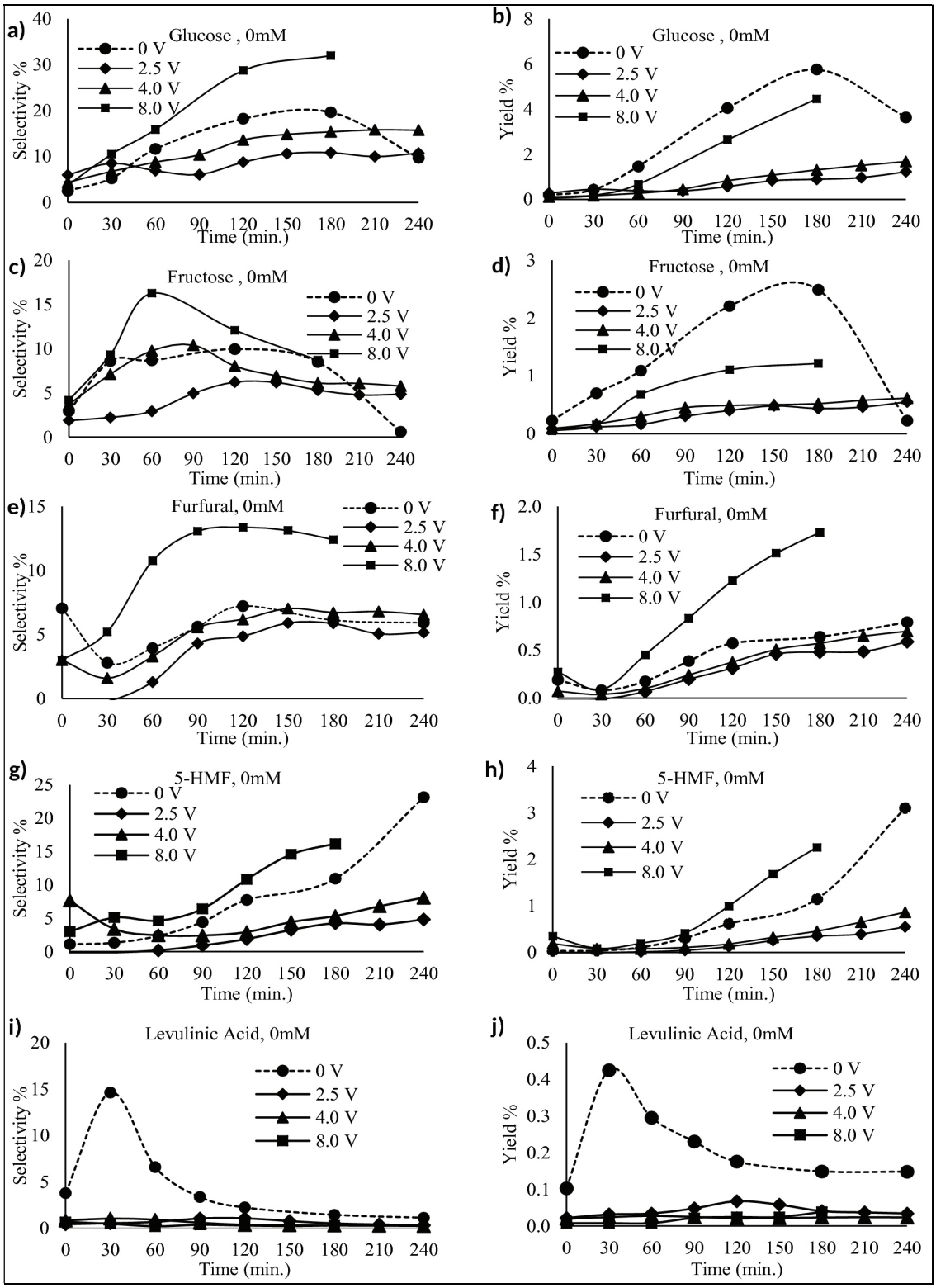

Figure 8.3. Selectivity and yield values of MCC degradation products in products a-b) glucose, c-d) fructose, e-f) furfural, g-h) 5-HMF, i-j) levulinic acid by hydrothermal constant voltage electrolysis in acid free medium

Rehydration of 5-HMF resulted in formation of levulinic acid (Figure 8.3-i). Application of voltage limited the formation of levulinic acid as compared to the voltage free experiments. In constant current experiments, effect of external proton source (H_2SO_4) on product yields at concentration of 25 mM and 50 mM under hydrothermal conditions has been investigated in depth in Chapter 5. Statistical analysis showed that there was a coupled effect coupled effect of electrolysis and acid catalyst on TOC yield under hydrothermal conditions. However, constant current did not selectively alter the decomposition reaction. In this study, it was proposed that application of constant voltage may alter the decomposition of cellulose in a selective way. Thus, yield and selectivity values of decomposition products under applied constant voltage of 2.5 V, 4.0 V and 8.0 V were investigated with addition of 5 mM (Figure 8.4) and 25 mM (Figure 8.5) of sulfuric acids into reaction medium. Addition of sulfuric acid (5mM) distinguished the diverse effect of applied voltage on glucose (Figure 8.4-b) and fructose (Figure 8.4-d) yields as it was in the case of electrolyte free reaction medium (0 mM). Application of constant voltage of 2.5 V selectively alter the reaction mechanism in favor of glucose (Figure 8.4-a) at first 30 minutes of reaction. Selectivity of glucose increased from 22.5% to 45% when 2.5 V of constant voltage was applied. Glucose selectivity decreased after 30 minutes of reaction due to the further reactions such as isomerization, dehydration, and retro-aldol condensation. The similar trend in glucose selectivity was also observed for voltage free hydrothermal reaction (Figure 8.4-a). Thus, addition of sulfuric acid increased the protonation of β-glyosidic bond and interaction of sulfuric acid with applied voltage resulted in the coupled effect on glucose selectivity that yield to 45% selectivity of glucose. In contrast, application 4.0 and 8.0 V of constant voltage declined the glucose selectivity in comparison to voltage free reaction medium at similar TOC yield (Figure 8.2). Similar TOC indicate that partial decomposition of cellulose yielded oligomers at higher voltage values within 30 minutes. High potential differences resulted in the formation of hydrogen gases instead of protonation of β(1-4),glyosidic bond of cellulose as found in GC-TCD analysis (Figure 8.6-a) of gaseous products. Moreover, our previous reported study also showed consistent results in terms of gaseous products formation at higher current values (Akin and Yuksel 2016).

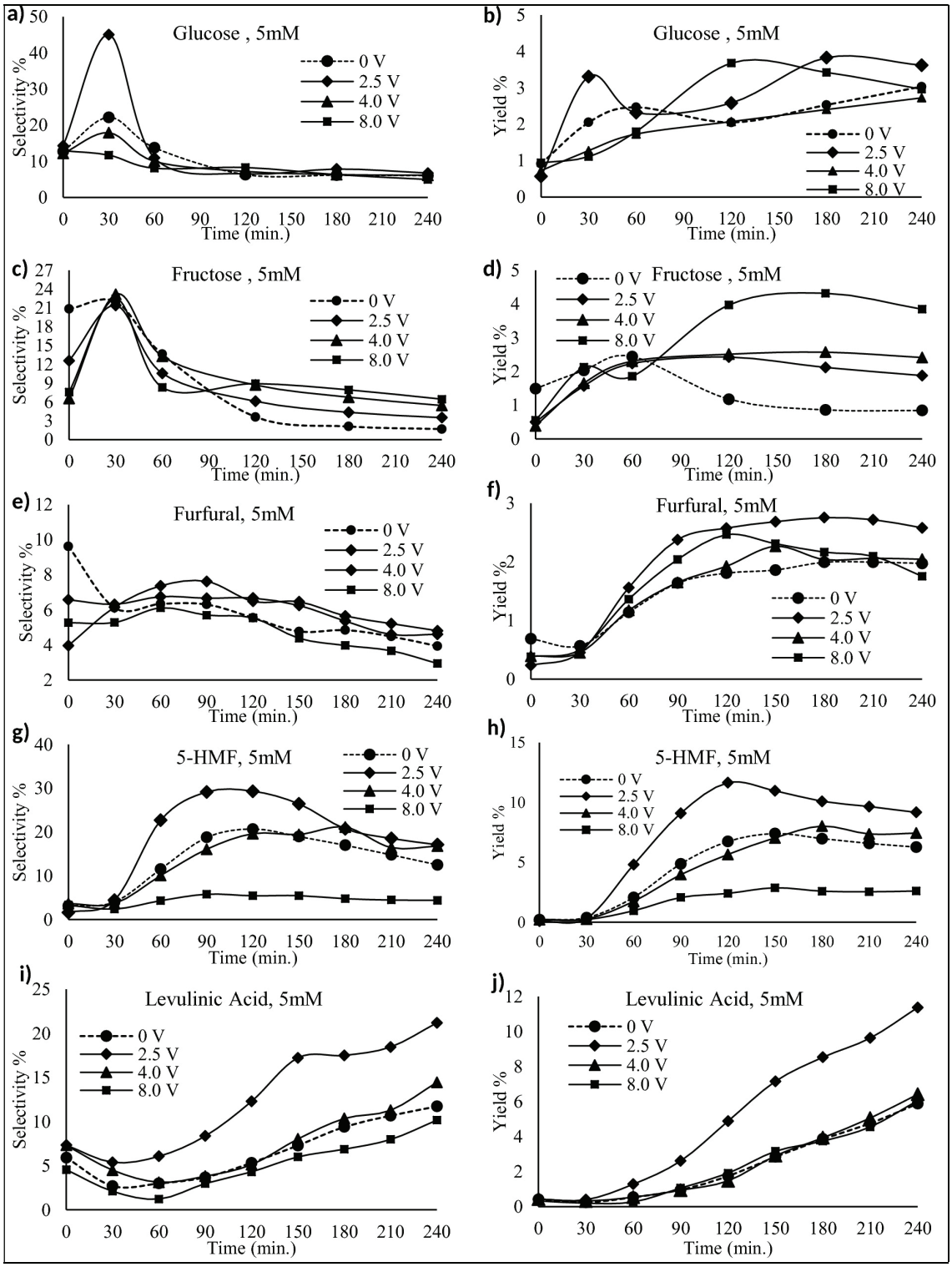

Figure 8.4. Selectivity and yield values of MCC degradation products in products a-b) glucose, c-d) fructose, e-f) furfural, g-h) 5-HMF, i-j) levulinic acid by hydrothermal constant voltage electrolysis in 5mM H_2SO_4

Addition of sulfuric acid under hydrothermal conditions increased the selectivity to fructose (21%, Figure 8.4-c) in comparison to acid free reaction medium

(10%, Figure 8.3-c). Application of constant voltage did not alter the selectivity of fructose in first 30 minutes of reaction. However, applied constant voltage resulted in higher fructose selectivity after the reaction time of 120 minutes in comparison to voltage free experiments. The selectivity values of degradation products such as 5-HMF (Figure 8.4-h) and levulinic acid (Figure 8.4-j) dramatically changed after 30 minutes of reaction. 5- HMF yield and selectivity reached to 11% and 29 % at 2.5 V within 120 minutes of reaction time, respectively. Under sub-critical water conditions (0 V), 5-HMF rehydrated to levulinic acid due to the thermal instability, which was also reported in literature (Sasaki et al. 2011). Therefore, levulinic acid was formed via rehydration of 5-HMF and its selectivity reached to 21% at 2.5 V within 240 minutes of reaction.

It was reported that Bronsted acid sites play crucial role in selective formation of 5-HMF via dehydration of fructose (Swift et al. 2014, Qi et al. 2012). Thus, the dramatic change in 5-HMF and levulinic acid selectivity values at 2.5 V potential could be due to the formation of sulfonated carbon particles that can act as catalyst in selective formation of 5-HMF. Formation of sulfone groups were detected via FTIR (Figure 8.7) of remaining solid residue collected at the end of reaction. FTIR patterns showed that formation of sulfur ester (S-R) and sulfoxide (S=O) groups became more obvious at 2.5 V of applied voltage (Figure 8.7-C). The detailed discussion is held on spectroscopic analysis part. Moreover, sulfonated carbon derived from biomass has been investigated and reported in selective production of 5-HMF (Shen, Yu, and Chen 2016, Kang et al. 2013, Qi et al. 2012). However, application of 4.0 V and 8.0 V of potential difference did not alter the selectivity values of 5-HMF and levulinic acid. In addition, application of 8.0 V decreased the product selectivity values in contrast to TOC yields. Application of higher voltage (8.0 V) decreased the pH value to 1.72 in comparison voltage free experiment in which pH was 2.0. Applied higher voltage could have resulted in further degradation of aldehydes and ketones to carboxylic acids due to the formation of highly active sulfate ion radicals. Effect of applied voltage at higher acid concentration (25 mM) on product yield and selectivity values was given in Figure 8.5. Under hydrothermal conditions, selectivity of 5-HMF (Figure 8.5-g) reached to 40% within 60 minutes and further reaction time (210 minutes) yielded levulinic acid (Figure 8.5-i) with selectivity of 23%. Application of voltage (4.0 V and 8.0V) showed diverse effect on 5-HMF selectivity even though the FTIR results showed that sulfone groups were formed at solid residuals.

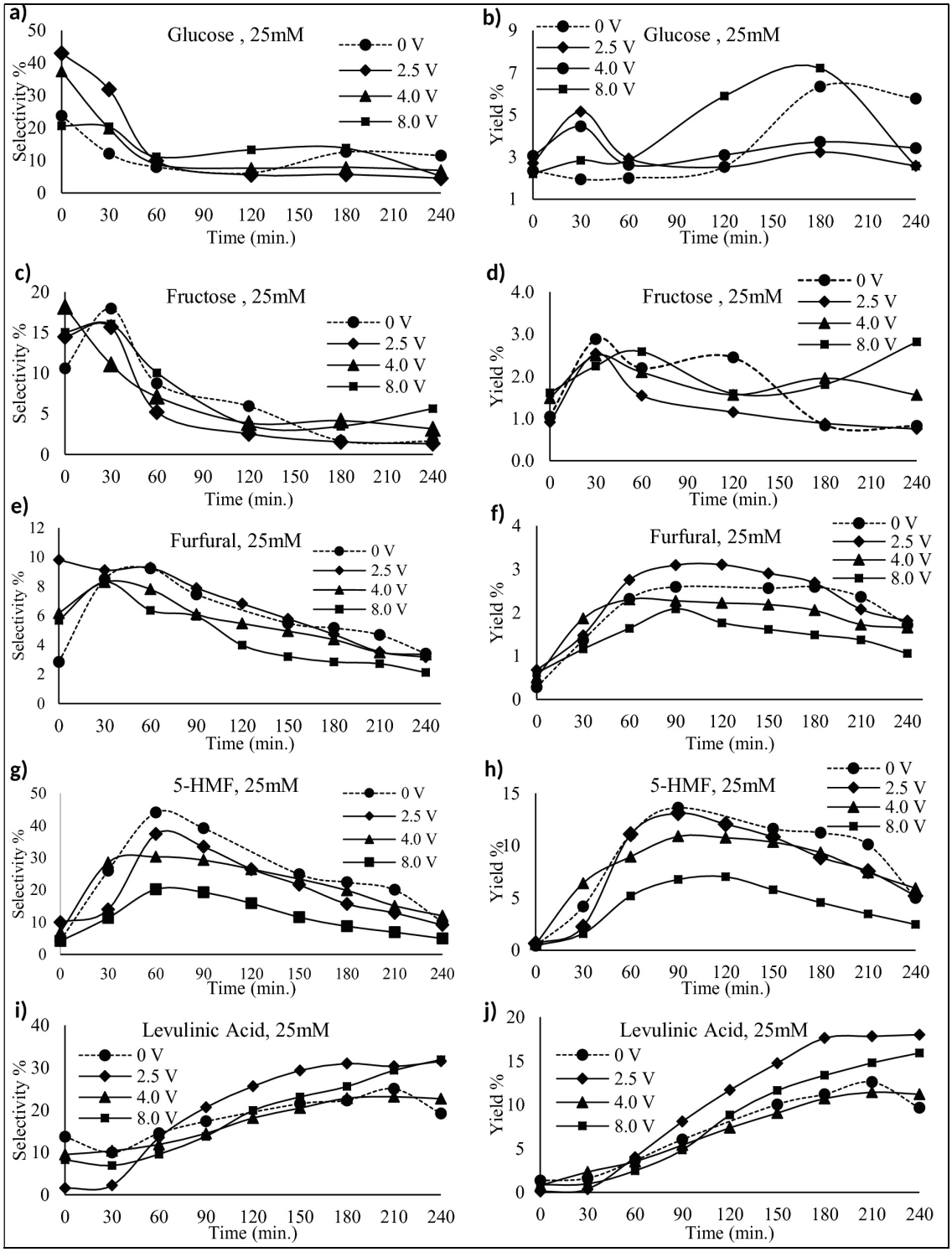

Figure 8.5. Selectivity and yield values of MCC degradation products in products a-b) glucose, c-d) fructose, e-f) furfural, g-h) 5-HMF, i-j) levulinic acid by hydrothermal constant voltage electrolysis in 25 mM H_2SO_4

Application of potential at relatively high concentration of sulfuric acid may yield high concentrations of reactive species such as sulfone ion radicals that hinders the effect

of sulfonated carbon particles. In contrast, levulinic acid selectivity increased from 23% (0 V) to 32% (2.5 V and 8.0 V) by application of voltage. GC-TCD (Figure 8.6) analysis showed that under hydrothermal conditions there was no significant production of gaseous products, however, as the potential applied, carbon monoxide and carbon dioxide formation increased. Thus, application of voltage under 25 mM acid yielded the formation of gaseous product due to further decomposition based on radical mechanism (Sasaki, Adschiri, and Arai 2004).

8.4. Gaseous Products of Electrochemical Decomposition of Microcrystalline Cellulose under Constant Voltage in Hot-Compressed Water

Gas samples were collected at the end of reaction (240 minutes) into PP bags and analyzed by GC-TCD. Hydrolysis of cellulose first yielded to aldehydes and ketones and further decomposition resulted in formation of carboxylic acids that could be decomposed to the gases under hydrothermal conditions. Application of potential difference to the reaction medium resulted in the formation of hydrogen and oxygen gases because of reduction and oxidation reactions of ionic products of water. Moreover, addition of sulfuric acid resulted in the formation of radical species that end-up formation of gaseous products due to radical based decomposition mechanism. Formation of gas products such as hydrogen (Figure 8.6-a), carbon monoxide (Figure 8.6-b) and carbon dioxide (Figure 8.6-c) were investigated. Application of potential of 2.5 V decreased carbon dioxide (Figure 8.6-b) formation in electrolyte free and 5 mM sulfuric acid containing reaction mediums. Decrease in the carbon dioxide could be explained by the electrochemical reduction at cathode surface (Jitaru et al. 1997) and possible further reactions with aldehydes and ketones. Further increase in voltage resulted in higher concentration of gaseous product. Moreover, when 8.0 V of potential was applied, methane was produced in the presence of 5 mM and 25 mM sulfuric acid. Electrochemical reduction of carbon dioxide might result in the formation of methane.

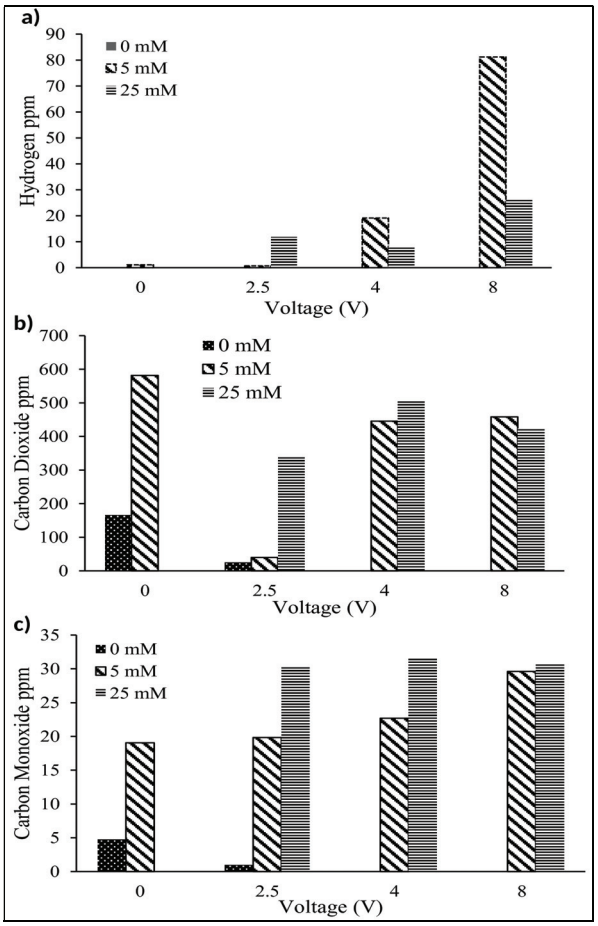

Figure 8.6. Production of gaseous products a) hydrogen, b) carbondioxide, c) carbonmonoxide under hydrothermal and applied voltage conditions

8.5. FT-IR Spectrum of Solid Residue of Electrochemical Decomposition of MCC under Constant Voltage in Hot-Compressed Water

The FTIR spectrums of solid residues of acid free (Figure 8.8) experiments and with 5 mM H_2SO_4 hydrothermal electrolysis reactions (Figure 8.7) were investigated. Raw material microcrystalline cellulose showed the stretching vibrations at 3341 and 2877 cm^{-1} which are attributed to O-H and C-H bonds, respectively. In addition, the peak at 902 cm^{-1} is attributed to the β-D-glucopyranosyl that disappeared by the application of 8.0 V of potential under acidic conditions (Figure 8.7-B). In contrast, application of 4.0 V did not totally diminish the intermolecular hydrogen bond peak, however, 2.5 V application was almost destruct the β-D-glucopyranosyl. The main characteristic peaks of cellulose were observed at spectrum of 1033 and 1059 cm^{-1} and were assigned as

C-OH and C-O stretching vibrations, respectively. The peaks of microcrystalline cellulose at 1104 and1160 cm^{-1} could be attributed to C–O and C–C stretching vibration of cellulose ether. Application of voltage in sulfuric acid reaction medium yielded the formation of sulfonate functionalities at solid residues. The peak of sulfur ester (S-OR) and sulfoxide (S=O) were observed at wavenumber of 811 cm^{-1} and 1030-1060 cm^{-1}, respectively. The sulfoxide peaks were overlapped with the characteristic peaks of cellulose and it was hard to distinguish. However, the shoulder (Figure 8.7, arrow) at 1033 cm^{-1} of cellulose was separated at spectrums of 2.5 V and 8.0 V. Moreover, the relative peak height at 1060 cm^{-1} became higher than 1030 cm^{-1} at 2.5 V potential, indicating that sulfoxide bond formation took place. The change in spectrums at 1030 and 1060 cm^{-1} (shoulder) with applied voltage was not observed in acid free reaction medium (Figure 8.8). Change in the selectivity of product distributions by application of 2.5 V potential can be explained by the formation of sulfonate groups in solid residuals. Moreover, application of voltage resulted in the formation of carboxylic acid (C=O) functional group at stretching vibration of 1705 cm^{-1} (Nakhate and Yadav 2016). Primary alcohol group of cellulose could be oxidized via cyclic or acyclic ways that resulted in formation of carboxylic acid (Figure 8.9), aldehyde and ketone functionality (Rajalaxmi et al. 2010). FTIR spectrum of 2.5 V and 8.0 V (Figure 8.7-B and E) indicated that higher carbonyl band intensity was higher under applied voltage. This intensity was a sign of oxidation of primary or secondary alcohol group of cellulose to carboxylic acid functionality. FTIR spectrums of solid residual also supported the idea of catalytic effect of solid particle within the reaction medium under applied voltage because of formed sulfonated and carboxylic acid groups.

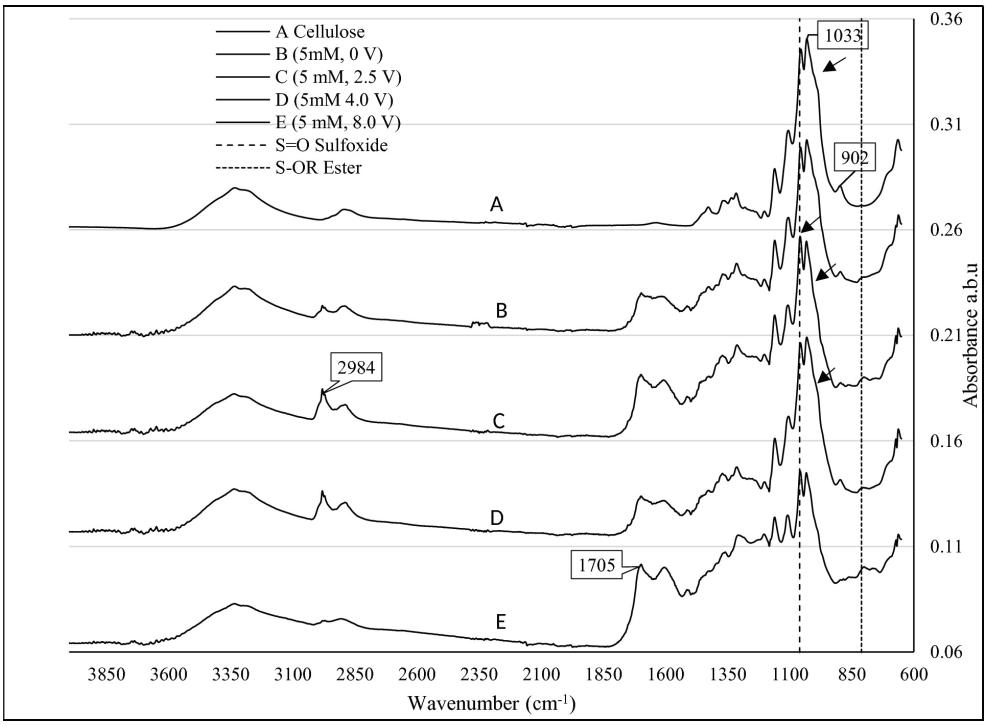

Figure 8.7. FT-IR spectrum of cellulose (A) and solid residue of hydrothermal (B), constant voltage (C, D, E) experiments in 5mM of H_2SO_4.

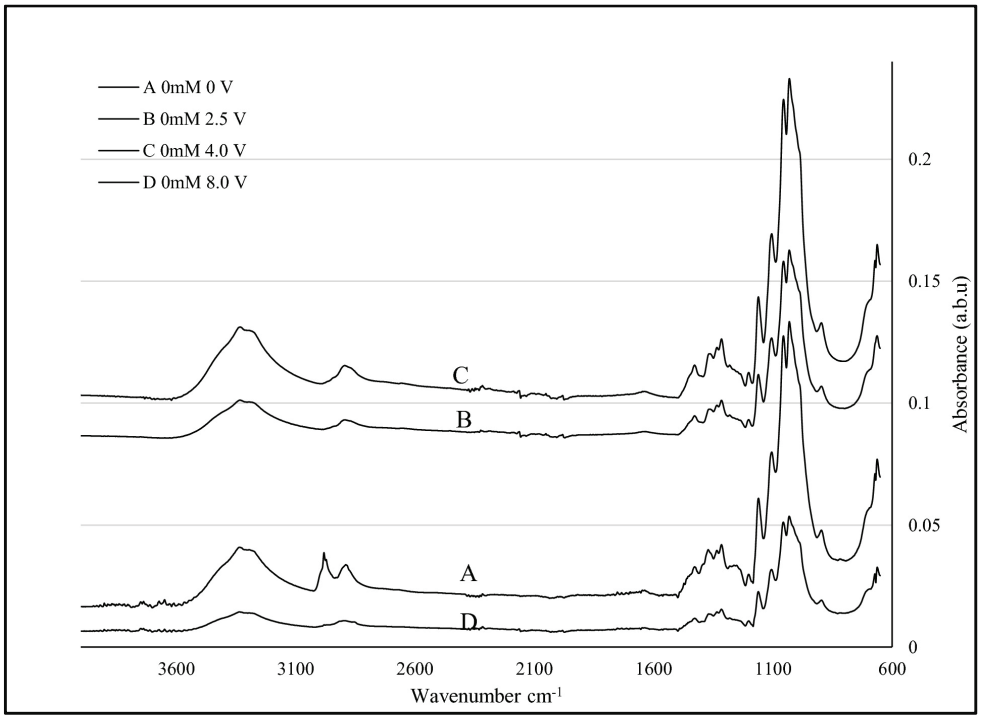

Figure 8.8. FT-IR spectrum of solid residue of hydrothermal (A) and constant voltage (B, C, D) experiments in acid free medium.

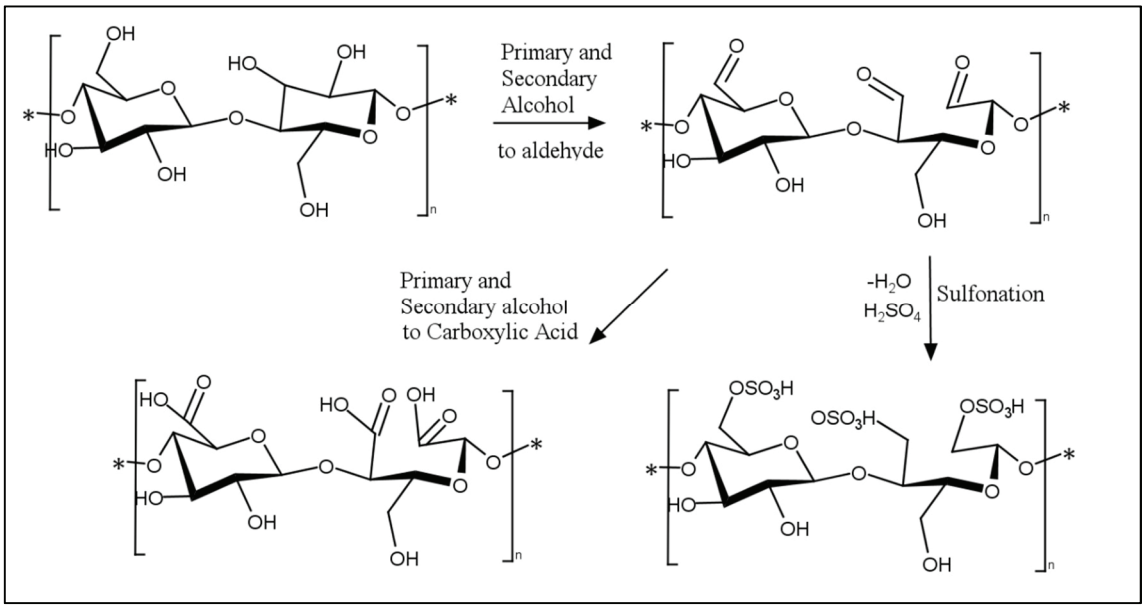

Figure 8.9. Reaction mechanism of carboxylic acid and sulfoxide functional groups by oxidation of primary and secondary alcohol group of cellulose

CHAPTER 9

DETAILED REACTION MECHANISM OF CELLULOSE HYDROLYSIS UNDER APPLIED DIRECT CURRENT

In this chapter, detailed reaction mechanism of microcrystalline cellulose hydrolysis under applied direct current is discussed. Hydrolysis products under application of direct current in constant voltage mode were analyzed by GC-MS analysis. The details of GC-MS analysis and detected product list were given in experimental study section (Chapter 6). Under hydrothermal conditions levulinic acid further involves dehydration and decarboxylation reactions. The detailed discussion is held by investigating the product distribution and effect of applied voltage on product distribution in details.

9.1. Decomposition Reaction Pathway of Cellulose in Hot-Compressed Water by Applied Direct Current

As a result of protonation of β(1-4),glycosidic bond of cellulose, hydrolysis reaction takes place. Under hydrothermal conditions high ionic product concentration of cellulose yield hydrolysis reaction. In our hypothesis, application of voltage under hydrothermal conditions enhance the reaction medium in terms of ionic and radical products. TOC analysis results supports the idea of enhancement in reaction medium since, TOC yield indicates the decomposition of cellulose.

Ionic based decomposition mechanism of cellulose is favored in subcritical water conditions. On the other hand, radical based decomposition mechanism of cellulose is favored in supercritical water conditions (Promdej and Matsumura 2011) and cellobiose decomposition mechanism in sub- and supercritical conditions was also reported in details (Kabyemela et al. 1998). They reported formation of glucosyl-glycoaldehyde, glucosyl-eryhtrose and glycoaldehyde was observed under supercritical water conditions. As the application of constant voltage resulted in formation of ionic and radical species, decomposition mechanism of cellulose via ionic and radical based pathways is postulated (Figure 9.1). It is hard to distinguished the radical and ionic based mechanism due to

common product distribution. The most dramatic change was observed in formation of Levoglucosenone (Figure 9.2). GC-MS results showed that application of 8.0 V maximize the production of Levoglucosenone (Figure 9.2-a) in 5 mM of sulfuric acid reaction medium. The increase in Levoglucosenone concentration along with the TOC yield at 8.0 V indicates that cellulose decomposition pathway altered in a way of radical mechanism. Moreover, application of 8.0 V in 25 mM of sulfuric acid concentration, increase the Levoglucosenone concentration (Figure 9.2-b). Showing that under certain potential decomposition of cellulose favors the radical mechanism.

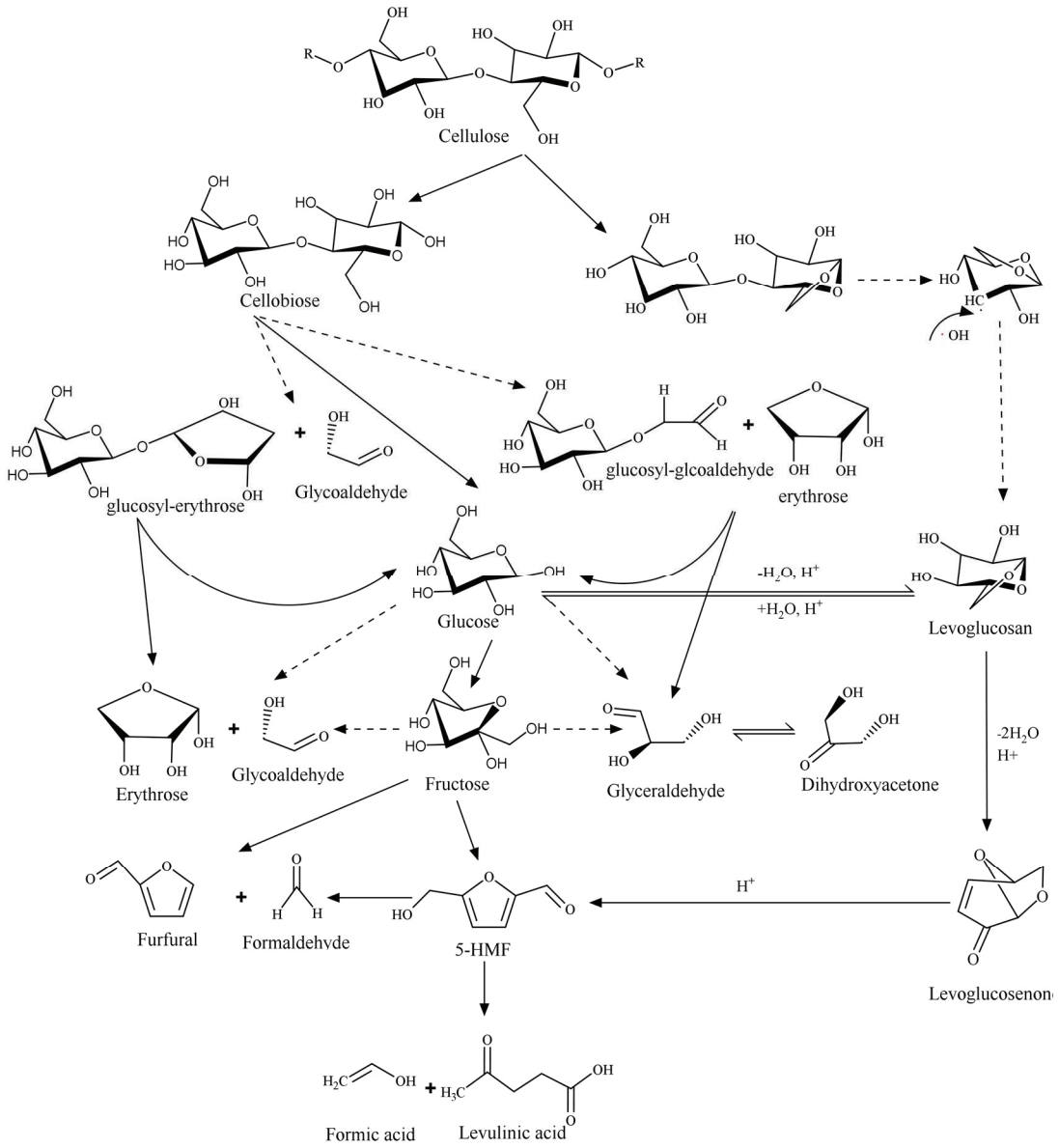

Figure 9.1. Postulated reaction pathways of cellulose decomposition by radical (dashed line arrow) and ionic (solid line arrow) species based mechanism

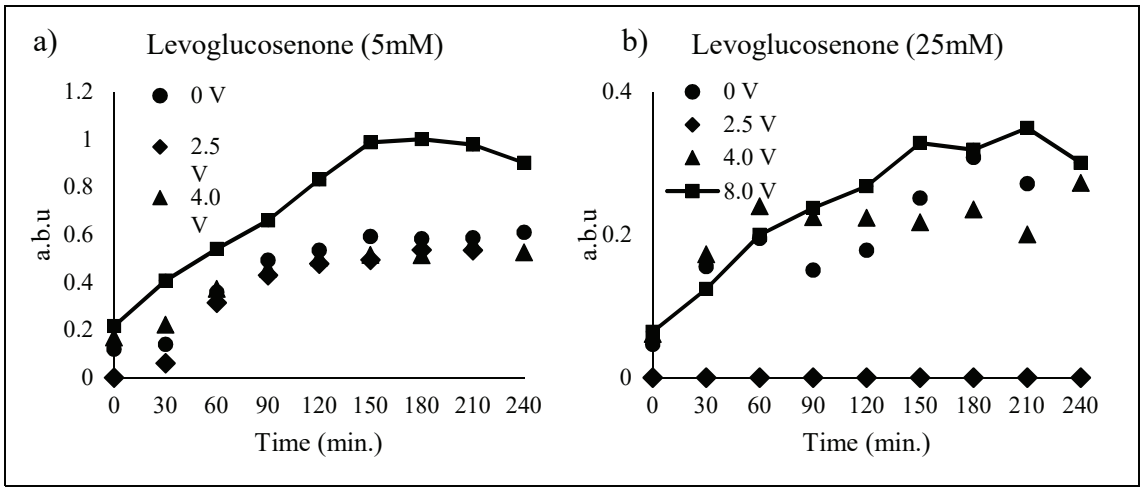

Figure 9.2. GC-MS results of Levoglucosenone formation under applied constant voltage in sulfuric acid concentration of a) 5mM and b) 25 mM

9.2. Further Reactions of Levulinic Acid by Hydrothermal Electrolysis in Hot-Compressed Water

Levulinic acid involves further reactions such as dehydration and decarboxylation under hydrothermal conditions (Figure 9.3). Dehydration of levulinic acid yields to formation of lactones such as β-angelica lactone and α-angelica lactone. As the lactones are unstable in hydrothermal conditions, they polymerize to tarry material. Moreover, hydrogenation of lactones results in the formation of gamma-valerolactone (GVL) and further protonation of GVL yields to 2-pentenoic acid. Methylvinylketone (MVK), 2-butanone are also formed by hydrogenation and dehydration reactions, respectively.

Electrochemical decarboxylation of levulinic acid to 2-butanone is reported by Nilges and coworkers (Nilges et al. 2012). Kolbe reaction of levulinic acid resulted in the decarboxylation via electrochemical reaction pathway and yields to formation of 2-butanone (Figure 9.4).

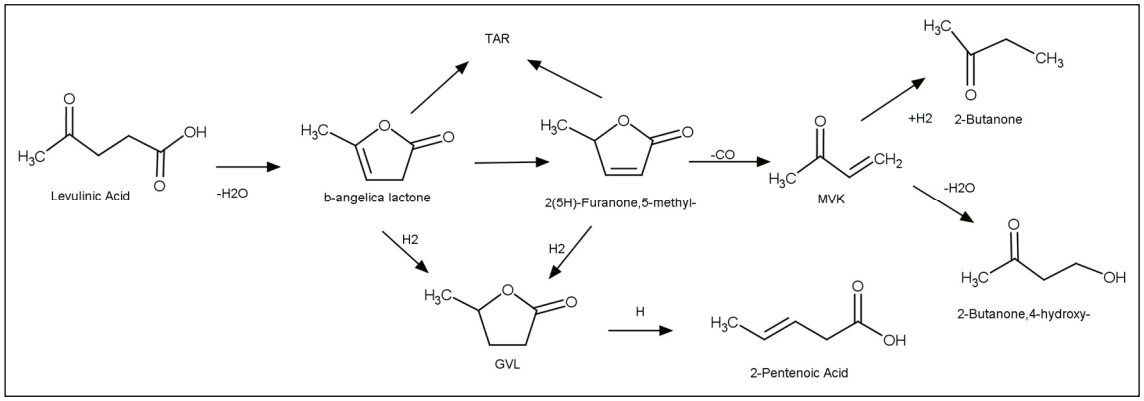

Figure 9.3. Reaction pathway of levulinic acid dehydration reaction under hydrothermal conditions

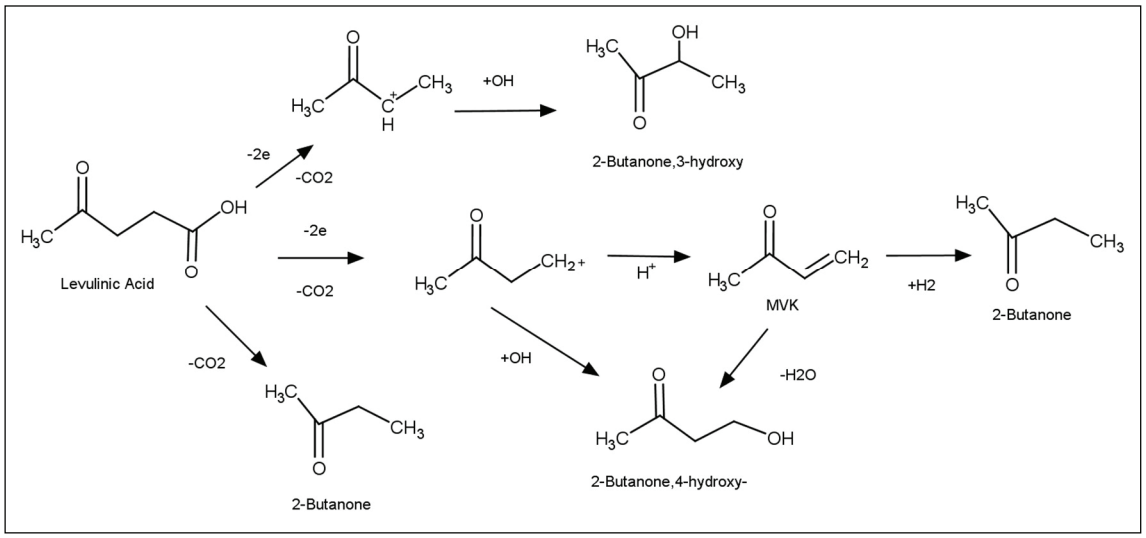

Figure 9.4. Decarboxylation reaction of levulinic acid via electrochemical pathway

Figure 9.5 indicates the formation of products of levulinic acid as a result of dehydration and decarboxylation under hydrothermal electrolysis conditions. Application of 2.5 V of constant voltage resulted in the higher yield in 5 mM of sulfuric acid conditions. As the most significant effect of voltage was observed in 5 mM of sulfuric acid solution, analysis was conducted for the experiments of containing 5 mM electrolyte. The effect of 2.5 V on product distribution is clearly seen in Figure 9.3. GVL was selectively produced by the application of 2.5 V of constant voltage into reaction medium. There was no formation of GVL under hydrothermal and applied voltage values of 4.0 and 8.0. However, degradation product of GVL which is 2-pentanoic acid was formed by applied voltage at 4.0 and 8.0 V. Moreover, 2.5 V of potential difference was resulted in the formation of 2-pentonic acid, however GVL was also formed and its degradation to

2-pentonic acid was hindered by applied voltage at 2.5 V. Increase in the product concentration is mainly due to the high TOC values. Therefore, enhancement in the reaction pathway cannot be conducted clearly, however, formation of GVL at 2.5 V of applied constant voltage supports the idea of enhancement in reaction pathway selectively to production of both GVL and levulinic acid.

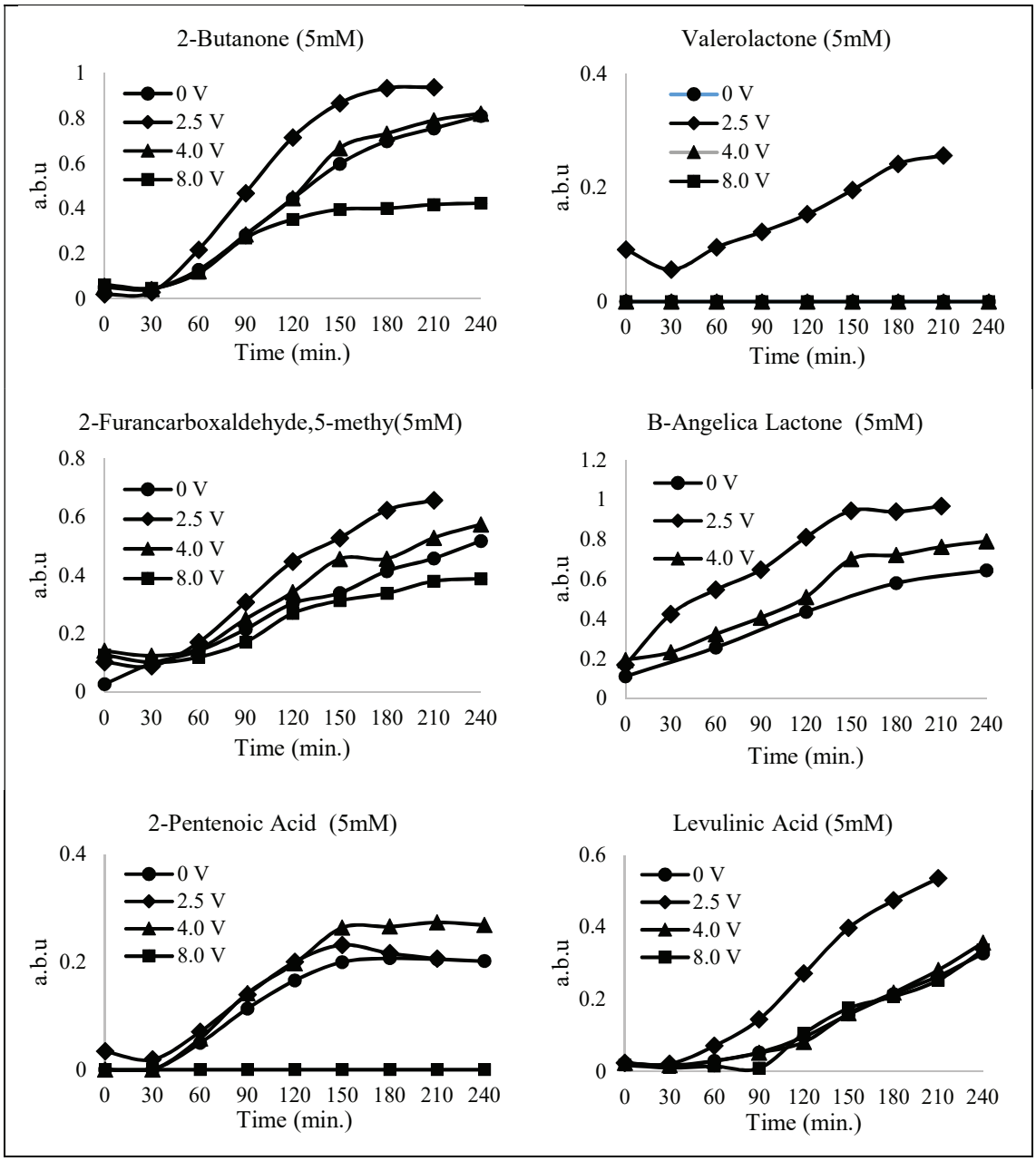

Figure 9.5. GC-MS result of hydrolysis and decarboxylation products of levulinic acid under hydrothermal electrolysis conditions

CHAPTER 10

CONCLUSION

Electrolysis of microcrystalline cellulose in sub-critical water conditions were carried out by application of constant current and constant voltage to the reaction medium. Interaction of constant current with reaction temperature, time and electrolyte concentration was investigated by building ½ fractional factorial design and application of ANOVA test to responses such as product yields, TOC and cellulose conversion. The significance of the interaction indicated that, direct current had major impact on cellulose hydrolysis. Maximum cellulose conversion (82%) was achieved at 230 ºC and 30 minutes of reaction time in 50mM of H_2SO_4. Application of 1 A of applied current to the reaction medium at reaction temperature of 200 ºC increased the TOC conversion (62%) by diminishing the reaction temperature from 230 ºC to 200 ºC and acid concentration from 50 mM to 1 mM in comparison with current-free experiments. Thus, the idea of electrochemically generated acid layer due to the dissociation of water around anode is supported. However, at higher constant current (2A), TOC yield decreased in contrast to an increase in hydrogen production. This can be attributed to increase in hydrolysis reaction rate of water at higher current values. No significant enhancement was achieved in product selectivity values by application of constant current in hydrothermal conditions.

In order to investigate the effect of voltage on product selectivity, electrolysis of MCC were carried out under constant potential range of 2.5 V-8.0 V. Formation of organic compounds (TOC) and product selectivity values were investigated in the presence and absence of electrolyte solution. As an electrolyte sulfuric acid was used in concentration of 5 mM and 25 mM. In the absence of electrolyte, application of voltage (2.5 V and 4.0 V) decreased TOC yield of reaction under hydrothermal conditions. Diverse effect was conducted with the redox reaction of ionic products water, which might hinder the protonation of β-glyosidic bond of cellulose under applied potential. In contrast, higher potential 8.0 V resulted in higher yield of TOC (13%) showing that applied over potential might result in the formation of more reactive species as hydroxyl radical ($OH^{\bullet -}$) that could trigger the cleavage of β-glyosidic bond. Moreover, application of 8.0 V altered the decomposition mechanism to furfural with the increased selectivity

of 13% in comparison to current free experiment (%7). Application of 2.5 V in 5 mM sulfuric acid solution also altered the TOC yield (54%) but most dramatic changes were observed in selectivity values of 5-HMF (30%) and levulinic acid (21%). The change in the selectivity values of degradation products and the structural changes in solid residues of electrochemically reacted MCC was conducted by Fourier Transform Infrared Spectroscopy (FTIR) and it was found that MCC particles functionalized by carboxylic acid and sulfonated groups by the application of constant voltage to reaction medium. Under certain potential difference (2.5 V), functionalization of primary and secondary alcohol groups of cellulose to carboxylic acid and sulfoxide became more obvious in FTIR results. Thus, it was suggested that, functionalization of particles may alter the selectivity of decomposition products of cellulose since formation of sulfoxide and carboxylic acid functionality has catalytic effect on decomposition of cellulose.

REFERENCES

Adschiri, T., S. Hirose, R. Malaluan, and K. Arai. 1993. "Noncatalytic Conversion of Cellulose in Supercritical and Subcritical Water." *Journal of Chemical Engineering of Japan* 26 (6):676-680

.

Ahola, S., X. Turon, M. Osterberg, J. Laine, and O. J. Rojas. 2008. "Enzymatic Hydrolysis of Native Cellulose Nanofibrils and Other Cellulose Model Films: Effect of Surface Structure." *Langmuir* 24 (20):11592-11599.

Aida, T. M., Y. Sato, M. Watanabe, K. Tajima, T. Nonaka, H. Hattori, and K. Arai. 2007. "Dehydration Of D-glucose in high temperature water at pressures up to 80 MPa." *Journal of Supercritical Fluids* 40 (3):381-388.

Akin, Okan, and Asli Yuksel. 2016. "Novel hybrid process for the conversion of microcrystalline cellulose to value-added chemicals: part 1: process optimization." *Cellulose* 23 (6):3475-3493. doi: 10.1007/s10570-016-1054-3.

Alvarez, V. A., and A. Vazquez. 2004. "Thermal degradation of cellulose derivatives/starch blends and sisal fibre biocomposites." *Polymer Degradation and Stability* 84 (1):13-21.

Amarasekara, A. S., and B. Wiredu. 2011. "Degradation of Cellulose in Dilute Aqueous Solutions of Acidic Ionic Liquid 1-(1-Propylsulfonic)-3-methylimidazolium Chloride, and p-Toluenesulfonic Acid at Moderate Temperatures and Pressures." *Industrial & Engineering Chemistry Research* 50 (21):12276-12280.

Annamalai, N., M. V. Rajeswari, and T. Balasubramanian. 2014. "Enzymatic saccharification of pretreated rice straw by cellulase produced from Bacillus carboniphilus CAS 3 utilizing lignocellulosic wastes through statistical optimization." *Biomass & Bioenergy* 68:151-160.

Antal, M. J., W. S. L. Mok, and G. N. Richards. 1990. "Kinetic-Studies of the Reactions of Ketoses and Aldoses in Water at High-Temperature .1. Mechanism of Formation of 5-(Hydroxymethyl)-2-Furaldehyde from D-Fructose and Sucrose." *Carbohydrate Research* 199 (1):91-109.

Asghari, F. S., and H. Yoshida. 2008. "Electrodecomposition in subcritical water using o-xylene as a model for benzene, toluene, ethylbenzene, and xylene pollutants." *Journal of Physical Chemistry A* 112 (32):7402-7410.

Ashadi, R. W., K. Shimokawa, and K. Ogawa. 1996. "The mechanism of enzymatic cellulose degradation .1. Purification and some properties of cellulolytic enzymes from Aspergillus niger UC." *Journal of General and Applied Microbiology* 42 (2):93-102.

Badgujar, K. C., and B. M. Bhanage. 2016. "The green metric evaluation and synthesis of diesel-blend compounds from biomass derived levulinic acid in supercritical carbon dioxide." *Biomass & Bioenergy* 84:12-21.

Bandura, Andrei V., and Serguei N. Lvov. 2006. "The Ionization Constant of Water over Wide Ranges of Temperature and Density." *Journal of Physical and Chemical Reference Data* 35 (1):15-30. doi: 10.1063/1.1928231.

Bodirlau, R., I. Spiridon, and C. A. Teaca. 2010. "Enzymatic Degradation of LDPE / Corn Starch Blends Treated with [EMIM][Cl] Ionic Liquid." *Materiale Plastice* 47 (2):126-129.

Brunner, G. 2009. "Near critical and supercritical water. Part I. Hydrolytic and hydrothermal processes." *Journal of Supercritical Fluids* 47 (3):373-381.

Brunner, Gerd. 2014. *Hydrothermal and Supercritical Water Processes*, *Supercritical Fluid Science and Technology*. Burlington: Elsevier. Book.

Cantero, D. A., M. D. Bermejo, and M. J. Cocero. 2013. "Kinetic analysis of cellulose depolymerization reactions in near critical water." *Journal of Supercritical Fluids* 75:48-57.

Cantero, D. A., M. D. Bermejo, and M. J. Cocero. 2015. "Governing Chemistry of Cellulose Hydrolysis in Supercritical Water." *Chemsuschem* 8 (6):1026-1033.

Cao, X., X. Peng, S. Sun, L. Zhong, W. Chen, S. Wang, and R. C. Sun. 2015. "Hydrothermal conversion of xylose, glucose, and cellulose under the catalysis of transition metal sulfates." *Carbohydr Polym* 118:44-51. doi: 10.1016/j.carbpol.2014.10.069.

Castello, D., A. Kruse, and L. Fiori. 2013. "Biomass gasification in supercritical and subcritical water: The effect of the reactor material." *Chemical Engineering Journal* 228:535-544.

Chen, S. L., and D. B. Wilson. 2007. "Proteomic and transcriptomic analysis of extracellular proteins and mRNA levels in Thermobifida fusca grown on cellobiose and glucose." *Journal of Bacteriology* 189 (17):6260-6265.

Chen, Y., G. Li, F. Yang, and S. M. Zhang. 2011. "Mn/ZSM-5 participation in the degradation of cellulose under phosphoric acid media." *Polymer Degradation and Stability* 96 (5):863-869.

Chung, C., M. Lee, and E. K. Choe. 2004. "Characterization of cotton fabric scouring by FT-IR ATR spectroscopy." *Carbohydrate Polymers* 58 (4):417-420.

Chuntanapum, A., and Y. Matsumura. 2009. "Formation of Tarry Material from 5-HMF in Subcritical and Supercritical Water." *Industrial & Engineering Chemistry Research* 48 (22):9837-9846.

Chuntanapum, A., T. Shii, and Y. Matsumura. 2011. "Acid-Catalyzed Char Formation from 5-HMF in Subcritical Water." *Journal of Chemical Engineering of Japan* 44 (6):431-436.

Chuntanapum, A., T. L. K. Yong, S. Miyake, and Y. Matsumura. 2008. "Behavior of 5-HMF in subcritical and supercritical water." *Industrial & Engineering Chemistry Research* 47 (9):2956-2962.

Connors, KA. 1990. "Chemical Kinetics: The Study of Reaction Rates in Solution; VCH: New York, 1990." *There is no corresponding record for this reference*:99-101.

Davis, J., J. C. Baygents, and J. Farrell. 2014. "Understanding Persulfate Production at Boron Doped Diamond Film Anodes." *Electrochimica Acta* 150:68-74.

Dibenedetto, A., M. Aresta, C. Pastore, L. di Bitonto, A. Angelini, and E. Quaranta. 2015. "Conversion of fructose into 5-HMF: a study on the behaviour of heterogeneous cerium-based catalysts and their stability in aqueous media under mild conditions." *Rsc Advances* 5 (34):26941-26948.

Ding, H. Z., and Z. D. Wang. 2008. "On the degradation evolution equations of cellulose." *Cellulose* 15 (2):205-224.

Dinjus, E., and A. Kruse. 2004. "Hot compressed water - a suitable and sustainable solvent and reaction medium?" *Journal of Physics-Condensed Matter* 16 (14):S1161-S1169.

dos Santos, T. R., P. Nilges, W. Sauter, F. Harnisch, and U. Schroder. 2015. "Electrochemistry for the generation of renewable chemicals: electrochemical conversion of levulinic acid." *Rsc Advances* 5 (34):26634-26643.

Franck, E. U. 1970. Water and aqueous solutions at high pressures and temperatures. In *Pure and Applied Chemistry*.

Gao, Y., X. H. Wang, H. P. Yang, and H. P. Chen. 2012. "Characterization of products from hydrothermal treatments of cellulose." *Energy* 42 (1):457-465.

Goto, M., and Y. Yokoe. 1996. "Ammoniation of barley straw. Effect on cellulose crystallinity and water-holding capacity." *Animal Feed Science and Technology* 58 (3-4):239-247.

Harvey, Allan H., and Daniel G. Friend. 2004. "Chapter 1 - Physical properties of water⋆." In *Aqueous Systems at Elevated Temperatures and Pressures*, 1-27. London: Academic Press.

Jeong, T. S., B. H. Um, J. S. Kim, and K. K. Oh. 2010. "Optimizing Dilute-Acid Pretreatment of Rapeseed Straw for Extraction of Hemicellulose." *Applied Biochemistry and Biotechnology* 161 (1-8):22-33.

Jitaru, M., D. A. Lowy, M. Toma, B. C. Toma, and L. Oniciu. 1997. "Electrochemical reduction of carbon dioxide on flat metallic cathodes." *Journal of Applied Electrochemistry* 27 (8):875-889. doi: 10.1023/a:1018441316386.

Kabyemela, B. M., T. Adschiri, R. M. Malaluan, and K. Arai. 1999. "Glucose and fructose decomposition in subcritical and supercritical water: Detailed reaction pathway, mechanisms, and kinetics." *Industrial & Engineering Chemistry Research* 38 (8):2888-2895.

Kang, S. M., J. Ye, Y. Zhang, and J. Chang. 2013. "Preparation of biomass hydrochar derived sulfonated catalysts and their catalytic effects for 5-hydroxymethylfurfural production." *Rsc Advances* 3 (20):7360-7366.

Kilic, E., and S. Yilmaz. 2015. "Fructose Dehydration to 5-Hydroxymethylfurfural over Sulfated TiO2-SiO2, Ti-SBA-15, ZrO2, SiO2, and Activated Carbon Catalysts." *Industrial & Engineering Chemistry Research* 54 (19):5220-5225.

Klingler, D., and H. Vogel. 2010. "Influence of process parameters on the hydrothermal decomposition and oxidation of glucose in sub- and supercritical water." *Journal of Supercritical Fluids* 55 (1):259-270.

Knezevic, D., W. P. M. van Swaaij, and S. R. A. Kersten. 2009. "Hydrothermal Conversion of Biomass: I, Glucose Conversion in Hot Compressed Water." *Industrial & Engineering Chemistry Research* 48 (10):4731-4743.

Kruse, A., and E. Dinjus. 2007. "Hot compressed water as reaction medium and reactant - Properties and synthesis reactions." *Journal of Supercritical Fluids* 39 (3):362-380.

K. Liu, Zur Hydrolyse von Biopolymeren in Wasser und Kohlendioxid unter erho¨hten Dru¨cken und Temperaturen, Ph.D. Dissertation, Hamburg University of Technology, Hamburg, Germany, 2000

Lee, Y. H., M. M. Gharpuray, and L. T. Fan. 1982. "Reactor Optimization for Enzymatic-Hydrolysis of Cellulose." *Biotechnology and Bioengineering*:121-138.

Li, J., Y. B. Huang, Q. X. Guo, and Y. Fu. 2014. "Production of Acetic Acid from Lignocellulosic Biomass in the Presence of Mineral Acid and Oxygen under Hydrothermal Condition." *Acta Chimica Sinica* 72 (12):1223-1227.

Li, M. H., W. Z. Li, Y. J. Lu, H. Jameel, H. M. Chang, and L. L. Ma. 2017. "High conversion of glucose to 5-hydroxymethylfurfural using hydrochloric acid as a catalyst and sodium chloride as a promoter in a water/gamma-valerolactone system." *Rsc Advances* 7 (24):14330-14336.

Luijkx, Gerard C. A., Fred van Rantwijk, and Herman van Bekkum. 1993. "Hydrothermal formation of 1,2,4-benzenetriol from 5-hydroxymethyl-2-furaldehyde and d-fructose." *Carbohydrate Research* 242:131-139.

Marshall, W. L., and E. U. Franck. 1981a. "Ion Product of Water Substance, O-Degrees-C-1000-Degrees-C, 1-10,000 Bars - New International Formulation and Its Background." *Journal of Physical and Chemical Reference Data* 10 (2):295-304.

Marshall, W.L., and E.U. Franck. 1981b. "Ion product of water substance, 0--1000 /sup 0/C, 1--10,000 bars New International Formulation and its background." *J. Phys. Chem. Ref. Data; (United States)*:Medium: X; Size: Pages: 295-304.

Nagamori, M., and T. Funazukuri. 2004. "Glucose production by hydrolysis of starch under hydrothermal conditions." *Journal of Chemical Technology and Biotechnology* 79 (3):229-233.

Nakhate, A. V., and G. D. Yadav. 2016. "Synthesis and Characterization of Sulfonated Carbon-Based Graphene Oxide Monolith by Solvothermal Carbonization for Esterification and Unsymmetrical Ether Formation." *Acs Sustainable Chemistry & Engineering* 4 (4):1963-1973.

Nilges, P., T. R. dos Santos, F. Harnisch, and U. Schroder. 2012. "Electrochemistry for biofuel generation: Electrochemical conversion of levulinic acid to octane." *Energy & Environmental Science* 5 (1):5231-5235.

Oomori, T., S. H. Khajavi, Y. Kimura, S. Adachi, and R. Matsuno. 2004. "Hydrolysis of disaccharides containing glucose residue in subcritical water." *Biochemical Engineering Journal* 18 (2):143-147.

Pasangulapati, V., K. D. Ramachandriya, A. Kumar, M. R. Wilkins, C. L. Jones, and R. L. Huhnke. 2012. "Effects of cellulose, hemicellulose and lignin on thermochemical conversion characteristics of the selected biomass." *Bioresource Technology* 114:663-669.

Pearson, Ralph G. 1981. *Kinetics and mechanism*: New York : Wiley, c1981. 3rd ed. Book.

Peterson, A. A., F. Vogel, R. P. Lachance, M. Froling, M. J. Antal, and J. W. Tester. 2008. "Thermochemical biofuel production in hydrothermal media: A review of sub- and supercritical water technologies." *Energy & Environmental Science* 1 (1):32-65.

Pinkowska, H., P. Wolak, and A. Zlocinska. 2011. "Hydrothermal decomposition of xylan as a model substance for plant biomass waste - Hydrothermolysis in subcritical water." *Biomass & Bioenergy* 35 (9):3902-3912.

Pospisil, L., R. Trskova, R. Fuoco, and M. P. Colombini. 1995. "Electrochemistry of S-Triazine Herbicides - Reduction of Atrazine and Terbutylazine in Aqueous-Solutions." *Journal of Electroanalytical Chemistry* 395 (1-2):189-193.

Prado, J. M., T. Forster-Carneiro, M. A. Rostagno, L. A. Follegatti-Romero, F. Maugeri, and M. A. A. Meireles. 2014. "Obtaining sugars from coconut husk, defatted grape seed, and pressed palm fiber by hydrolysis with subcritical water." *Journal of Supercritical Fluids* 89:89-98.

Promdej, C., and Y. Matsumura. 2011. "Temperature Effect on Hydrothermal Decomposition of Glucose in Sub- And Supercritical Water." *Industrial & Engineering Chemistry Research* 50 (14):8492-8497.

Qi, X. H., H. X. Guo, L. Y. Li, and R. L. Smith. 2012. "Acid-Catalyzed Dehydration of Fructose into 5-Hydroxymethylfurfural by Cellulose-Derived Amorphous Carbon." *Chemsuschem* 5 (11):2215-2220.

Radha, K. V., V. Sridevi, and K. Kalaivani. 2009. "Electrochemical oxidation for the treatment of textile industry wastewater." *Bioresource Technology* 100 (2):987-990.

Rajalaxmi, D., N. Jiang, G. Leslie, and A. J. Ragauskas. 2010. "Synthesis of novel water-soluble sulfonated cellulose." *Carbohydrate Research* 345 (2):284-290.

Rajkumar, D., and K. Palanivelu. 2004. "Electrochemical treatment of industrial wastewater." *Journal of Hazardous Materials* 113 (1-3):123-129.

Resende, F. L. P., and P. E. Savage. 2010. "Kinetic Model for Noncatalytic Supercritical Water Gasification of Cellulose and Lignin." *AIChE Journal* 56 (9):2412-2420.

Rogalinski, T., K. Liu, T. Albrecht, and G. Brunner. 2008. "Hydrolysis kinetics of biopolymers in subcritical water." *Journal of Supercritical Fluids* 46 (3):335-341.

Rossmeisl, J., A. Logadottir, and J. K. Nørskov. 2005. "Electrolysis of water on (oxidized) metal surfaces." *Chemical Physics* 319 (1–3):178-184. doi: http://dx.doi.org/10.1016/j.chemphys.2005.05.038.

Saito, T., M. Sasaki, H. Kawanabe, Y. Yoshino, and M. Goto. 2009. "Subcritical Water Reaction Behavior of D-Glucose as a Model Compound for Biomass Using Two Different Continuous-Flow Reactor Configurations." *Chemical Engineering & Technology* 32 (4):527-533.

Sasaki, M., B. Kabyemela, R. Malaluan, S. Hirose, N. Takeda, T. Adschiri, and K. Arai. 1998. "Cellulose hydrolysis in subcritical and supercritical water." *Journal of Supercritical Fluids* 13 (1-3):261-268.

Sasaki, M., Z. Fang, Y. Fukushima, T. Adschiri, and K. Arai. 2000. "Dissolution and hydrolysis of cellulose in subcritical and supercritical water." *Industrial & Engineering Chemistry Research* 39 (8):2883-2890.

Sasaki, M., T. Adschiri, and K. Arai. 2004. "Kinetics of cellulose conversion at 25 MPa in sub- and Supercritical water." *AIChE Journal* 50 (1):192-202.

Sasaki, M., K. Yamamoto, M. Sakaguchi, M. Goto, and T. Hirose. 2005. "Hydrothermal decomposition and electrolysis of bio-related materials." *Abstracts of Papers of the American Chemical Society* 229:U284-U284.

Sasaki, M., Wahyudiono, A. Yuksel, and M. Goto. 2010. "Applications of hydrothermal electrolysis for conversion of 1-butanol in wastewater treatment." *Fuel Processing Technology* 91 (9):1125-1132.

Sasaki, M., T. Oshikawa, H. Watanabe, Wahyudiono, and M. Goto. 2011. "Reaction kinetics and mechanism for hydrothermal degradation and electrolysis of glucose for producing carboxylic acids." *Research on Chemical Intermediates* 37 (2-5):457-466.

Savage, Phillip E., Sudhama Gopalan, Thamid I. Mizan, Christopher J. Martino, and Eric E. Brock. 1995. "Reactions at supercritical conditions: Applications and fundamentals." *AIChE Journal* 41 (7):1723-1778. doi: 10.1002/aic.690410712.

Schwald, W., and O. Bobleter. 1989. "Hydrothermolysis of Cellulose under Static and Dynamic Conditions at High-Temperatures." *Journal of Carbohydrate Chemistry* 8 (4):565-578.

Shen, Z. Q., X. M. Yu, and J. Z. Chen. 2016. "Production of 5-Hydroxymethylfurfural from Fructose Catalyzed by Sulfonated Bamboo-Derived Carbon Prepared by Simultaneous Carbonization and Sulfonation." *Bioresources* 11 (2):3094-3109.

S. Noguchi, R. Uehara, M. Sasaki, M. Goto, "Thermal stability of monosaccharides in subcritical water." *Proceedings 8th International Symposium on Supercritical Fluids*, November 5–8, Kyoto, Japan; Paper PB 2-47, 2006.

Swift, T. D., C. Bagia, V. Choudhary, G. Peklaris, V. Nikolalds, and D. G. Vlachos. 2014. "Kinetics of Homogeneous Bronsted Acid Catalyzed Fructose Dehydration and 5-Hydroxymethyl Furfural Rehydration: A Combined Experimental and Computational Study." *Acs Catalysis* 4 (1):259-267.

Tolonen, L. K., M. Juvonen, K. Niemela, A. Mikkelson, M. Tenkanen, and H. Sixta. 2015. "Supercritical water treatment for cello-oligosaccharide production from microcrystalline cellulose." *Carbohydrate Research* 401:16-23.

Uematsu, M., and E. U. Frank. 1980. "Static Dielectric Constant of Water and Steam." *Journal of Physical and Chemical Reference Data* 9 (4):1291-1306. doi: 10.1063/1.555632.

Waldvogel, Siegfried R. 2015. "Fundamentals and Applications of Organic Electrochemistry. Synthesis, Materials, Devices. By Toshio Fuchigami, Mahito Atobe and Shinsuke Inagi." *Angewandte Chemie International Edition* (34):9751. doi: 10.1002/anie.201505828.

Watanabe, M., T. Sato, H. Inomata, R. L. Smith, K. Arai, A. Kruse, and E. Dinjus. 2004. "Chemical reactions of C-1 compounds in near-critical and supercritical water." *Chemical Reviews* 104 (12):5803-5821.

Wu, L. L., M. Mascal, T. J. Farmer, S. P. Arnaud, and M. A. W. Chang. 2017. "Electrochemical Coupling of Biomass-Derived Acids: New C-8 Platforms for Renewable Polymers and Fuels." *Chemsuschem* 10 (1):166-170.

Wu, Y. Y., Z. H. Fu, D. L. Yin, Q. Xu, F. L. Liu, C. L. Lu, and L. Q. Mao. 2010. "Microwave-assisted hydrolysis of crystalline cellulose catalyzed by biomass char sulfonic acids." *Green Chemistry* 12 (4):696-700.

Xu, B., B. G. Zhang, M. Li, W. W. Huang, N. Chen, C. P. Feng, and L. J. Yao. 2014. "Production of reducing sugars from corn stover by electrolysis." *Journal of Applied Electrochemistry* 44 (7):797-806.

Yan, X. Y., F. M. Jin, K. Tohji, A. Kishita, and H. Enomoto. 2010. "Hydrothermal Conversion of Carbohydrate Biomass to Lactic Acid." *AIChE Journal* 56 (10):2727-2733.

Yin, S. D., and Z. C. Tan. 2012. "Hydrothermal liquefaction of cellulose to bio-oil under acidic, neutral and alkaline conditions." *Applied Energy* 92:234-239.

Yu, J. C., M. M. Baizer, and K. Nobe. 1988. "Electrochemical Generated Acid Catalysis of Cellulose Hydrolysis." *Journal of the Electrochemical Society* 135 (1):83-87.

Yuksel, A., M. Sasaki, and M. Goto. 2011. "A new green technology: hydrothermal electrolysis for the treatment of biodiesel wastewater." *Research on Chemical Intermediates* 37 (2-5):131-143.

Zhang, Y. M., Y. Peng, X. L. Yin, Z. H. Liu, and G. Li. 2014. "Degradation of lignin to BHT by electrochemical catalysis on Pb/PbO2 anode in alkaline solution." *Journal of Chemical Technology and Biotechnology* 89 (12):1954-1960.

Zheng, X. J., X. C. Gu, Y. Ren, Z. H. Zhi, and X. B. Lu. 2016. "Production of 5-hydroxymethyl furfural and levulinic acid from lignocellulose in aqueous solution and different solvents." *Biofuels Bioproducts & Biorefining-Biofpr* 10 (6):917-931.

Zhu, G. Y., Y. H. Ma, and X. Zhu. 2010. "Reactions of Cellulose in Supercritical Water." *Chinese Journal of Organic Chemistry* 30 (1):142-148.

APPENDIX A

HIGH PRESSURE LIQUID CHROMOTOGRAM CALIBRATION

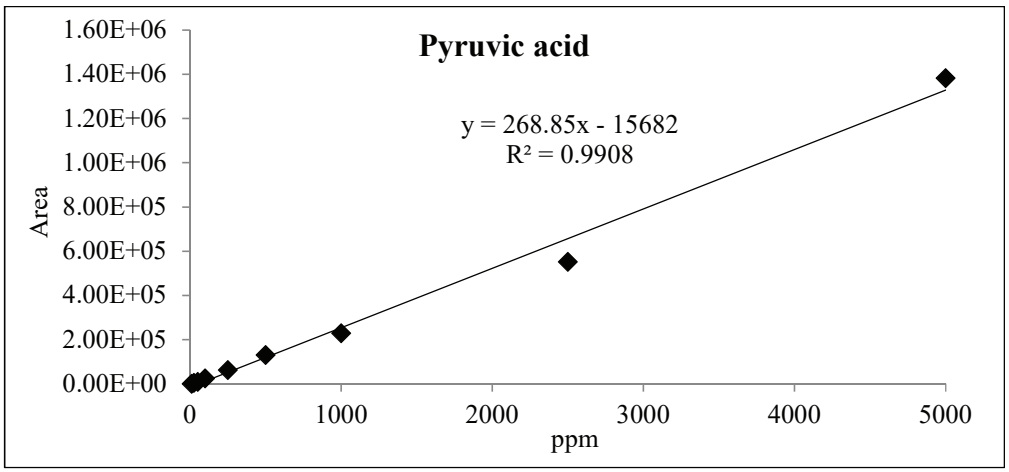

Figure A.1. HPLC calibration curve and fitting line equation of pyruvic acid

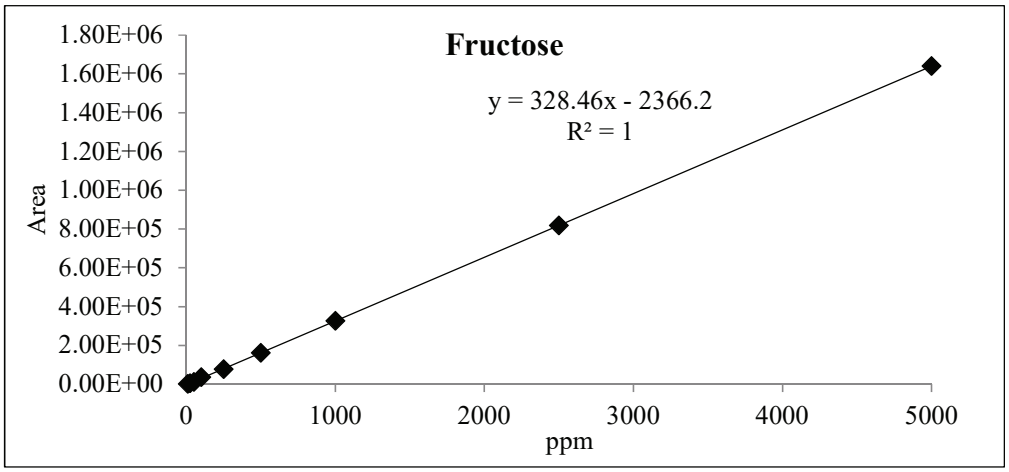

Figure A.2. HPLC calibration curve and fitting line equation of fructose

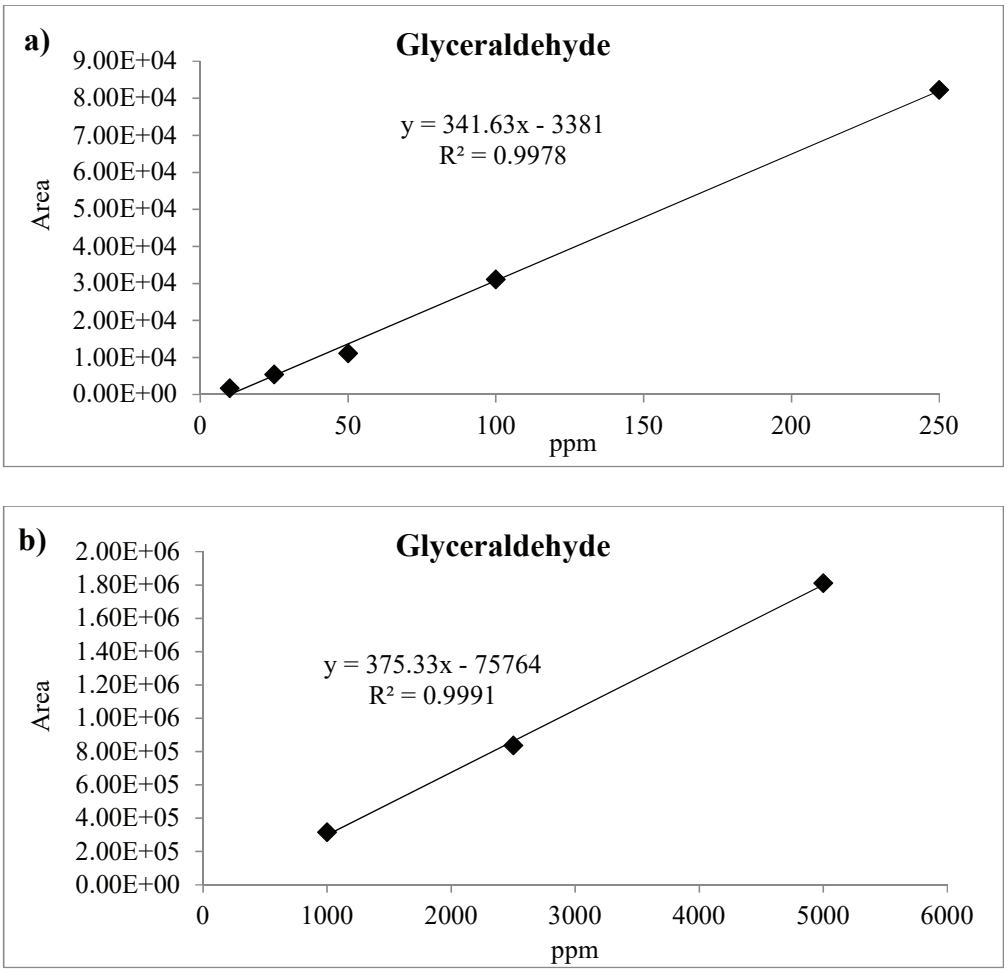

Figure A.3. HPLC calibration curve and fitting line equation of glyceraldehyde a)10-250 ppm, b) 1000-5000 ppm

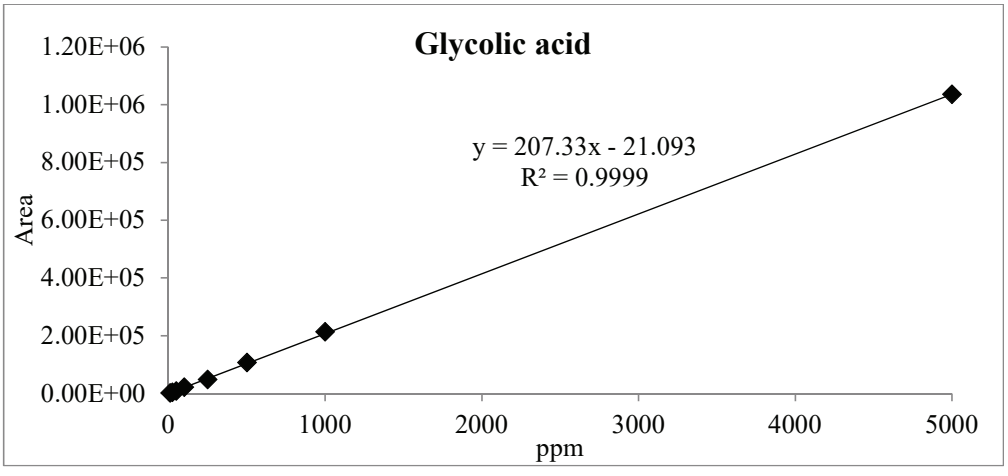

Figure A.4. HPLC calibration curve and fitting line equation of glycolic acid

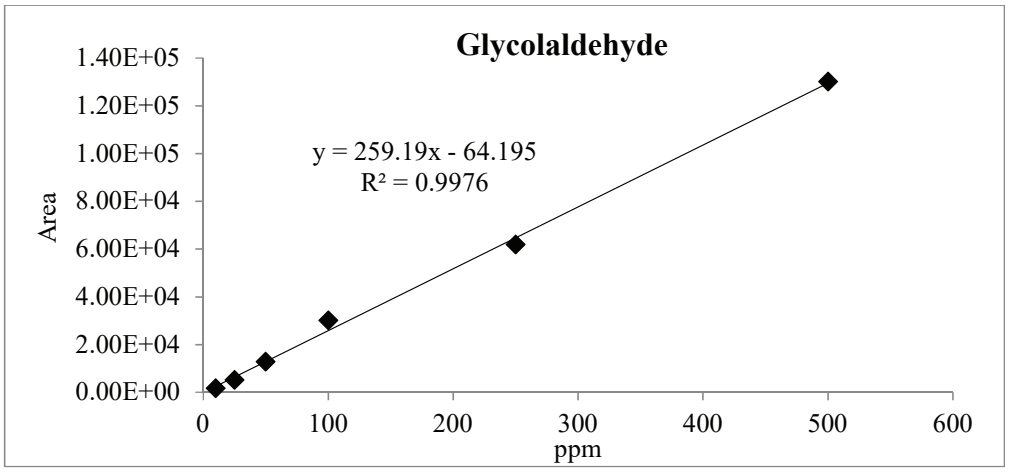

Figure A.5. HPLC calibration curve and fitting line equation of glycoaldehyde

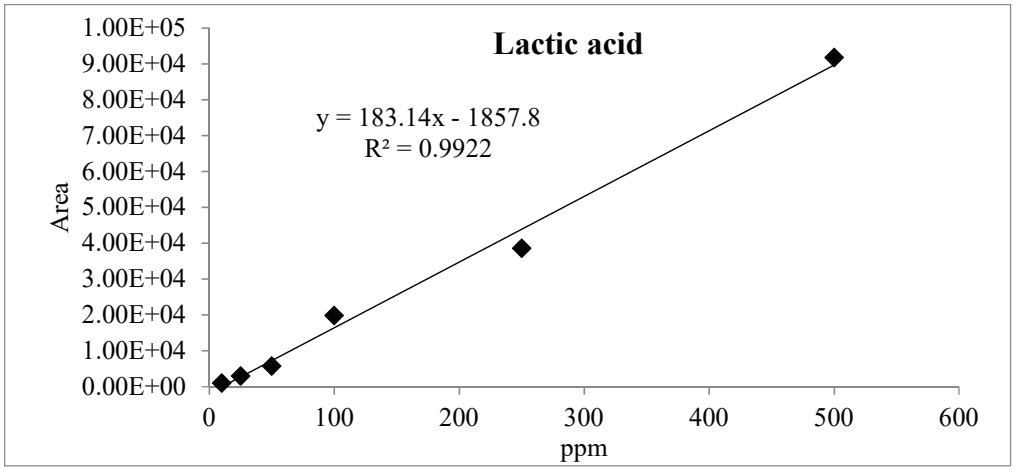

Figure A.6. HPLC calibration curve and fitting line equation of lactic acid

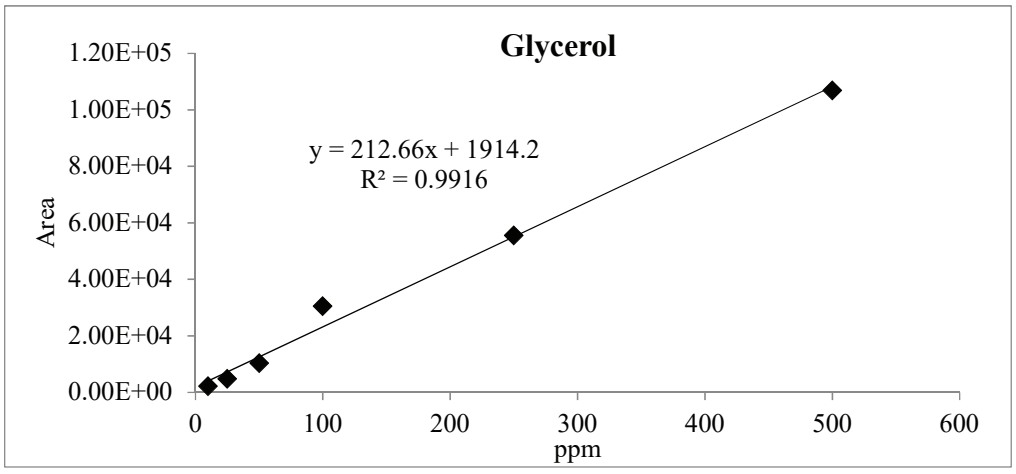

Figure A.7. HPLC calibration curve and fitting line equation of glycerol

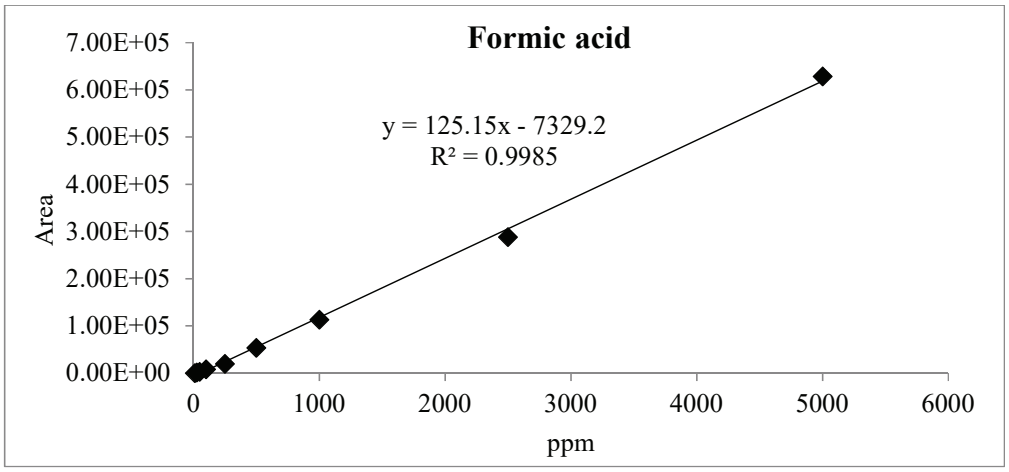

Figure A.8. HPLC calibration curve and fitting line equation of formic acid

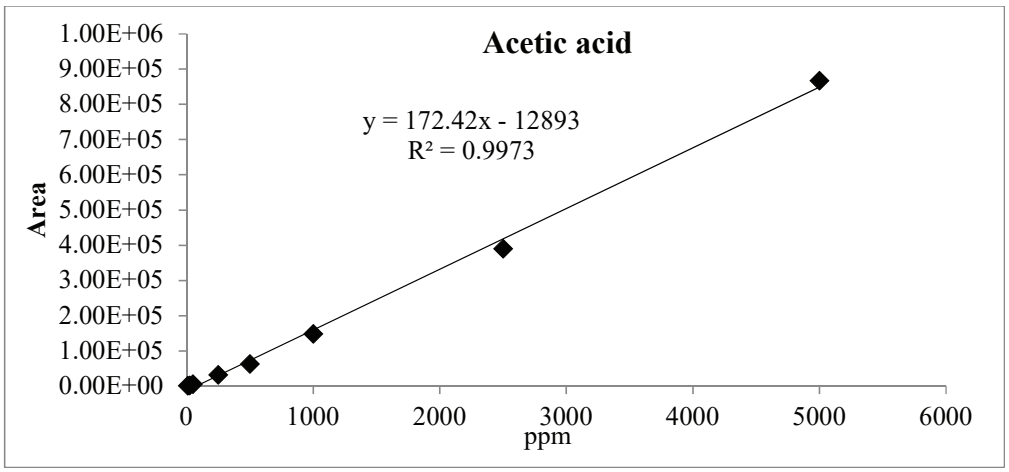

Figure A.9. HPLC calibration curve and fitting line equation of acetic acid

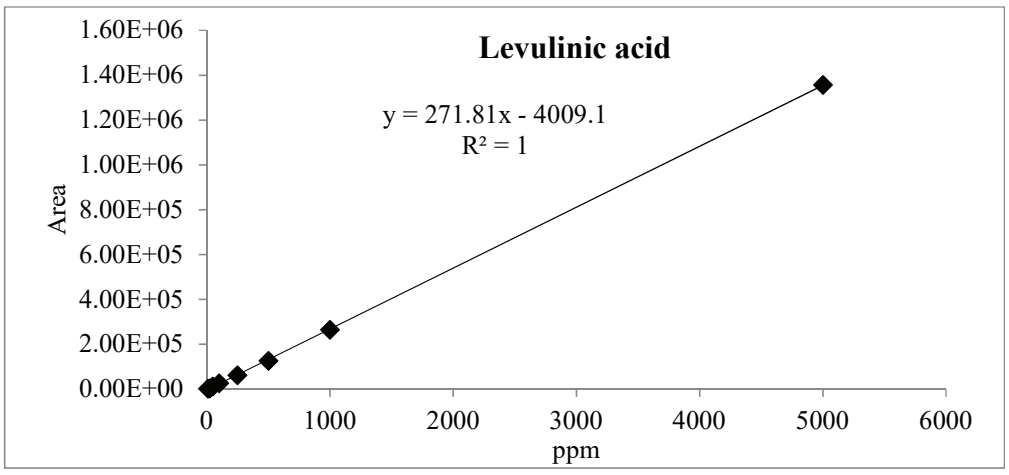

Figure A.10. HPLC calibration curve and fitting line equation of levulinic acid

APPENDIX B

RESIDUAL PLOTS

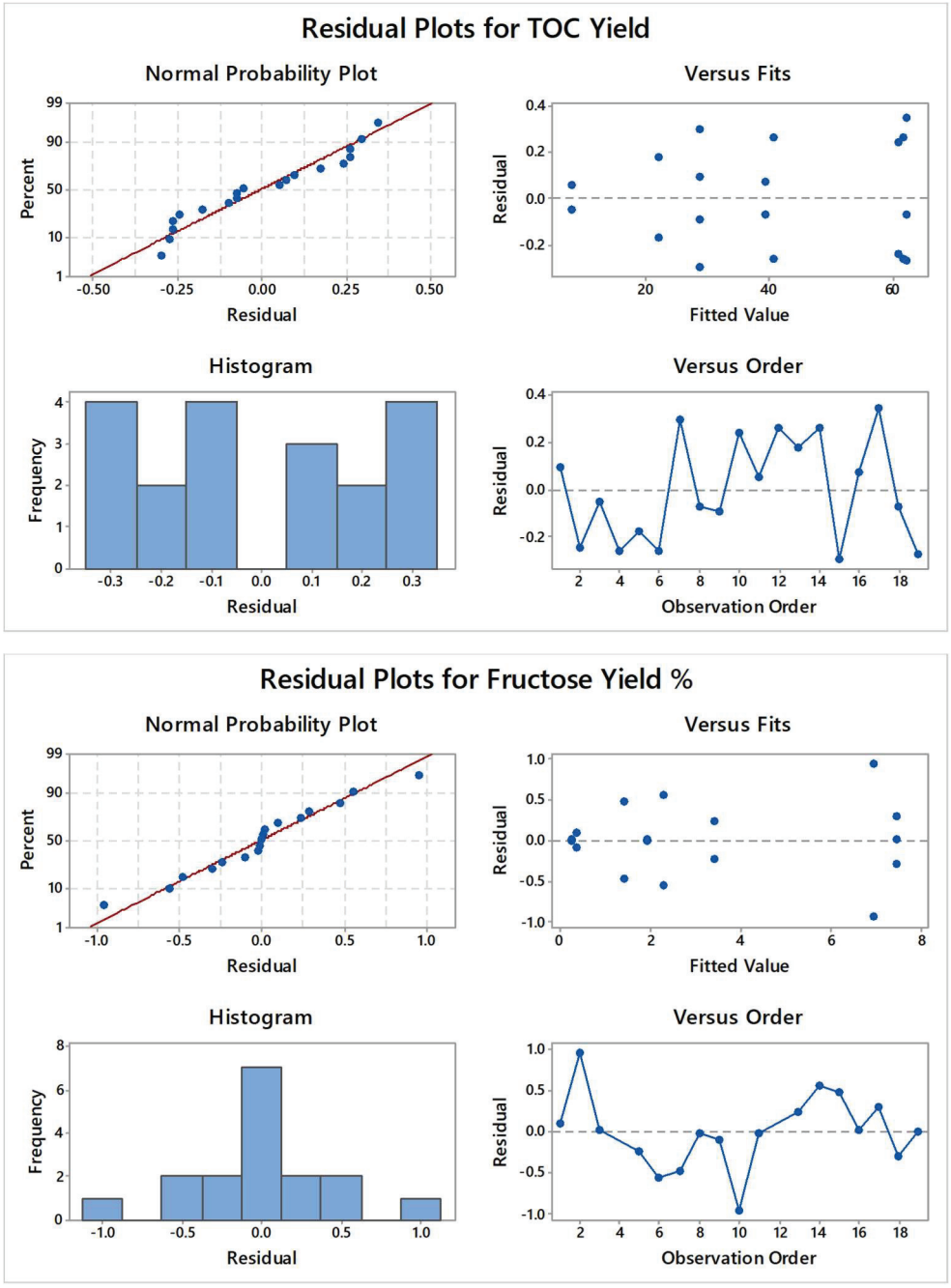

Figure B.1. Residual plots of a) TOC yield, and b) Fructose yield

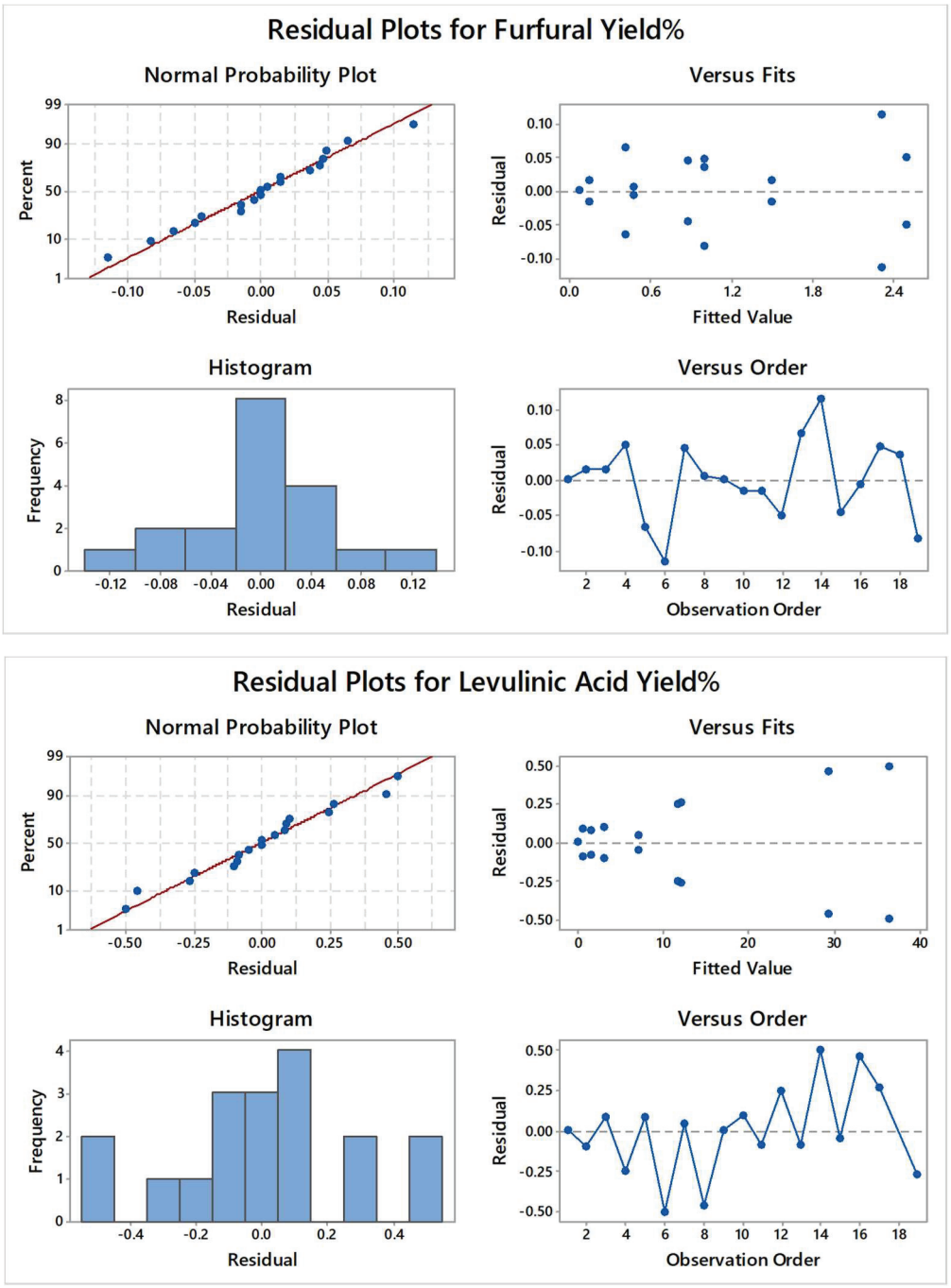

Figure B.2. Residual plots of a) Furfural, and b) Levulinic acid yields

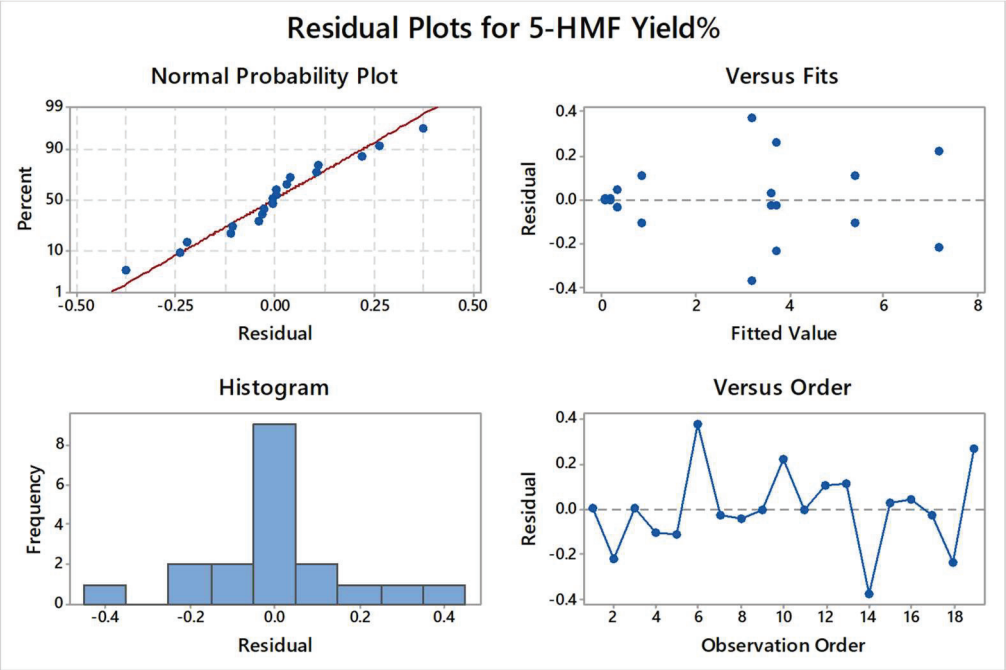

Figure B.3. Residual plots for 5-HMF yield

APPENDIX C

SAMPLE CALCULATION OF HPLC ANALYSIS

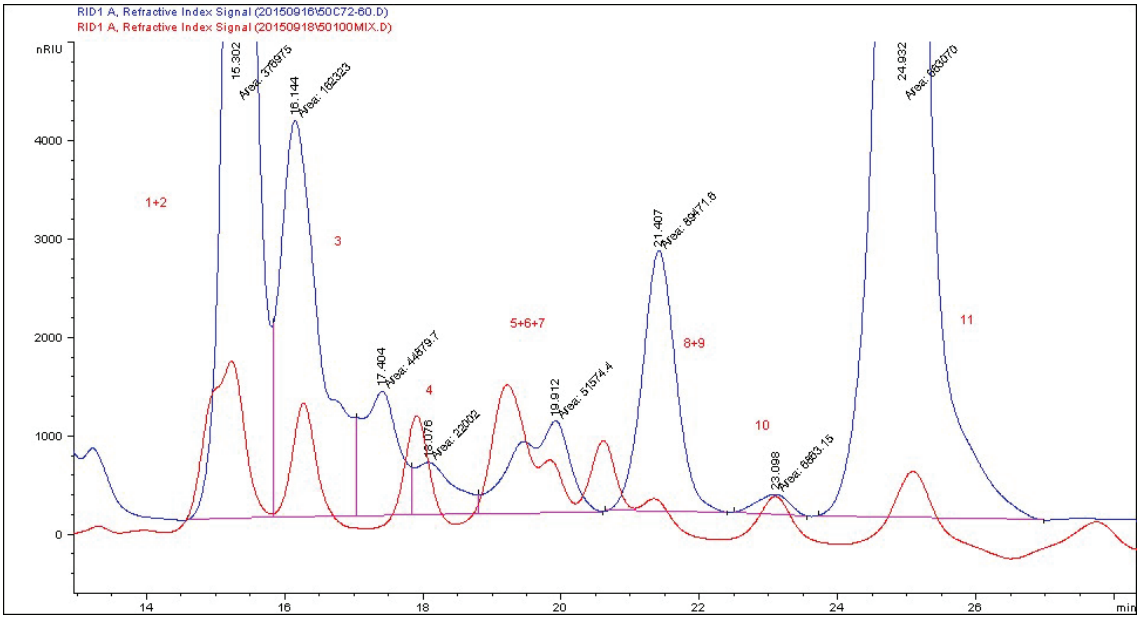

Figure C.1. HPLC chromtogram of sample taken at 60th min. in reaction conditions of (200 ℃, 1 A and 25 mM)

Area of 11th peak (levulinic acid): 663070

y=271.81x-4009.1

y: peak area

x: levulinic acid concentration

x=(y+4009.1)/271.81

x=(663070+4009.1)/271.81

x=2454 ppm of levulinic acid

OKAN AKIN

RESEARCH EXPERINCE

PhD Dissertation 2013-2017
"Synthesis of Biomass Sourced Value Added Chemicals by Hydrothermal Electrolysis Technique in Sub-Critical Water" Supervisor: Assist. Prof. Dr. Asli Yüksel Özşen

Project Coordinator/Researcher (Elkomar Chemical) 2014-2017
"Development of Environmentally Friendly Biopolymer Based Antifouling Coating for Marine Applications"

MSc Dissertation 2009-2012
"Development of biopolymer based protective coatings for marble surfaces"
Supervisor: Prof. Dr. Funda Tihminlioglu

AWARDS

Honeywell UniSIM® Design Competition, Global Winner, 2016 and 2017
North Star Innovation Competition, 2nd Finalist Project, 2013

PUBLICATIONS

O. Akin, A. Yüksel**,** "Novel Hybrid Process for the Conversion of Microcrystalline Cellulose to Value-Added Chemicals: Part 2: Constant Voltage Effect on Product Selectivity", Journal of Cellulose, 2017, Accepted Manuscript

O. Akin, A. Yüksel**,** "Novel Hybrid Process for the Conversion of Microcrystalline Cellulose to Value-Added Chemicals: Part 1: Process Optimization", Journal of Cellulose, 2016

O. Akin, F. Tihminlioglu, "Effect of Organ-Modified Clay Addition on Properties of Polyhydroxy Butyrate Homo and Copolymer Nanocomposite Films", J. of Environmental and Polymer Science, 2017

J.C. Garcia Queseda, **O.Akin**, I.Kocabas, E.Gil, "Study of the Procesability of PVC Plastisols Containing a Poly (Hydroxybutyrate-Valerate) Copolymer", Journal of Vinyl and Additive Technology, March 2012

H. Oguzlu, O. Ozcalik, **O. Akin**, F. Tihminlioglu, "Biodegradable Polymer Layered Silicate Nanocomposites and Developments in their Food Packaging Applications Turkish Plastics Association (PAGEV) Journal of Plastics (Sector Journal), December 2010

CONFERENCE PRESENTATIONS

O. Akin, A. Yüksel, "Conversion of Microcrystalline Cellulose to Value Added Chemical by Applying Direct Current in Hot Compressed Water" 16th European Meeting of Supercritical Fluids, Lisbon, 2017

O. Akin, O. Deliismail**, "**Utilization of Biodiesel By-Product Glycerol: Energy Efficient Integrated Process for Bio-Gasoline Production" Honeywell User Group (HUG-2016), San Antonio, Texas, 2016

O.Akin, A. Yüksel, "Conversion of Microcrystalline Cellulose to Value Added Chemical in Hot Compressed Water" 1st Green Chemistry and Sustainable Technologies, Çeşme, İzmir, 2015

O.Akin, A. Yüksel, "Software Simulation of Electrolysis Reaction of Biomass under Hydrothermal Conditions", Amadeus- 4th International Solvothermal and Hydrothermal Association Conference, Bordeaux, France, 2014